THERMAL PERFORMANCE OF THREE FREEZE PROTECTION METHODS AS APPLIED TO A LARGE SOLAR ENERGY SYSTEM

by

JAMES PATRICK KUMMER

A thesis submitted in partial fulfillment of the
requirements for the degree of

MASTER OF SCIENCE

(Mechanical Engineering)

at the

UNIVERSITY OF WISCONSIN - MADISON

1986

THERMAL PERFORMANCE OF THREE FREEZE PROTECTION
METHODS AS APPLIED TO A LARGE SOLAR ENERGY SYSTEM

by James P. Kummer

Under the Supervision of Professor William A. Beckman

Liquid flat plate solar collectors are devices that convert radiant energy from the sun into thermal energy, in the form of a heated liquid. A common problem for any solar collector using water as the collector fluid, is that of freezing, which has been known to cause extensive damage to many solar energy systems. Methods must be incorporated in solar energy systems using liquid flat plate collectors to prevent freeze damage.

The three most common methods of freeze protection are "drain-back, "dual fluid", and "recirculation." These three freeze protection schemes were investigated to determine possible control strategies and predict the annual thermal performance of solar energy systems incorporating them.

The analysis was done using the computer simulation program, TRNSYS, with models based on the large solar energy system installed at the Indian Health Facility in Chinle, Arizona. New component models, for use in TRNSYS, were developed to include thermal capacitance in the collectors, to include pipe wall thermal capacitance in the pipes, and to allow changing fluid volumes in both the collectors and pipes. This project was also intended to provide quidelines on the modeling requirements for each freeze protection method.

The drain-back freeze protection scheme using the "open return" control strategy had the highest solar fraction (22.8%) for the Chinle system. The lowest solar fractions

were for the recirculation schemes, with a decrease in solar fraction of up to 7% relative to the drain-back method. The modeling requirements were the most stringent for recirculation, as system dynamics become important. Finally, dual fluid freeze protection showed a decrease in solar fraction of 3% relative to drain-back. The dual fluid system performs closer to the drain-back system than might be expected, because the Chinle system incorporates a collector to storage heat exchanger with all freeze protection schemes.

ACKNOWLEDGEMENTS

Many thanks go to my advisors, Professors Jack Duffie and Bill Beckman, who provided much needed direction to a randomly steered "ship." I also thank Professors Sandy Klein and John Mitchell who have made the Solar Energy Laboratory "a place that counts."

I must offer praise, thanks, and "my first born child," to the graduate students, friends, and staff of the Solar Energy Laboratory. These people make a difference, day in and day out, and have turned my 19 months here into a worthwhile and memorable experience. An added special thanks to Jim Braun. I don't know why or how, but he let my problems become his problems, and many of my problems would not have been solved otherwise.

Of course there are the "special people": Grandma Tek, Sharon, Connie, Greg, Bridget, Danny, Keith, Ryan, Dave, Jerry, and Sue. I owe you more than I can ever pay back. Two other special people came into my life during "all this," Cindy and Kristi. These were the women behind this man and his work. "Thanks HUN."

Financial support for this work was provided by the U.S. Department of Energy. Thanks to all who knowingly and unknowingly supported me through their tax dollars.

Finally, but foremost:

Keith and Marge

"Dad and Mom"

Everything I do is because of you and is with you in mind. I felt your presence throughout this experience, and only wish I could say to you in person, "Love and Thanks."

TABLE OF CONTENTS

LIST OF FIGURES

FIGURE PAGE

FIGURE	PAGE

LIST OF TABLES

TABLE PAGE

NOMENCLATURE

A_c	collector area
A_n	collector area for one node
A_{xm}	pipe metal cross sectional area
C_{Pf}	specific heat of fluid
C_{Pm}	specific heat of metal
CAP_E	effective collector capacitance
$CAP_{E,NF}$	effective collector capacitance without fluid
F'	collector efficiency factor
F_R	collector heat removal factor
G_T	rate at which radiant energy is incident on the collector surface
$K_{\tau\alpha}$	incidence angle modifier
L	length
L_{eq}	equivalent pipe length
m_{cf}	mass of fluid in the collector
m_{feq}	equivalent fluid mass
m_{in}	mass of fluid entering the pipe
m_m	mass of metal
m_{pf}	mass of fluid within the pipe
$m_{pf,ave}$	average mass of fluid within the pipe over a timestep
$\dot{m}$	fluid flowrate
$\dot{m}_{drain}$	fluid flowrate during a draining process
$\dot{m}_{in}$	inlet fluid flowrate

$\dot{m}_{out}$	outlet fluid flowrate
$(mC_P)_{pf}$	capacitance of fluid within the pipe
n	collector node number
n_{total}	total number of collector nodes
Q_{aux}	auxiliary energy
Q_{col}	collected energy
Q_{env}	heat loss to the environment
Q_{load}	energy delivered to the load
Q_{rec}	energy used for recirculation
Q_{solar}	solar energy delivered (energy delivered from the collector storage tanks)
$\dot{Q}_{env}$	heat loss to the environment (rate)
$\dot{Q}_u$	useful energy collected (rate)
S	solar energy absorbed by the collector
SF	solar fraction ($1 - Q_{aux} / Q_{load}$)
t	time
t_{ff}	time for the fluid front to move through the collector
t_{nd}	time to fill one collector node
t_{tf}	time for the thermal front to move through the collector
Δt	TRNSYS timestep
T_{amb}	ambient temperature
T_{env}	environment temperature
T_i	temperature of pipe fluid element
T_{in}	inlet fluid temperature
T_{mix}	collector fluid temperature after "mixing" all of the nodes

T_n	temperature of collector node
T_{out}	outlet fluid temperature
T_P	collector plate temperature
T_{pf}	temperature of fluid within the pipe
U_L	overall collector heat loss coefficient
$(UA)_i$	heat loss coefficient for pipe element i based on inside pipe diameter
$(UA)_{id}$	overall heat loss coefficient based on inside pipe diameter
V_c	volume of collector fluid
V_i	volume of collector fluid in one node
V_{min}	minimum fluid volume, used to model the pipe wall thermal capacitance
ρ_m	density of pipe metal
$(\tau\alpha)$	transmittance - absorptance product
$(\tau\alpha)_n$	transmittance - absorptance product for radiation normal to the collector surface

CHAPTER I: INTRODUCTION

Active solar energy systems are mechanical systems used to convert radiant energy from the sun into usable thermal energy, such as hot water and hot air for domestic or industrial use. A common device for converting the sun's energy is a liquid flat plate solar collector, shown in figure 1.1. Water or any other suitable fluid is circulated through the riser tubes, where it is heated by the suns energy, which has been collected by the absorber plate. The absorber is nothing more than a metal plate, usually copper, and sometimes has its outer surface treated to enhance its ability to collect solar radiation. The heated water can then be pumped or delivered to any process where thermal energy is required.

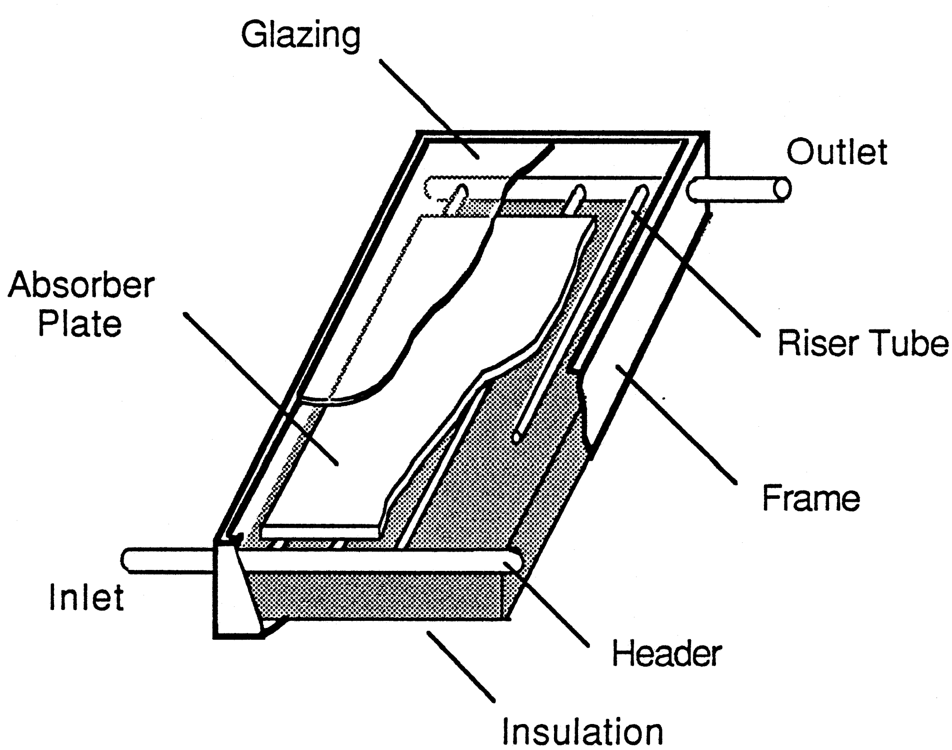

FIGURE 1.1 Cutaway view of a liquid flat plate solar collector.

Solar collectors perform best with as much direct sunlight as possible, which means they are located outdoors and exposed to the environment. A problem for almost all solar collectors using water as the energy transfer medium, is freezing. Freezing water inside a solar collector can cause extensive damage, and in one large industrial system resulted in over one million dollars in damages (Hicks, 1986). Most locations throughout the world can and do experience freezing conditions at one time or another. In locations far from the equator, freezing is more than just an occasional problem. Methods must be incorporated in solar energy systems to prevent freeze damage.

This report summarizes the results of an investigation of the three most common methods of freeze protection. Computer simulations were used to study the control and thermal requirements of each method. The major emphasis of the project consisted of developing and using a computer model to predict the annual performance of one particular solar energy system, using each of the three freeze protection schemes.

I.1 FREEZE PROTECTION METHODS

The three most common types of freeze protection are drain-back, dual fluid, and recirculation. The schemes are only briefly described here, with greater detail presented in the chapter on each method.

In a drain-back system the fluid is removed from the collectors anytime that freezing conditions are approached. The fluid is drained into storage tanks, normally located indoors, where it is stored until freezing conditions no longer exist and solar energy can be collected. A similar scheme known as "drain-down", is where the fluid is dumped to the ground or down the drains instead of to a storage tank. Drain-down is only practical for small systems located in mild climates, as make-up water costs can become significant. Drain-down was not included in this study, although the annual thermal performance of systems using drain-down should be very close to that for drain-back.

In a dual fluid system an anti-freeze and water mixture is used as the collector fluid. Freeze protection is provided by the fact that the freezing temperature of the collector fluid is well below expected ambient temperatures. This type of system requires a heat exchanger to separate the anti-freeze/water mixture from pure water in the rest of the system. Different fluids are on each side of the heat exchanger, thus the name, "dual fluid" system.

The recirculation method uses a portion of the energy collected during the day, to warm the collectors and prevent freezing at night or other times of freezing conditions. Water that was heated by solar energy, earlier in the day, and held in storage tanks, is pumped into the collectors, replacing the cold collector fluid that is about to freeze. The cold fluid normally is returned to the storage and mixed with the warm water. The pumps in this system continually cycle on and off as the temperature of the fluid in the collectors approach freezing and need to be replaced by warm fluid. As this method incurrs an energy cost to the system, it is only suitable for mild climates where only occasional freezing problems exist.

I.2 THE SYSTEM

The three freeze protection methods were compared, by applying them to a computer model of the large solar energy system installed at the Indian Health Facility located in Chinle, Arizona. The system was installed as part of the Solar in Federal Buildings program, which was a project of the United States government in an effort to develop solar technology and stimulate the solar industry.

The solar energy system consists of over 10,000 square feet of liquid flat plate collectors and is designed to supplement the space heating (SPH) and domestic hot water (DHW) requirements of the Chinle health facility. The system was designed so that it could operate as a drain-back system using water in the collector loop or as a dual fluid system with a water-glycol anti-freeze mixture in the collector loop. The system could also be modified to incorporate recirculation freeze protection.

Presently drain-back is used for freeze protection. At the time of this writing no performance data were available for this system. Only "expected" and design loads were available, which were used for sizing the components used in the computer model.

I.3 THE SIMULATION PROGRAM

The costs of actually installing each freeze protection scheme and performing tests to determine the system performance are prohibitive. Computer simulations provide a relatively inexpensive means to test a variety of system configurations and control strategies. However, caution must be used in relating computer predicted performance to real life system performance.

A transient system simulation program, known as TRNSYS, developed at the University of Wisconsin Solar Energy Laboratory, was used for simulating the Chinle system. (TRNSYS 1983). This is a well documented program that is extremely versatile in modeling an unlimited number of system configurations. Although initially developed to analyze solar energy systems, the program can be used for modeling HVAC, power plant, and other energy systems.

The program consists of many individual subroutines, called "components", which each model the performance of an individual piece of equipment, such as a pipe, pump, solar collector, or storage tank. The user can connect any number of these components, in any fashion, in order to model a system. Each component must be supplied with a list of parameters to determine the component performance. A main program performs the simulation and handles information passing amongst the components. Information passed between components generally consists of mass flowrates, temperatures, energy transfer rates, and control signals.

The system is defined in a "deck", which is a computer file containing a list of components, parameter specifications, interconnection information, and other data required to run a simulation. The deck is a description of the system and determines the set of equations which must be solved in order to determine the system performance. The simulation must be driven by forcing functions, normally the solar radiation and other environmental data. These data are available for an average year, known as typical mean year (TMY) data (Hall *et. al.*, 1978), which includes the temperatures and solar radiation on a horizontal surface for every hour of the year. The user determines a "timestep", which is the increment of time that the program uses to march through a simulation. At each timestep, TRNSYS solves all of the equations defining system performance. The solution method is by successive substitution.

As an example, consider the system shown in figure 1.2, with a solar collector, storage tank, and pump. Consider the pump to be constantly circulating water around this loop. After TRNSYS finishes one timestep, the TMY data is read and processed by TRNSYS to determine the ambient temperature and solar radiation during the next timestep. The collector inlet fluid temperature at the end of the last timestep is considered

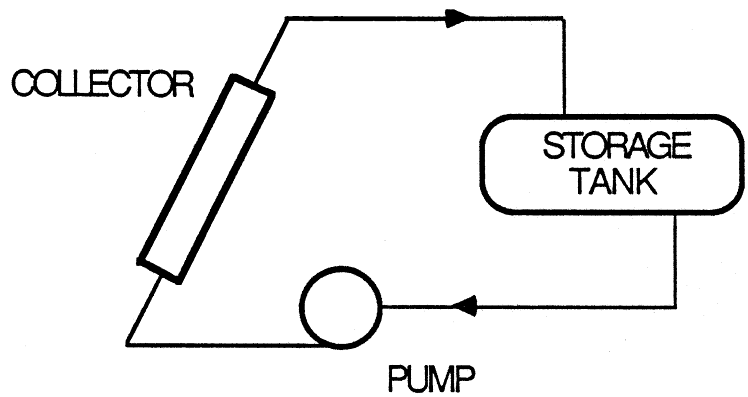

FIGURE 1.2 Example system with solar collector, storage tank, and pump.

the inlet fluid temperature during this timestep. Using the radiation data, ambient temperature, mass flowrate into the collector, and inlet fluid temperature, the collector component equations are solved to determine the fluid temperature leaving the collector. This fluid temperature and flowrate information is passed to the storage tank component, where differential equations are solved to determine new tank temperatures and the outlet fluid temperature. With the new tank temperature and the ambient temperature, heat losses from the tank can be determined. The temperature and flowrate of the fluid leaving the tank then passes to the pump component and finally back to the collector. The collector uses the same radiation data and ambient temperature, but now has a new inlet fluid temperature which it uses to calculate a new outlet temperature and thus the process repeats. This iterative process continues until the information passed to each component converges within a user specified tolerance. The timestep is now complete. All of the temperatures, flowrates, and energy transfer rates (such as heat losses) are considered constant over the timestep. The energy rates can be integrated over the timestep, which is just the energy rate times the timestep, and totals stored by the main part of TRNSYS in order to produce a summary of results at the end of the simulation. Another step in time (timestep) is taken and the whole process is repeated until all the timesteps of a simulation are completed. Timesteps can be on the order of seconds or hours and simulations can be over a period of seconds or years.

CHAPTER II: COMPONENT MODELS

In this chapter pipe and collector component models used in TRNSYS will be described. For various reasons, new pipe and collector models are used in the system simulations instead of the current TRNSYS models. Two philosophies were followed in model selection and development. First, the existing TRNSYS models were used as much as possible. Second, existing TRNSYS computer code was modified instead of developing new components from scratch.

II.1 PIPE MODELS

In this section several steps in the development of a pipe model will be discussed. A model was desired to account for the thermal capacitance of the pipe walls and allow the pipe to be drained and filled. Draining the fluid from the pipe is required to model systems incorporating drain-back freeze protection. The current TRNSYS pipe model ignores the wall thermal capacitance and considers the pipe to be full of fluid at all times.

In section II.1.1 the current TRNSYS pipe model is is reviewed. Section II.1.2 describes a simple pipe model which will be extended in sections II.1.3 and II.1.4 to account for pipe capacitance and changing fluid volumes.

II.1.1 PLUG-FLOW PIPE MODEL

The plug-flow pipe model used in version 12.1 of TRNSYS is reviewed here for comparison to other models presented in this section. At any given time the pipe is considered to be divided into fluid segments, each at a uniform temperature, but not necessarily of uniform size. The fluid entering the pipe in a given timestep forms a new segment which displaces an equal mass from the exit of the pipe. The fluid leaving the pipe can be made up of several fluid segments or parts of segments, which are mixed to determine an outlet temperature over the timestep. Figure 2.1 illustrates this concept.

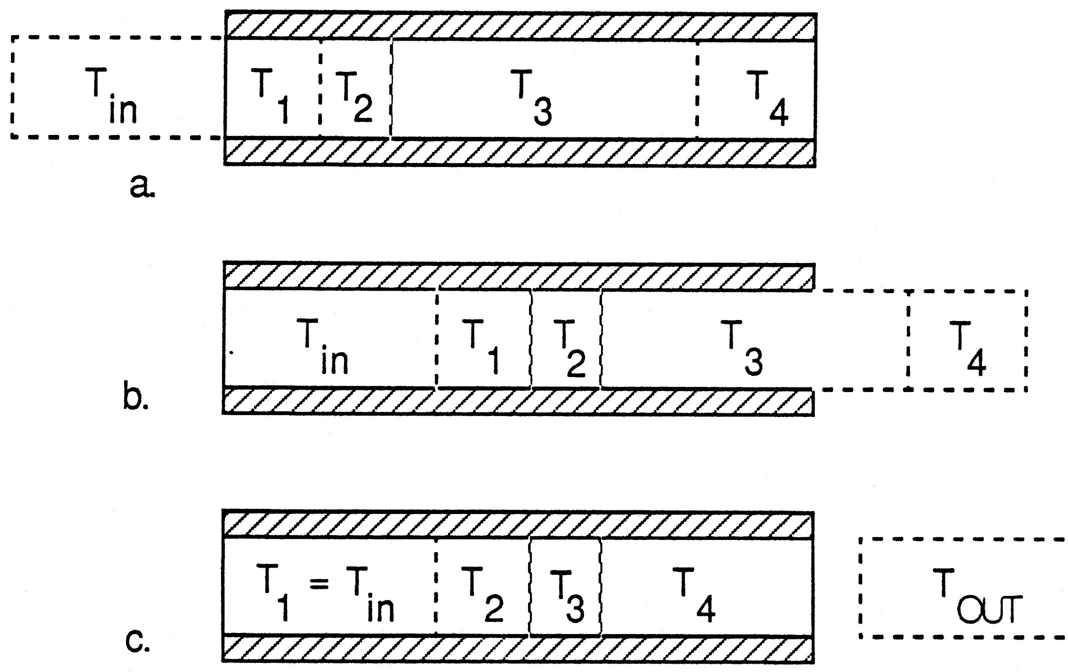

FIGURE 2.1 Plug-flow pipe model.

A fluid segment enters the pipe with a mass (figure 2.1.a):

$$m_{in} = \dot{m}_{in}\,\Delta t \tag{2.1.1}$$

where:

m_{in} = fluid mass entering pipe

$\dot{m}_{in}$ = fluid flowrate

Δt = TRNSYS timestep

The entering fluid pushes the same amount of fluid, which consists of segment 4 and part of segment 3, out the exit of the pipe (figure 2.1.b). The outlet temperature is the mass weighted average of the exiting fluid.

$$T_{out} = \frac{m_{3'} T_3 + m_4 T_4}{m_{3'} + m_4} \qquad (2.1.2)$$

$$m_{out} = m_{3'} + m_4 = m_{in} \qquad (2.1.3)$$

where:

$m_{3'}$ = mass of the portion of segment 3 which exits the pipe

Heat losses to the environment are calculated separately for each fluid segment by analytically solving equation 2.1.4. For elements leaving the pipe during the timestep, losses are calculated for only the time while in the pipe. The segments are renumbered at the end of the timestep as shown in figure 2.1.c and their temperatures adjusted to reflect the heat loss.

$$m_i \, C_{Pf} \frac{dT_i}{dt} = - (UA)_i \; (T_i - T_{env}) \qquad (2.1.4)$$

where:

m_i = fluid mass in element i

T_i = temperature of fluid element i

C_{Pf} = specific heat of fluid

$(UA)_i$ = loss coefficient for element i based on inside pipe area

T_{env} = temperature of environment around pipe

t = time

Temperature fronts moving through pipes are simulated with the plug-flow model by tracking the location and temperature of each segment. This can be important for simulating controller dynamics in systems with long pipe runs, where a significant amount of time is required for fluid to pass through the pipes.

II.1.2 FULLY MIXED PIPE MODEL

This section presents a pipe model, less complicated than the plug-flow model, which assumes that the fluid within the pipe is fully mixed and that fluid entering the pipe is instantly mixed with the existing fluid. The mixed temperature pipe is shown in figure 2.2. This model considers the pipe to be always full, so that the flowrate in equals the flowrate out. An energy balance on the fluid in the pipe yields equation 2.1.5, which is solved analytically to determine the fluid temperature.

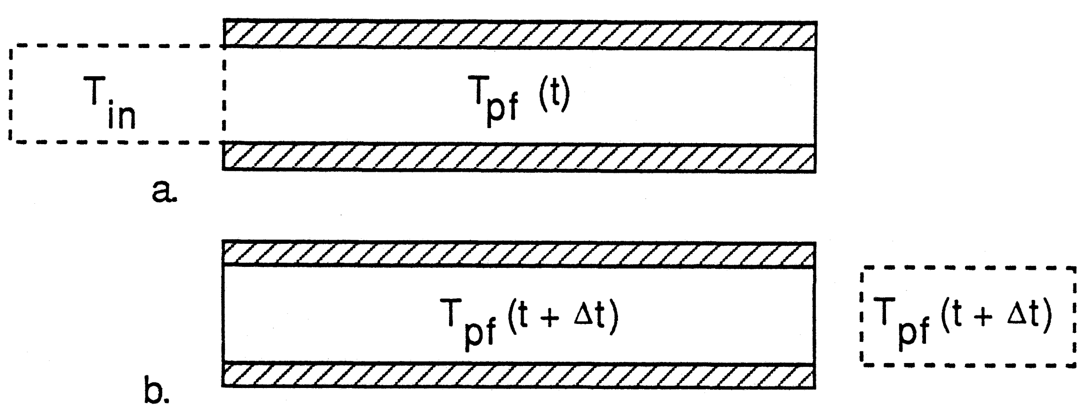

FIGURE 2.2 Mixed temperature pipe model.

$$(m\,C_P)_{pf}\frac{dT_{pf}}{dt} = \dot{m}_{in}\,C_P\,(T_{in} - T_{pf}) - (UA)_{id}\,(T_{pf} - T_{env}) \qquad (2.1.5)$$

where:

$(mC_P)_{pf}$ = capacitance of pipe fluid

T_{pf} = temperature of pipe fluid

T_{in} = inlet fluid temperature

$(UA)_{id}$ = loss coefficient based on the inside pipe area

Figure 2.3 shows the outlet temperature of a pipe, after a step change in inlet temperature, for both the plug-flow (sec. II.1.1) and fully mixed models. The fully mixed model does not track the temperature front, but the energy associated with each curve is approximately the same.

During transient conditions, the fully mixed model predicts slightly different heat losses than the plug-flow model. As the pipes reach steady-state temperatures the heat losses are the same. Consider a pipe with a step increase in the inlet temperature. With the fully mixed pipe, the outlet temperature will instantly begin to rise, while the plug-flow pipe outlet temperature will be unaffected until the temperature front has moved through the pipe. The difference in heat loss occurs because the fully mixed model transmits energy through and out the pipe faster than the plug-flow model, so that the fully mixed pipe will have a lower average temperature than the plug-flow pipe. The mixed temperature model underpredicts the pipe losses for a step increase in inlet temperature and overpredicts for a step decrease in inlet temperature. The errors are small and tend to cancel each other out in typical simulations, so that the overall difference in predicted pipe losses will generally be insignificant.

The Chinle system has long piping runs of 600 feet for the inlet and outlet of the collectors. Results for simulations using the plug-flow model and the fully mixed model for the collector piping are shown in table 2.1. The results show an insignificant

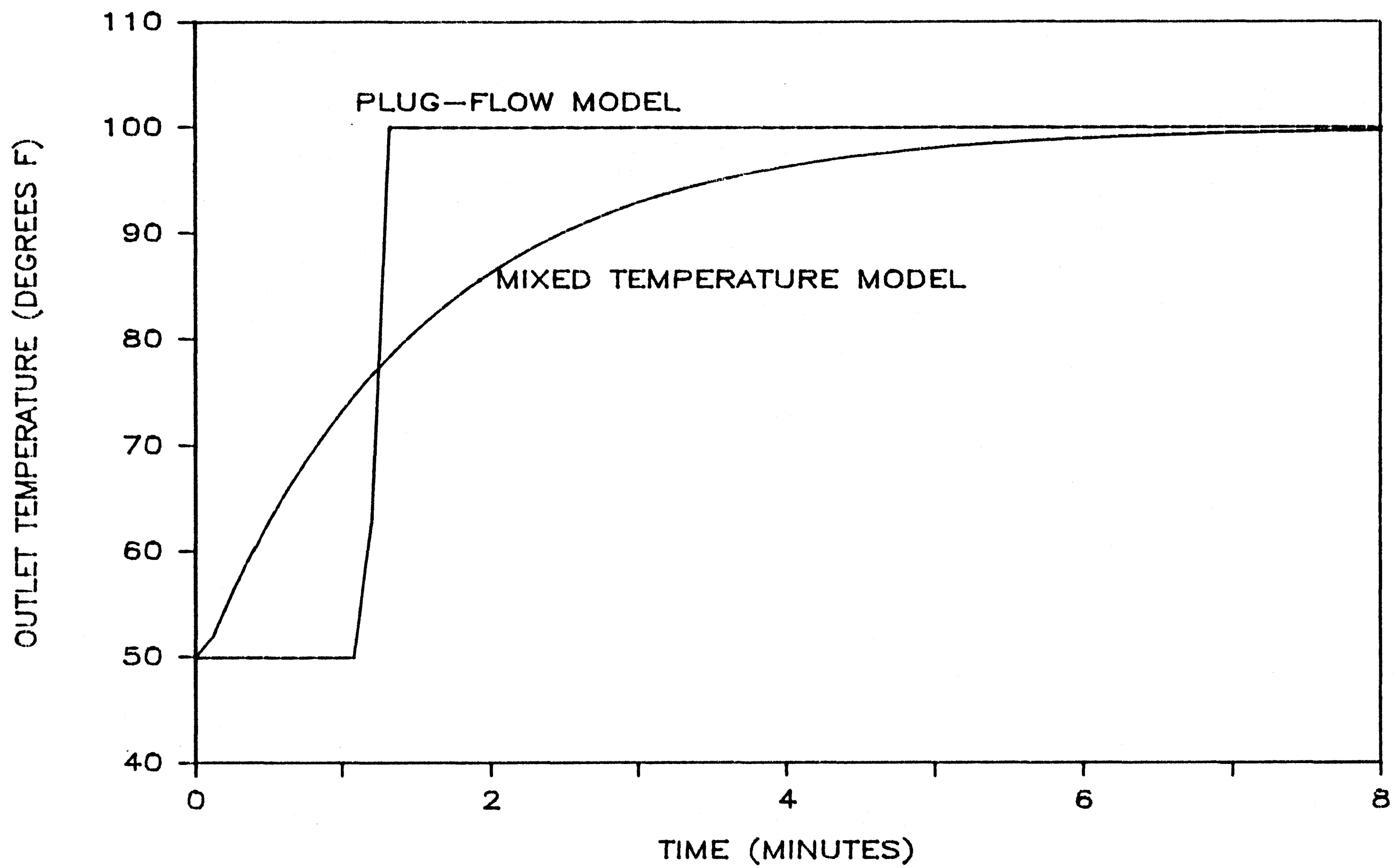

FIGURE 2.3 Pipe models response to a step change in inlet termperature. (Pipe length = 600 ft.; Diameter = 4 in;. Flowrate = 160170 lbm / hr)

difference between the plug-flow and fully mixed models in predicting heat losses and overall system performance.

MODEL	Q_{col} Btu x10^{-9}	Q_{env} Btu x10^{-9}	Q_{env} / Q_{col} Percent	Q_{aux} Btu x10^{-9}	Q_{load} Btu x10^{-9}	SF Percent
Plug-flow pipes	2.902	0.2618	9.0	9.022	11.62	22.36
Fully mixed pipes	2.892	0.2620	9.1	9.026	11.62	22.32

Q_{col} = total solar energy collected
Q_{env} = heat losses from the collector loop piping
Q_{aux} = total auxiliary energy
Q_{load} = total energy delivered to the load (space heating plus hot water)
SF = solar fraction (1- Q_{aux} / Q_{load})

TABLE 2.1 Annual thermal energy usage predicted with the Chinle model using the plug-flow and fully mixed pipe models. (Note that for these simulations the heat loss coefficient for the pipes was twice the value calculated for the Chinle pipes.)

For any simulation it should be determined whether the dynamics modeled by a plug-flow model are important. Tracking temperature fronts may be important for simulating controller dynamics. However, for typical yearly TRNSYS simulations, the solar fraction predicted by the fully mixed pipe model and the plug-flow pipe model are essentially identical.

II.1.3 PIPE WALL THERMAL CAPACITANCE

In this section a method is given to account for pipe wall capacitance using the fully mixed pipe model from section II.1.2. Pipe wall capacitance can be important when considering the energy required to warm the pipes after a night of cooling. This energy includes not only pre-warming during morning start-up, but warming the pipe from its morning start-up temperature, to its final operating temperature when the system shuts down for the day.

The pipe wall capacitance can be modeled by adding an extra length of pipe to the actual pipe length, so that the extra fluid has the same capacitance as the walls of the original pipe. This added pipe length volume is specified as a minimum fluid volume, so that if the pipe is drained, this "equivalent" pipe wall capacitance always remains in the pipe. As an example consider the following pipe:

4 inch nominal pipe size; 600 feet long
O.D. = 4.5 inches; I.D.= 4.026 inches
A_{xm} (metal cross section) = 3.137 in^2
A_{xf} (fluid cross section) = .0884 ft^2

schedule 40 carbon steel pipe
$\rho_m = 487\ lbm / ft^3$; $Cp_m = .113\ Btu / (lbm\ °F)$

fluid: water
$\rho_w = 62.4\ lbm / ft^3$; $Cp_w = 1\ Btu / (lbm\ °F)$

mass of metal:

$$m_m = (A_{xm})(L)(\rho_m)$$

$$m_m = (3.137\ in^2)(1\ ft / 144\ in^2)(600\ ft)(487\ lbm / ft^3) = 6365\ lbm$$

metal capacitance:

$$(mCp)_m = (m_m)(Cp_m)$$

$$(mCp)_m = (6365\ lbm)(.113\ Btu / (lbm\ °F)) = 719\ Btu / °F$$

equivalent fluid mass:

$$m_{feq} = \frac{(mCp)_m}{Cp_f} = \frac{719\ Btu / °F}{1\ Btu / °F} = 719\ lbm$$

equivalent pipe length:

$$L_{eq} = \frac{m_{feq}}{\rho_f \, A_{xf}} = \frac{719 \text{ lbm}}{(62.4 \text{ lbm / ft}^3)\ (.0884 \text{ ft}^2)} = 130.3 \text{ ft}$$

volume of L_{eq}:

$$V_{min} = \frac{m_{feq}}{\rho_f} = \frac{719 \text{ lbm}}{62.4 \text{ lbm / ft}^3} = 11.52 \text{ ft}^3$$

In this example the 600 foot pipe would be modeled as a 730 foot pipe ($L + L_{eq}$). A minimum fluid volume of 11.52 ft^3 would be specified in order to account for the pipe wall capacitance. If the pipe is drained, this minimum fluid volume remains in the pipe and continues to lose energy to the environment. Fluid that begins to fill the pipe is mixed with the minimum fluid volume. In effect, this models the pipe wall as a lumped parameter, with an infinite heat transfer coefficient between the pipe wall and fluid.

II.1.4 VARIABLE VOLUME PIPE MODEL

The fully mixed pipe model of section II.1.2 is easily modified to allow filling and draining the pipe fluid, which is needed for simulating drain-back solar energy systems. A mass and energy balance on the pipe fluid results in differential equations 2.1.6 and 2.1.7, which describe the rate of change in mass and internal energy.

$$\frac{dm_{pf}}{dt} = \dot{m}_i - \dot{m}_o \tag{2.1.6}$$

$$(C_P)_{pf} \frac{d\,(mT)_{pf}}{dt} = \dot{m}_{in}\, C_P\, T_{in} - \dot{m}_{out}\, C_P\, T_{pf} - (UA)_{id}\,(T_{pf} - T_{env}) \tag{2.1.7}$$

where:

m_{pf} = mass of fluid within the pipe

Simultaneous solution of equations 2.1.6 and 2.1.7 gives the time temperature history of the pipe fluid. In TRNSYS the temperature and mass of the fluid in the pipe at the end of the timestep is used as initial conditions in the next timestep. The inlet fluid temperature and flowrate are considered constant over the timestep, therefore equations 2.1.6 and 2.1.7 can solved for the temperature and mass at the end of the timestep. Equations 2.1.8 and 2.1.9 can be used with 2.1.6 and 2.1.7 to find the average temperature and mass over the TRNSYS timestep, which are the values passed to other component models during simulations.

$$m_{pf,ave} = \frac{1}{\Delta t} \int_0^{\Delta t} m_{pf}\, dt \qquad (2.1.8)$$

$$T_{pf,ave} = \frac{1}{\Delta t} \int_0^{\Delta t} T_{pf}\, dt \qquad (2.1.9)$$

A conductance term (UA) for heat losses is needed for equation 2.1.7. In an actual pipe the conductance term between the fluid and environment would be based on the resistor network shown figure 2.4.

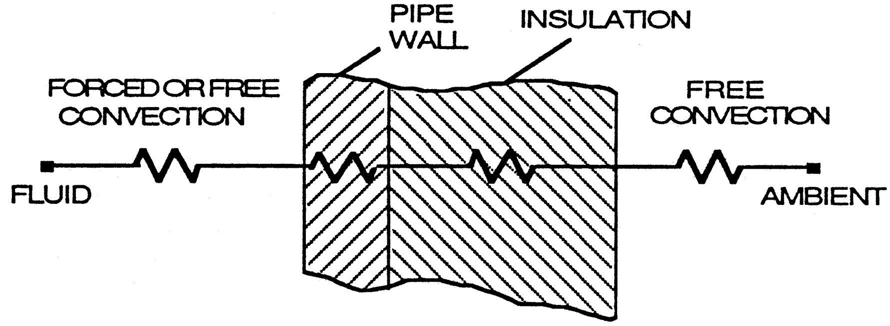

FIGURE 2.4 Resistor network for determining the conductance between the pipe fluid and environment.

In section II.1.3 a method was presented for including the effects of pipe wall capacitance by adding an equivalent pipe length. The heat transfer coefficient between the fluid and walls is considered infinite. The resistance due to the pipe wall is negligible for metal pipes, therefore the loss coefficient for the model is based on the outside pipe area and includes only the conductance through the insulation and into the environment. The area associated with conduction is for the actual pipe length and does not include the added equivalent length for wall capacitance.

To use the variable volume pipe model in a TRNSYS model of a drain-back system, a few constraints are required. For filling an empty or partially empty pipe in an actual system, the inlet flowrate is determined by the specific system. TRNSYS models this situation with the flowrate determined by the pump component. The filling time is dependent on the pump flowrate and pipe size. For draining the pipe, the actual drain time will depend on the pipe slope and system configuration. For compatibility with existing TRNSYS components, the variable volume pipe is forced to empty in one timestep, independent of pipe size. A control signal is input to the pipe model to initiate the draining process.

Instead of writing a new TRNSYS component model for a filling and draining pipe, the existing variable volume tank model (type 39) was modified. The variable volume tank component models a fully-mixed tank that contains a variable quantity of fluid and is based on equations 2.1.6 and 2.1.7. A mixed temperature pipe can be considered a long narrow tank. The variable volume tank model was modified to drain in one timestep and calculate heat losses based on the outside pipe area.

II.2 COLLECTOR MODELS

Numerous computer models have been developed to simulate collector performance, ranging in complexity from the simple steady-state models to detailed finite difference models. (Klein *et. al.*, 1974; Chiou, 1982; De Ron, 1979) Several new models were written for this project. These models were kept simple in order to minimize the computational effort required to use them. Although not as accurate as more detailed models, their purpose was to provide first approximations of the effect various freeze protection methods have on system performance.

These new collector models were all slightly changed versions of the existing TRNSYS code. Three of the steps in the evolution of a new collector component are summarized in this section. The first model is the existing zero capacitance collector component in TRNSYS. The second model accounts for capacitance and the final model allows for draining and filling the collector.

Collector capacitance must be taken into account when modeling recirculation freeze protection. As the collector reaches a set minimum temperature, the pump is turned on to recirculate warm fluid and prevent collector freezing. After the collector is warmed up, the pump is turned off and the collector cools down. A collector model in this case must include thermal capacitance to simulate the cooling down time, which is important for modeling controller response.

In order to simulate a drain-back freeze protection system, a collector model must account for draining and filling. The effects of draining a collector are to remove the fluid and reduce the overall thermal capacitance of the collector.

II.2.1 ZERO CAPACITANCE COLLECTOR MODEL

The existing TRNSYS collector model is briefly described here. Only the linear efficiency mode (mode one in TRNSYS) was used for this project. The TRNSYS model is based on the Hottel-Whillier equation: (Duffie and Beckman, 1980)

$$\dot{Q}_u = A_c F_R [S - U_L (T_{in} - T_{amb})] \tag{2.2.1}$$

where:

$\dot{Q}_u$ = useful energy gain (energy rate)

A_c = collector area

F_R = collector heat removal factor

S = absorbed solar radiation (per unit area)

U_L = overall loss coefficient (per unit area)

T_{in} = inlet fluid temperature

T_{amb} = ambient temperature

The absorbed solar radiation (S) is equal to the difference between the incident solar radiation and optical losses. The heat removal factor (F_R) is the ratio of the actual energy collected to the energy collected if the whole collector is at the inlet fluid temperature. The overall loss coefficient (U_L) includes all the radiation, conduction, and convection heat transfer losses that occur from a collector.

The useful energy gain from equation 2.2.1 is also equal to the energy transferred to the fluid.

$$\dot{Q}_u = \dot{m}\, C_P (T_{out} - T_{in}) \tag{2.2.2}$$

where:

$\dot{m}$ = collector flowrate

T_{out} = outlet fluid temperature

TRNSYS solves equation 2.2.2 for the outlet temperature anytime there is flow through the collector. For no flow conditions, a steady-state stagnation temperature is found. The stagnation temperature is found by setting Q_u to zero in Eqn. 2.2.1 and solving for T_{in}. Since there is no flow, T_{in} is considered to be the uniform plate temperature, (T_p). Eqn. 2.2.3 is the steady-state equation for the stagnation temperature.

$$T_p = \frac{S}{U_L} + T_{amb} \tag{2.2.3}$$

Since the TRNSYS collector model has no capacitance, the steady-state conditions are reached instantaneously. Klein (1973) found that yearly simulations using collector models neglecting capacitance have an error of 1% to 5% in collected energy. For further information on the TRNSYS collector model see the TRNSYS manual (1983).

II.2.2 COLLECTOR CAPACITANCE

A collector model accounting for thermal capacitance is described in this section. Capacitance can be important in simulations where the time-temperature behavior of a collector influence the control decisions. The analysis of transient heat transfer in a solar collector is similar to that for classical heat exchangers. (Myers *et. al.*, 1967 and 1970; Kays and London, 1964) A combination lumped parameter and finite difference analysis is used as the basis for this model. An overall equivalent capacitance is determined which lumps the effects of the cover, absorber plate, fluid, tubes, insulation, and other collector materials. The collector is broken into a user determined number of nodes in the flow direction. Each node has a fraction of the overall capacitance.

A schematic collector is shown in figure 2.5, with its associated energy flows.

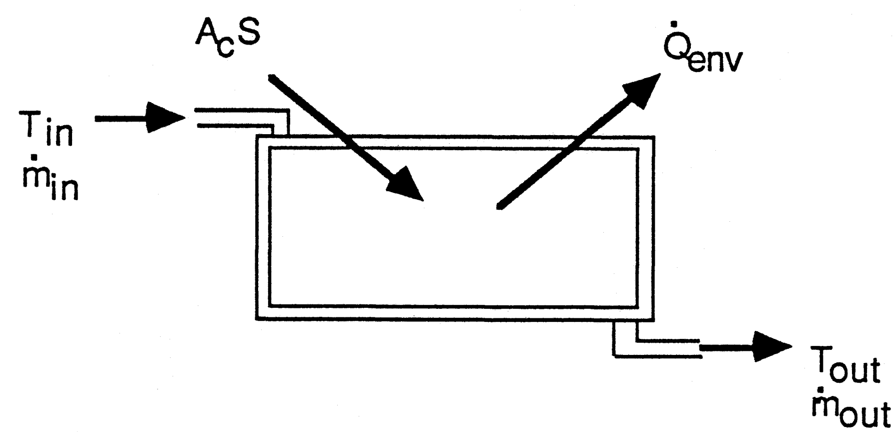

FIGURE 2.5 Schematic of flat plate solar collector. (Top view)

The same collector is shown in figure 2.6 divided into three nodes in the flow direction. The absorbed solar radiation, a thermal network for collector losses, and the mass flows are also represented in figure 2.6.

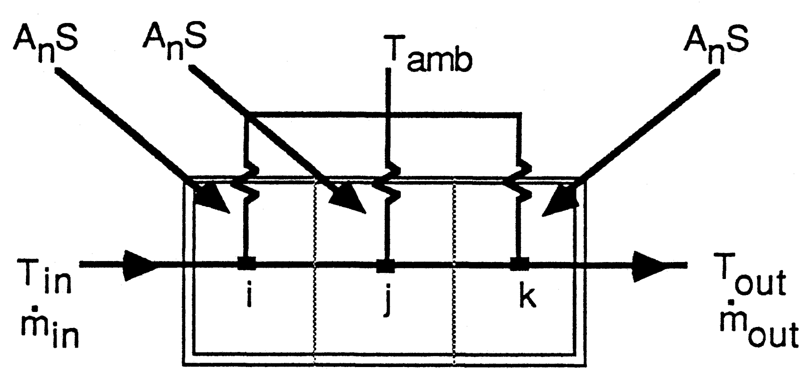

FIGURE 2.6 Multi-node collector.

An energy balance on any node n from figure 2.6 gives the following equations:

$$CAP_E \frac{dT_n}{dt} = F' [S - U_L (T_n - T_{amb})] - \frac{\dot{m}\, C_P}{A_n} (T_{out,n} - T_{in,n}) \qquad (2.2.4)$$

$$A_n = \frac{A_c}{n_{total}} \qquad (2.2.5)$$

$$T_{out,n} = T_n \qquad (2.2.6)$$

where:

A_n = node collector area

CAP_E = effective capacitance (per unit area)

F' = collector efficiency factor

n_{total} = total number of nodes

T_n = temperature of node

$T_{out,n}$ = fluid temperature leaving node n

$T_{in,n}$ = fluid temperature entering node n

The following list of assumptions are implicit to equation 2.2.4.

1. An infinite heat transfer coefficient between the fluid, tubes, and absorber plate.
2. Glass cover, insulation, and other collector material temperatures are the same as the local fluid temperature.
3. No conduction heat transfer in the flow direction within any of the collector materials or fluid.

4. Constant collector parameters. (F' and U_L)

Assumption 1 is generally made for liquid based collectors where the fluid to tube heat transfer coefficient is large compared to the overall loss coefficient between the fluid and environment. Assumption 2 allows one node to represent the total cross sectional area of the collector. This assumption can be made by using weighting factors for each collector material, in calculating an equivalent collector capacitance. The weighting factor method is described later in this section. Assumption 3 greatly simplifies the solution method required for solving the system of equations generated for all of the nodes. The temperature difference (about 10 °F) from collector inlet to outlet is small relative to the operating temperature of the collector (above 125 °F). This small temperature difference provides little potential for conduction heat transfer. The temperature throughout the collector is dominated by the inlet fluid temperature, and conduction has little affect on the temperature profile along the flow direction of the collector. Assumption 4 is often used for collector models and implies that all the factors in determining F' and U_L are constant, such as the wind heat transfer coefficient and collector material properties. Only very detailed models could be used without making this assumption.

By performing an energy balance on each node, a system of coupled, first order differential equations (eqn. 2.2.4) is obtained. A simple solution method is to solve the equations sequentially. The fluid conditions entering the collector are used as the conditions entering the first node. After solving the differential equation for the first node, the average fluid temperature from the first node is used as the inlet temperature for the second node. This scheme is repeated for each node and the fluid temperature in the last node is used as the collector outlet temperature. This model simulates a collector that is always full. Therefore the mass flow into and out of the collector and each node is constant.

The collector model based on equation 2.2.4 requires that an effective capacitance be determined for the collector. Klein (1973) gives a method to calculate an effective capacitance, which is not the sum of all the collector material capacities, but the sum of each collector material capacity multiplied by a weighting factor. The weighting factor is the ratio of the temperature change experienced by the material, to that experienced by the fluid, plate, and tubes. Typical weighting factors are given by Klein (1973). The weighting factor method requires detailed information on the collector geometry and materials.

A second method to determine the effective capacitance is to fit the collector model to the collector performance data. Only the time constant for the collector is needed, which is normally given in performance specifications. The time constant can be defined as the time required for fluid leaving a collector to attain 63.2 percent of its total change after a step change in incident radiation or inlet fluid temperature. A time constant for the model can be found by subjecting the model to a step change in inlet temperature or radiation, which is equivalent to the test method specified by ASHRAE (1977) to determine actual collector time constants. Figure 2.7 shows the model results in an attempt to determine the effective capacitance. for a given collector. The horizontal line represents 63.2 percent of the total change in outlet temperature and the vertical line is the time constant specified for this particular collector. A trial and error method is used to find the effective capacitance which gives a curve passing through the intersection of the two lines.

Equation 2.2.4 contains a term for the absorbed solar radiation, which may be given as: (Duffie and Beckman, 1980)

$$S = G_T \, K_{\tau\alpha} \, (\tau\alpha)_n \tag{2.2.7}$$

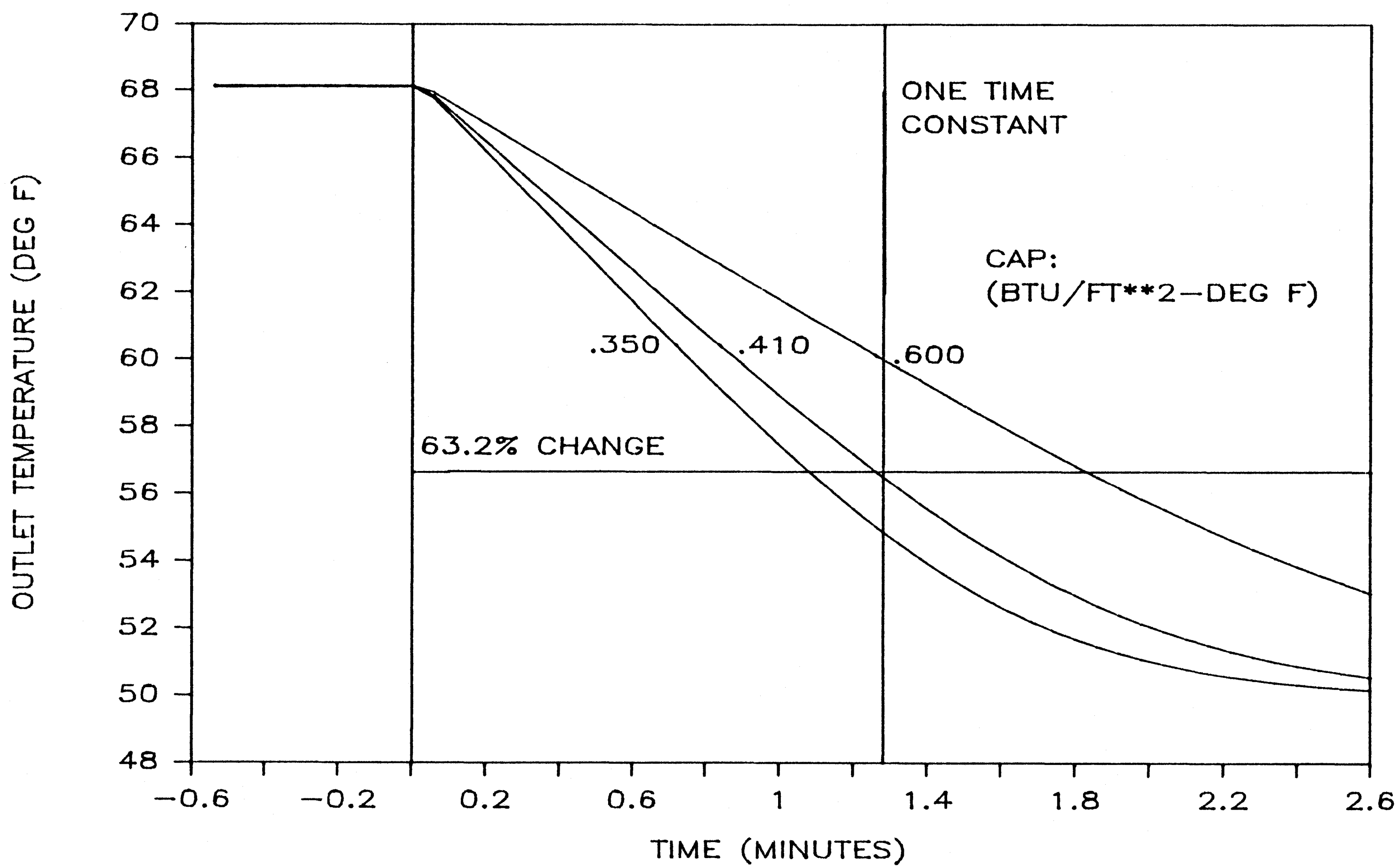

FIGURE 2.7 Collector response to a step change in radiation, from 300 to 0 Btu / hr-ft^2; for collectors with various effective capacitances.

$$K_{\tau\alpha} = \frac{(\tau\alpha)}{(\tau\alpha)_n} \tag{2.2.8}$$

where:

G_T = the rate at which radiant energy is incident on the collector surface

$K_{\tau\alpha}$= incidence angle modifier

$(\tau\alpha)$ = transmittance - absorptance product; defined as the ratio of total absorbed radiation to the incident radiation.

$(\tau\alpha)_n$ = transmittance - absorptance product for radiation normal to the collector surface.

Substituting Eqn. 2.2.7 into 2.2.4 yields:

$$C_n \frac{dT_n}{dt} = F' [\, G_T K_{\tau\alpha} (\tau\alpha)_n - U_L (T_n - T_{amb})\,] - \frac{\dot{m}\, C_P}{A_n} (T_{out,n} - T_{in,n}) \tag{2.2.10}$$

Eqn. 2.2.9 uses the collector efficiency factor (F'), while the steady-state eqn. 2.2.1 uses the collector heat removal factor (F_R). The collector efficiency factor represents the ratio of actual useful energy gain to the useful gain that would result if the collector absorbing surface had been at the local fluid temperature. In order to determine the collector response using F', the temperature profile in the flow direction of the collector must be known. By dividing the collector into nodes, an approximate temperature profile is represented in the model.

The heat removal factor (F_R) was developed so that collector performance could be determined knowing only the inlet temperature. Two terms that are used by the solar industry to rate collectors are the products $F_R(\tau\alpha)_n$ and F_RU_L. The solution to Eqn. 2.2.9 contains the products $F'(\tau\alpha)_n$ and $F'U_L$, which can be related to $F_R(\tau\alpha)_n$ and F_RU_L with the equations (Duffie and Beckman, 1980):

$$F' U_L = -\frac{\dot{m}\, C_P}{A_c} \ln\left(1 - \frac{F_R\, U_L\, A_c}{\dot{m}\, C_P}\right) \qquad (2.2.10)$$

$$\frac{F'}{F_R} = \frac{A_c\, F' U_L}{\dot{m}\, C_P}\left[\, 1 - \exp\left(\frac{-A_c\, F' U_L}{\dot{m}\, C_P}\right)\right]^{-1} \qquad (2.2.11)$$

The accuracy of the collector model and solution method described in this section is dependent on both the number of nodes that the collector is divided into and the size of timestep used in solving the differential equations. Consider a collector in equilibrium with the environment as shown in figure 2.8.

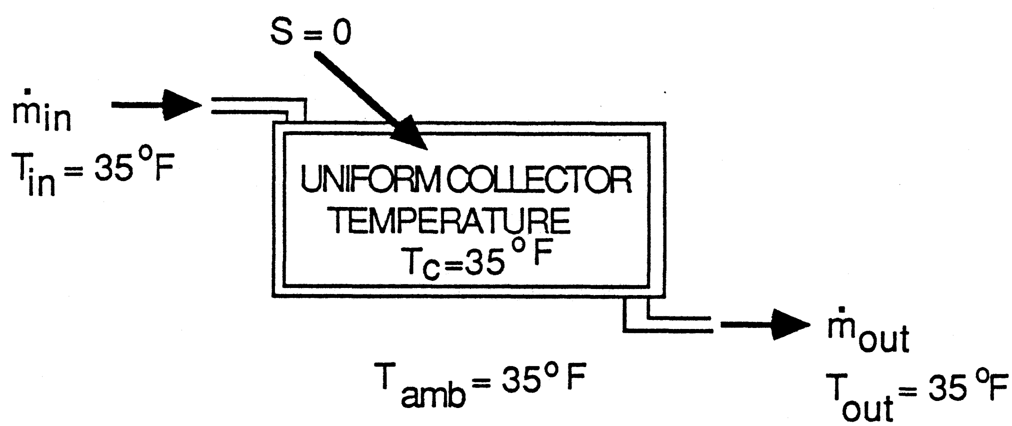

FIGURE 2.8 Collector in equilibrium with the surroundings.

Figure 2.9 shows the response of the collector, with an infinite heat transfer coefficient between the fluid and collector materials, to a step increase in inlet temperature. If equation 2.2.4 could be solved exactly for an infinite number of nodes, the calculated outlet temperature of the collector would look like figure 2.9. There are two fronts that pass through this collector. The first is a fluid front, which is at the head of the warmer inlet fluid and moves through the collector at the fluid velocity. The time for this front to push out the fluid initially in the collector is the collector volume divided by the fluid flow rate and is indicated as t_{ff} in figure 2.9. Until this time the collector outlet temperature will be at the initial collector temperature, 35 °F in this case.

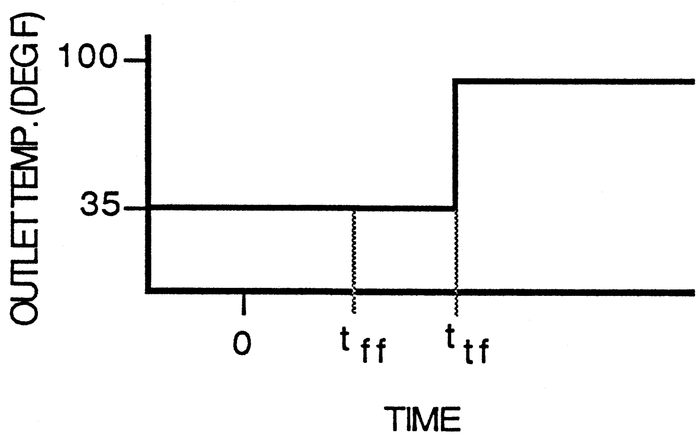

FIGURE 2.9 Collector response to a step change in inlet temperature, from 35 °F to 100 °F at time zero. The collector has an infinite heat transfer coefficient between the fluid and collector materials.

The second is a thermal front, and is associated with the time required for the entering fluid to warm the collector materials to the inlet fluid temperature. This can be estimated by:

$$t_{tf} = \frac{CAP_{E,NF}}{m\,C_P} \qquad (2.2.12)$$

$$CAP_{E,NF} = CAP_E - \frac{V_c\,\rho_{cf}\,C_P}{A_c} \qquad (2.2.13)$$

where:

t_{tf} = time for thermal front to pass through the collector

$CAP_{E,NF}$ = effective capacitance of collector with no fluid (per unit area)

V_c = collector fluid volume

ρ_{cf} = density of collector fluid

Equation 2.2.12 would be exact for the case of infinite heat transfer between the fluid and collector and zero heat loss to the environment. Until time t_{tf} the outlet temperature remains at 35 °F. The step form of the outlet temperature at time t_{tf} is due to the infinite heat transfer coefficient assumed between the fluid and collector materials.

Figure 2.10 shows the response of the collector model to a step change in inlet temperature as a function of the number of nodes. Figure 2.11 shows the collector model response for various timesteps. Either increasing the number of nodes or decreasing timestep size improves the accuracy of the model. In order to reach the ideal step change response, a very large number of nodes and extremely small timestep is required.

For a given number of nodes there is a minimum timestep size at which any further decrease in size produces a negligible change in results. Experience has shown this timestep size to be approximately equal to the time required to fill one node, and is calculated by equation 2.2.14.

$$t_{nd} = \frac{\dfrac{V_c \, \rho_{cf}}{n_{total}}}{\dot{m}} \tag{2.2.14}$$

where:

t_{nd} = time to fill one node

In typical yearly TRNSYS simulations, using a large number of nodes with small timesteps is not practical due to the computing effort required. Fewer nodes and larger timesteps can be used, but the consequences should be realized. Compare the ideal curve and case D in figures 2.10 and 2.11. The ideal step becomes smoothed and stretched as the number of nodes are decreased and timestep size increased. The

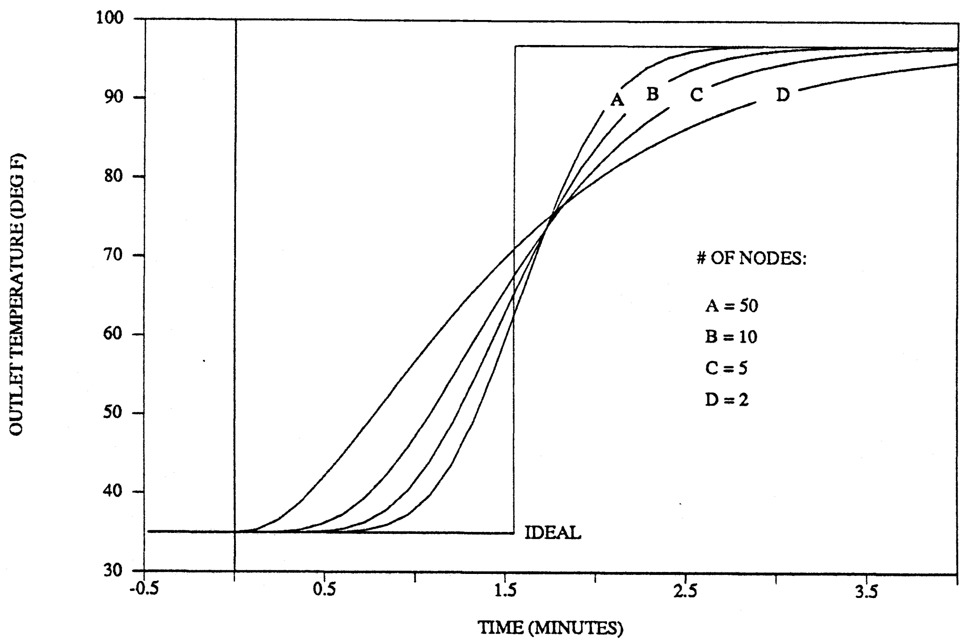

FIGURE 2.10 Collector response to a step change in inlet temperature for collectors modeled with various number of nodes. (timestep = 7.2 seconds)

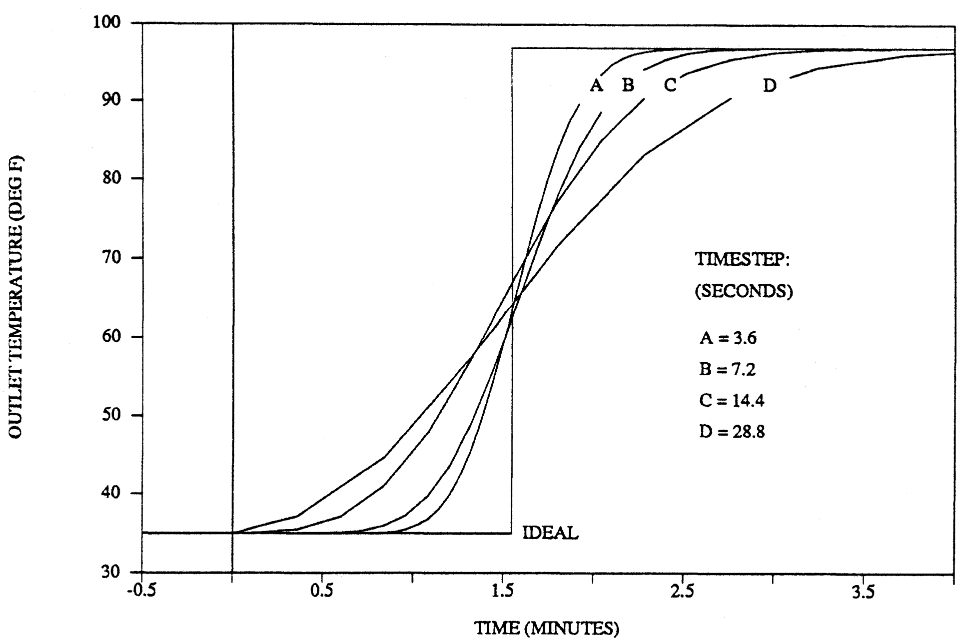

FIGURE 2.11 Collector response to a step change in inlet temperature for a 50 node collector and various timesteps.

collector in case D can be considered to transmit energy through the collector faster than the collector with the ideal step. This has two effects. The collector outlet temperature reacts sooner and it takes longer to reach steady-state. These effects can be important when modeling controls, but are normally insignificant when looking at the overall energy transfer. The amount of energy associated with each of the curves in figures 2.10 and 2.11 is close to identical. The response of a real collector to a step change in inlet was recorded by Goumaz (1981) and the form of the response is shown in figure 2.12.

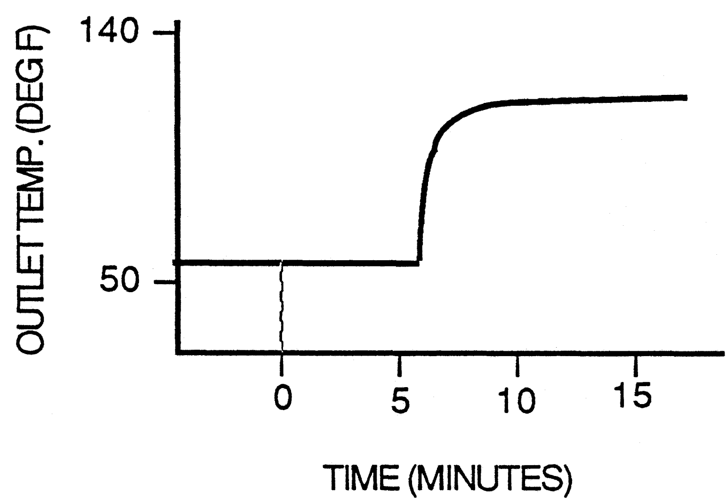

FIGURE 2.12 True collector response to a step change in inlet temperature.

As the thermal front reaches the exit of the real collector, the outlet temperature responds similar to the ideal step of figures 2.10 and 2.11. A sharp step does not occur because of fluid mixing and the heat transfer coefficient between the fluid and tubes is less than infinite in a real collector. Curves A through D of figures 2.10 and 2.11 have the same shape as the real collector curve as the response approaches steady-state. Therefore, choosing fewer nodes and larger timesteps than required to follow the step front, may actually give results closer to that of a real collector. In summary, decreasing the number of nodes and increasing the timestep size produce results different than the ideal step, but the results still account for the overall energy transfer.

Results for simulations of the Chinle system using collector models with and without capacitance, are shown in table 2.2. The simulation using the collector model accounting for thermal capacitance predicts about 1.5% less energy collected than the model neglecting capacitance.

MODEL	Qcol Btu x10^{-9}	Qsolar Btu x10^{-9}	Qaux Btu x10^{-9}	Qload Btu x10^{-9}	SF Percent
Col. capacitance	2.815	2.643	9.062	11.68	22.4
No col. capacitance	2.861	2.687	9.031	11.70	22.8

Q_{solar} = energy used for recirculation

TABLE 2.2 Annual thermal energy usage predicted with the Chinle model using collector models with and without accounting for thermal capacitance. (Chinle model with no freeze protection)

II.2.3 DRAINABLE COLLECTORS

In the previous section, a collector model accounting for capacitance was developed by modifying the zero capacitance model. In this section the capacitance model is modified in order to simulate drain-back solar energy systems. The same capacitance model from section II.2.2 is used, but with the added ability to drain and fill the collector.

The heat transfer involved in a filling or draining collector is difficult to handle analytically. A system of coupled partial differential equations need to be solved. The degree of complexity in modeling all of the dynamics is not warranted for normal use of TRNSYS. The approach taken is to simplify the modeling of the dynamics, but still account for the total energy transferred in the overall filling or draining process. This type of approach for TRNSYS is justified since the filling process takes only a few minutes, while weather data used for the simulations is typically on an hourly basis.

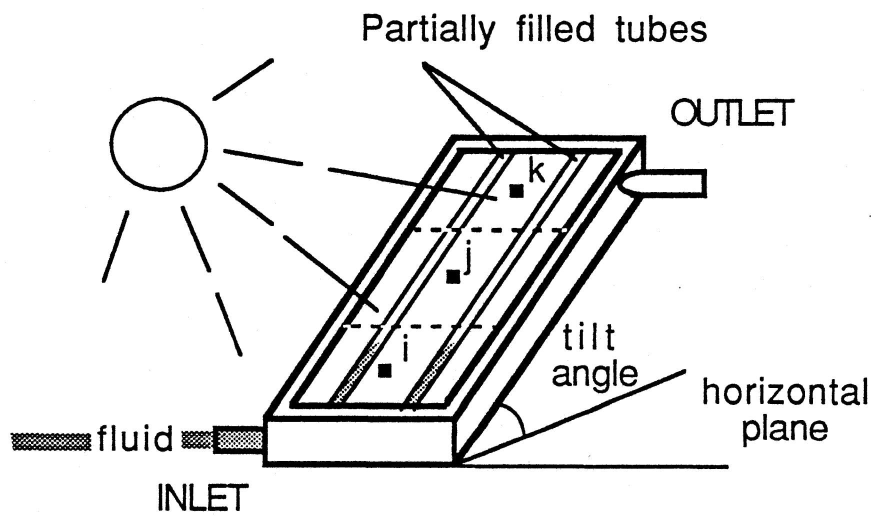

FIGURE 2.13 Typical collector filling with fluid.

The effect of filling or draining a collector is to change its overall thermal capacitance. The nodal model described in section II.2.2 is modified here to allow draining and filling the fluid. Collectors are normally mounted in an inclined position as shown in figure 2.13. The orientation of nodes in the collector model would mean that filling occurs in one node at a time. This can be modeled, but requires a complicated bookkeeping method to keep track of filled and partially filled nodes. An alternative is to divide the entering fluid equally amongst each node, as represented in figure 2.14 a and b. This would be the case if the collector in figure 2.13 is turned on its side and placed horizontally. This assumption simplifies the model as the capacitance is the same for each node and is calculated as:

$$C_n = CAP_{E,NF} + \frac{\dot{m}\ C_P\ \Delta t}{A_c} \tag{2.2.15}$$

For the draining case all the collector nodes are combined and a mixed temperature found.

$$T_{mix} = \sum_{i=1}^{n_{total}} \frac{V_i\, T_i}{V_c} \tag{2.2.16}$$

since

$$V_i = \frac{V_c}{n_{total}} \tag{2.2.17}$$

then

$$T_{mix} = \frac{1}{n_{total}} \sum_{i=1}^{n_{total}} T_i \tag{2.2.18}$$

where:

T_{mix} = collector temperature after mixing all of the nodes

V_i = fluid volume in one node

A representation of the draining case is shown in figure 2.14 c and d. All of the fluid draining from the collector is at the mixed temperature. In TRNSYS, mass is transferred from one component to another (*eg*: collector to storage tank) by passing flowrate information from one component to the next. In each component, the TRNSYS timestep is multiplied by the flowrate to determine the amount of fluid that transferred during that timestep. For the draining process, an assumption is made that all of the fluid is drained

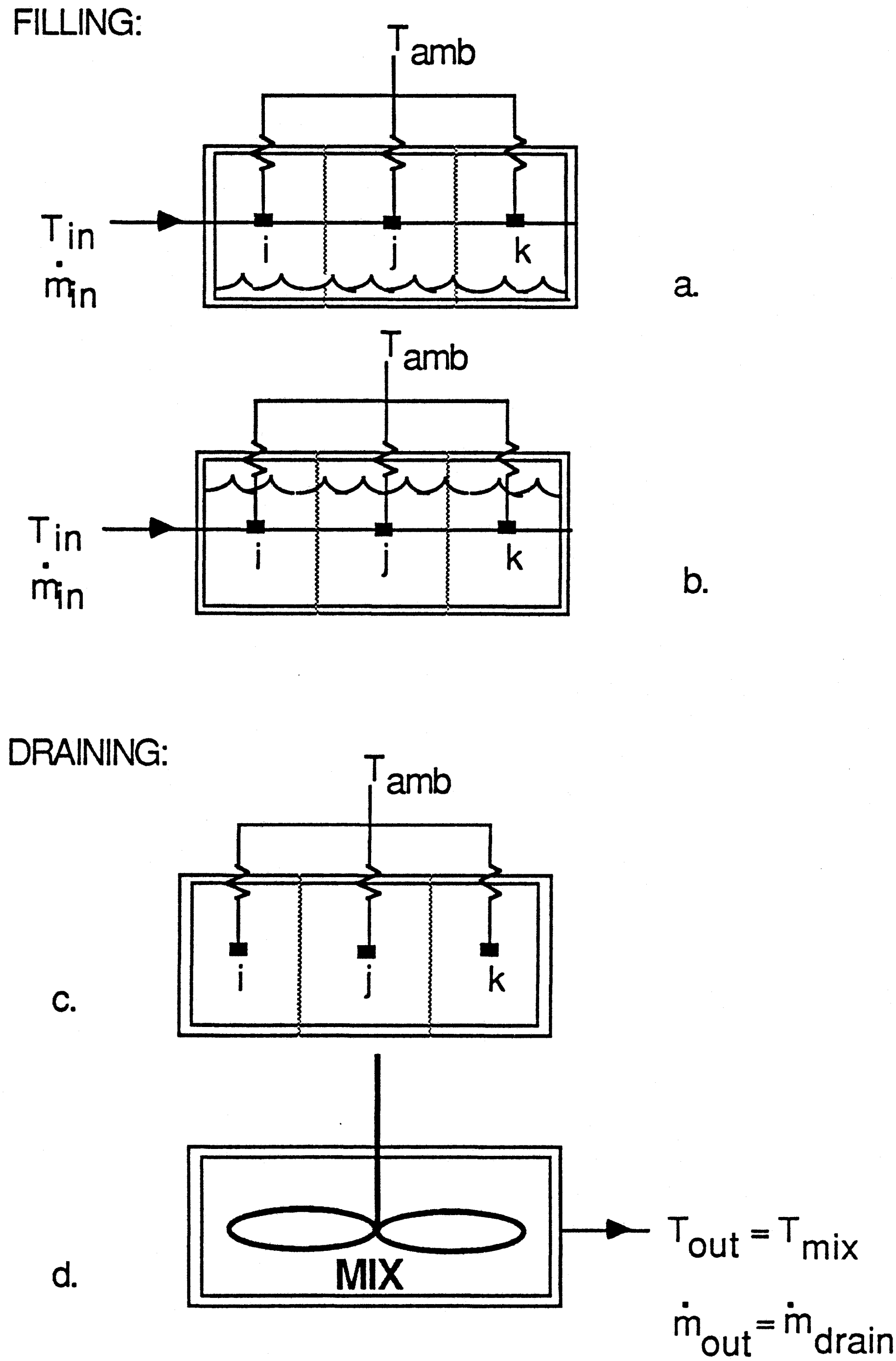

FIGURE 2.14 Schematic of filling (a & b) and draining (c & d) collector models. (Top view looking through glazing.) Note that the fluid shown in a & b would actually be inside collector tubes.

in one timestep. The flowrate during the timestep is determined as:

$$\dot{m}_{drain} = \frac{m_{cf}}{\Delta t} \tag{2.2.19}$$

where:

$\dot{m}_{drain}$ = the fluid flowrate used in TRNSYS during a draining process

m_{cf} = mass of fluid in the collector before draining

This drain flowrate is used instead of the actual rate for compatabillity with existing TRNSYS components.

In both the draining and filling case, assumptions have been made that do not represent the true dynamics of a collector. It was noted before that the filling and draining process happens in only a matter of minutes. Filling and draining normally occur during times of low solar radiation, so that incorrectly modeling the dynamics, results in an insignificant error in accounting for the energy .

CHAPTER III: THE CHINLE SYSTEM USING DRAIN-BACK FREEZE PROTECTION

This chapter describes both the actual Chinle solar energy system and the TRNSYS model used to simulate it. Annual energy performance predictions from the TRNSYS model are also presented. The last section discusses the various control strategies for drain-back freeze protection and presents results showing their effect on annual performance.

III.1 THE CHINLE SYSTEM

As part of the Solar In Federal Buildings program, a solar energy system was installed at the Indian Health Facility in Chinle, Arizona. Liquid flat plate collectors provide part of the space heating (SPH) and domestic hot water (DHW) requirements. The system was designed so that it could be operated as a drain-back system using water in the collector loop or a dual fluid system with a water / glycol mixture in the collector loop. The system is presently operated in the drain-back mode. A system schematic is shown in figure 3.1 and the various loops of the system are described in the following paragraphs.

The collector loop consists of 320 collectors with a total gross area of 10112 ft^2. The main inlet and outlet manifolds to the collector field are 4 inch pipes approximately 575 feet long, buried over 3 feet underground. A heat exchanger separates the fluids of the collector and storage loops. A 1500 gallon drain-back tank can store all of the collector loop fluid when the system is drained. Two 160 gpm pumps are connected in parallel and operate individually or simultaneously, depending on temperatures in the system.

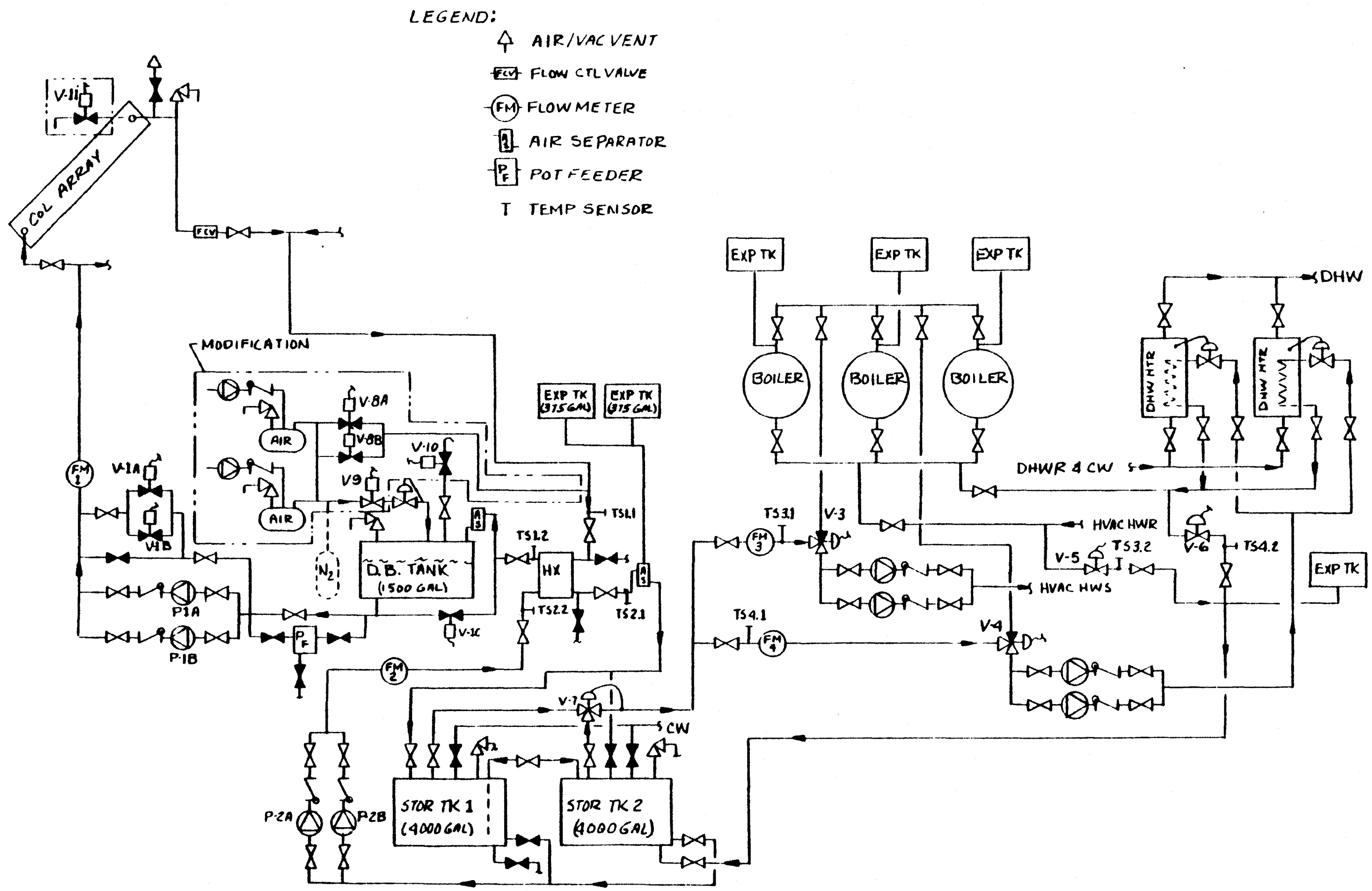

FIGURE 3.1 Schematic of the solar energy system on the Indian Health Facility in Chinle, Arizona.

Energy from the collector loop is transferred through the heat exchanger into the storage loop. Fluid is pumped from the storage side of the heat exchanger into two 4000 gallon storage tanks, connected in series. Two pumps, connected in parallel, move the fluid around the storage loop. Only one of the 281 gpm pumps is operated at any one time. Energy is transferred from the storage tanks to the load loops through a mixing valve (V-7 in fig. 3.1), which can supply fluid from either or both tanks.

The closed loop between the main storage tanks and the DHW storage tanks ("DHW HTR" in fig. 3.1) is considered the DHW loop. Two pumps, connected in parallel, move water from the main storage tanks through heating coils inside the DHW tanks and back to tank #2. Cold mains water is heated in the DHW tanks before being supplied to the load. There were no specifications available for the DHW loop equipment.

The closed loop between the main storage tanks and the water to air heat exchanger (not shown in figure 3.1) form the space heating loop. Two pumps circulate water through the heat exchanger and back to collector storage tank #2. There were no specifications available for the SPH loop equipment.

Auxiliary energy is supplied by three parallel connected water boilers. Both the DHW and SPH loops are connected so that energy can be supplied from either the auxiliary boilers or the collector storage tanks, but not both at once. For solar energy to be supplied to the DHW load, three-way valve V-3 in figure 3.1 is switched to connect the collector storage to the DHW pump inlet, and valve V-6 is opened to allow return fluid to the main storage tanks. For auxiliary energy to be supplied to the SPH loop, valve V-4 in figure 3.1 is switched to connect the auxiliary boilers to the SPH pump inlet, and valve V-5 is closed to force return fluid to the auxiliary boilers. All of the valves just mentioned are connected to a programmable controller.

Table 3.1 summarizes the major control functions for this system. The storage to load mixing valve (V-7 in fig. 3.1) is intended to keep the temperature in storage tank #2 as low as practical. Since storage tank #2 supplies the fluid to the heat exchanger of the collector loop, minimizing its temperature will maximize collector performance. A graphical representation of the mixing valve control strategy is given in figure 3.2.

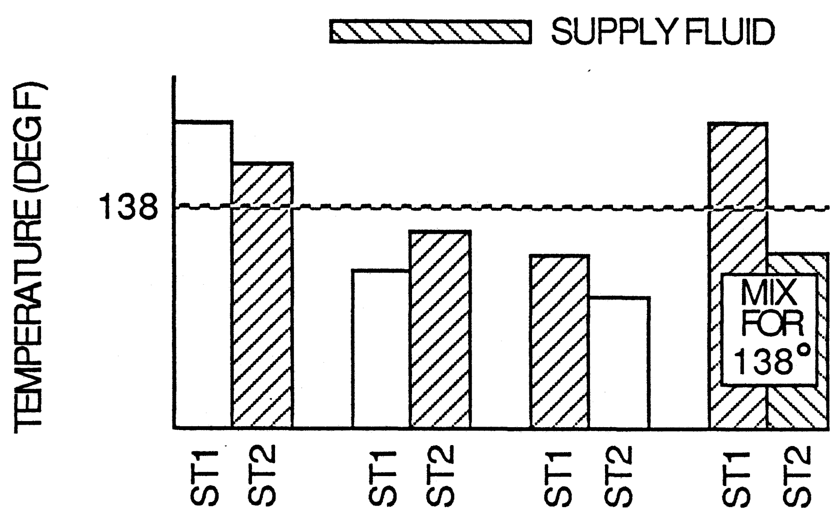

FIGURE 3.2 Mixing valve (V-7) control strategy.

III.2 TRNSYS MODEL OF THE CHINLE SYSTEM

In the previous section a brief description was given for the solar energy system on the Chinle Health Facility. The TRNSYS program (TRNSYS, 1983) was used to model this system and provide yearly simulations to determine the effects of various freeze protection methods. Several versions of the model (called "decks") using TRNSYS were generated. The initial decks were intended to model as much of the system dynamics as possible, while using standard TRNSYS components or making only minor

CODE:

T_c = collector plate temperature
T_{st1} = storage tank #1 temperature
T_{chx} = temperature of collector side inlet to the collector/storage heat exchanger
P_{c1} = collector loop lead pump
P_{c2} = collector loop lag pump
P_{st} = collector storage loop pump
P_{dhw} = domestic hot water loop pump
P_{sph} = space heating loop pump

DESCRIPTION	PUMP P_{c1}	PUMP P_{c2}
Collector Loop:		
1. System shut down	off	off
2. (T_c - T_{st1}) > 10 °F and P_{c1} off time > 14 minutes	on	on
3. For the next 14 minutes (minimum)	on	on
4. (T_{chx} - T_{st1}) < 2 °F	on	off
5. For the next 14 minutes (minimum)	on	off
6. (T_{chx} - T_{st1}) > 5 °F and P_{c2} off time > 14 minutes	on	on
7. For the next 14 minutes (minimum) **	on	on
8. (T_c - T_{st1}) < 2 °F	off	off
9. For the next 14 minutes (minimum)	off	off
10. T_{st1} > 220 °F or T_c < 45 °F	drain-back	

** note: control code #5 and #7 can be overriden by control #8

Storage Loop:	P_{st}
11. (T_{chx} - T_{st1}) > 3 °F and P_{c1} on	on
12. (T_{chx} - T_{st1}) < 2 °F or P_{c1} off	off

Space Heating Loop:	P_{sph}	Energy Supply
13. If no heating demand	off	-
14. If heating demand and T_{st1} > 125 °F	on	Solar
15. If heating demand and T_{st1} < 125 °F	on	Aux

Domestic Hot Water Loop:	P_{dhw}	Energy Supply
16. T_{st1} > 128 °F	on	Solar
17. T_{dhw} < 120 °F	on	Aux
18. T_{st1} < 128 °F and T_{dhw} > 130 °F	off	-

TABLE 3.1 Major control functions for the Chinle solar energy system.

alterations to existing components. It was hoped that this would save time and provide a test of the versatility of the existing TRNSYS program. This section describes the TRNSYS model for the present Chinle system, which uses drain-back freeze protection.

Figures 3.3 through 3.6 are schematics of the various Chinle system loops and the components used for the TRNSYS model. Lines connecting the components are not pipes, but information paths within the TRNSYS model. The "TY" or type numbers represent existing TRNSYS components, except for the TY numbers in quotes, which are components that were written for the Chinle model.

The collector loop is shown in figure 3.3. The collector was modeled as a multi-node lumped capacitance collector (TY "43") as described in chapter 2. A control signal, γ, is shown as an input to the collector and is used to signal when drain-back occurs. The collector inlet and outlet pipes were modeled with the fully mixed drainable pipe model including wall thermal capacitance (TY "36") as described in chapter 2. The pipes include an added length to account for the fluid volume of all the interconnecting collector array piping. In the Chinle system the major outdoor pipes are buried underground and are therefore exposed to an environment temperature different than the ambient air temperature. A constant temperature of 50 °F was used year round as the pipe's environment temperature. The control signal γ is also an input to the pipes to indicate drain-back conditions. A secondary set of lines (light lines) are shown in figure 3.3 from the collector, inlet pipe, and outlet pipe, which lead back to the drain-back tank. These are information paths needed in TRNSYS to account for the mass flows during a drain-back. A controller component (TY "45") was written to model the actual programable controller in the Chinle system. Control signals are generated to run the collector pumps, storage loop pump, and to initiate drain-back. The variable volume tank component (TY 39) models the drain-back tank as fully mixed and allows the fluid

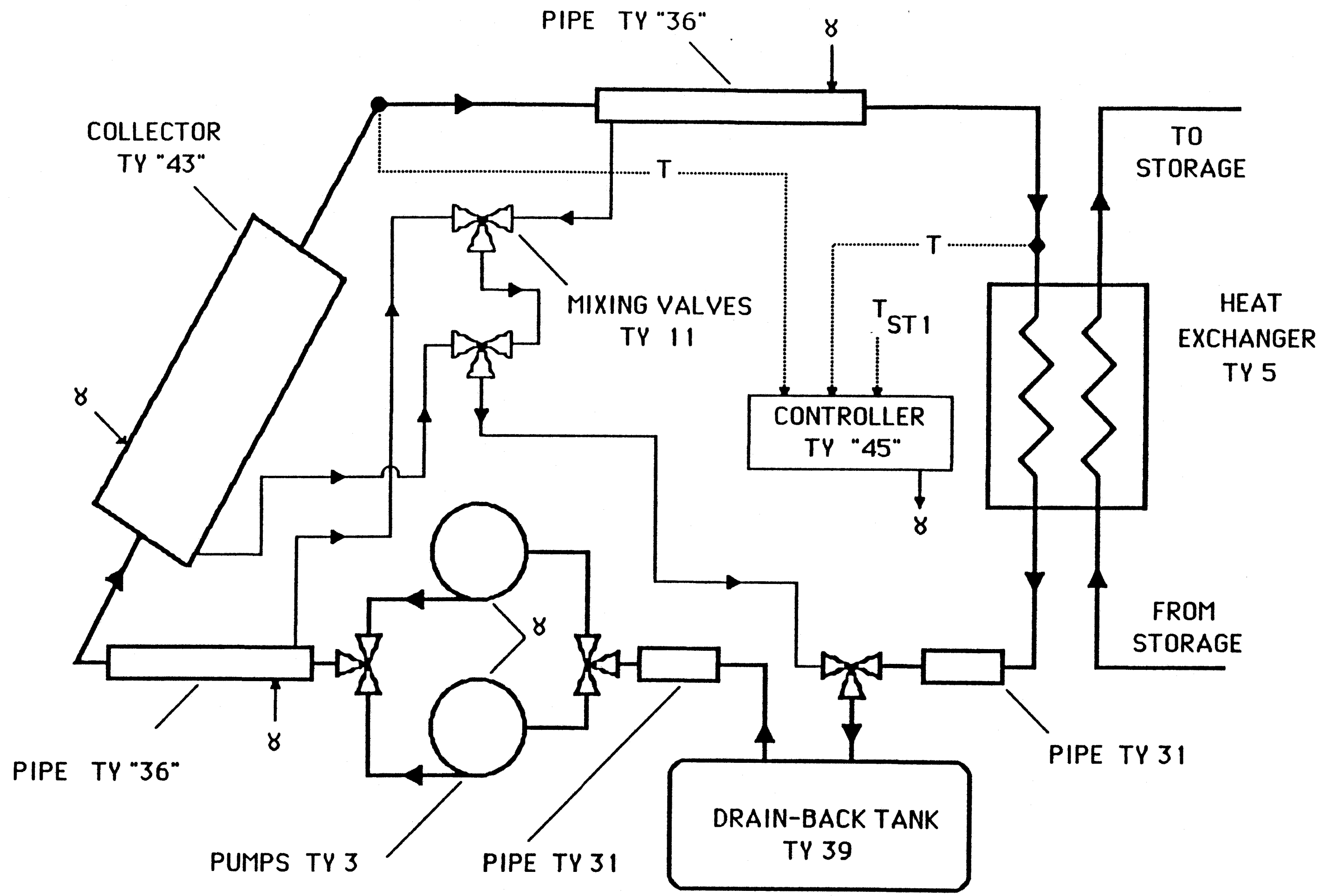

FIGURE 3.3 Chinle collector loop TRNSYS model. Lines between components represent information flow paths and not actual system piping.

volume to change during drain-back. Standard TRNSYS components were used to model the rest of the system as shown.

Figure 3.4 shows the Chinle storage loop and the components used in the TRNSYS model. This system uses all standard TRNSYS components except for the mixing valve (TY "49"). The control strategy for this valve was described in section III.1. The total mass flowrate required for the DHW and SPH loops is an input to this valve and it calculates the mass flowrate required from each storage tank. The storage tanks are modeled as fully mixed (TY 4 with 1 node) because the flow rates are very high in this system, which means the tanks will not be thermally stratified. The type 2 controller is used with a control signal, γ, input from the collector loop controller, so that the storage loop pump can run only if one of the collector loop pumps is running. The storage loop pump has two control signals, one from the storage loop controller for normal operation, and one from the collector loop controller used for recirculation freeze protection. Recirculation freeze protection is not used in the present Chinle system, but will be examined in chapter IV. None of the actual system piping in the storage loop are modeled in this deck. These pipes are short and well insulated and would have a negligible effect on system performance.

Figure 3.5 shows the DHW system and the components used in the TRNSYS model. All of the components are standard TRNSYS types. The type 11 flow diverters (V-4 and V-6) along with the controller determine if the DHW tanks are supplied by solar energy from the storage tanks or auxiliary energy from the boilers. Energy is supplied to the DHW storage tanks through external heat exchangers. In the actual Chinle system the energy is supplied through in-tank heat exchanger coils. There is presently noTRNSYS tank model that includes an internal heat exchanger coil. An internal heat exchanger coil can be modeled by using external heat exchangers with a constant mass

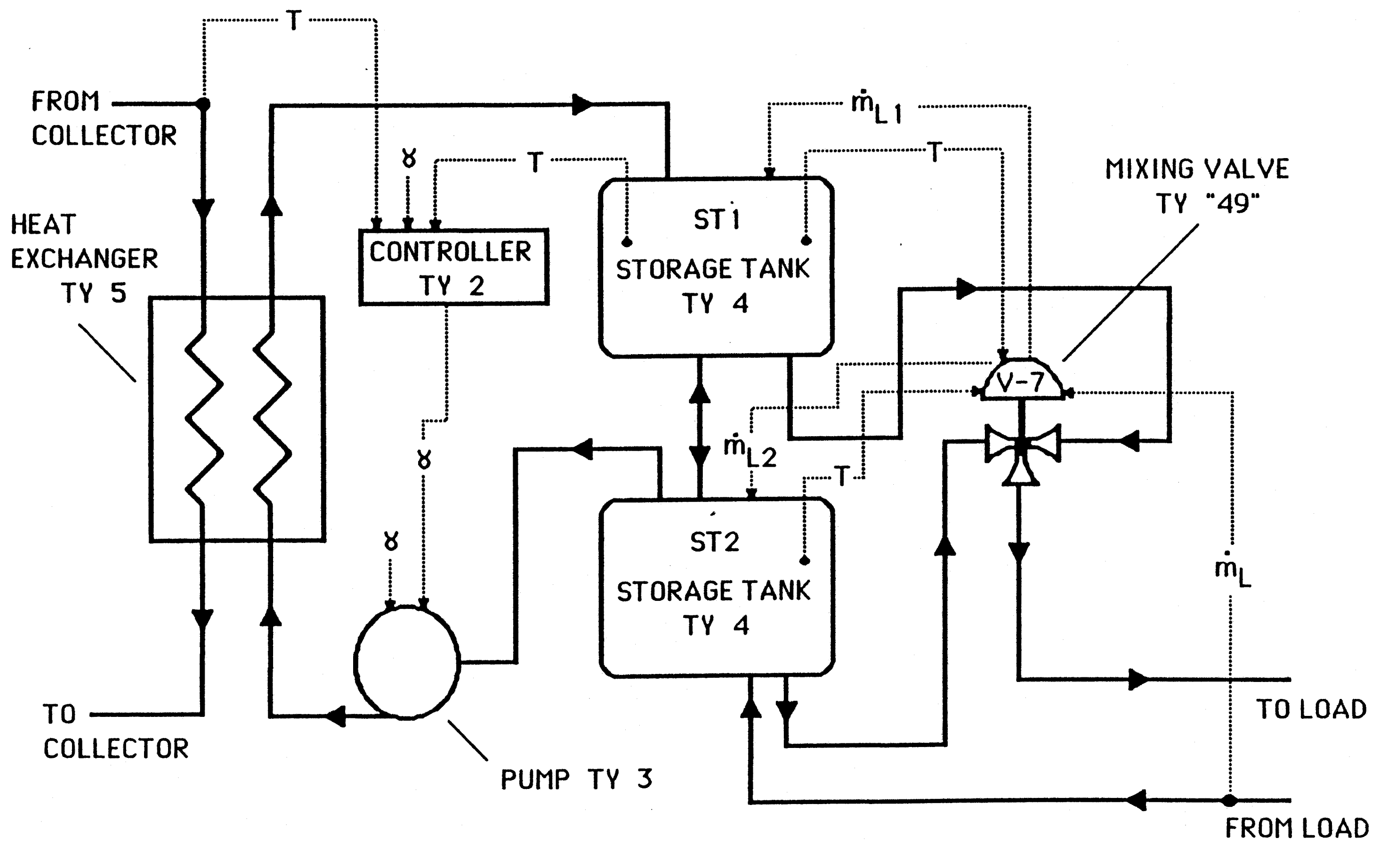

FIGURE 3.4 Chinle storage loop TRNSYS model. Lines between components represent information flow paths and not actual system piping.

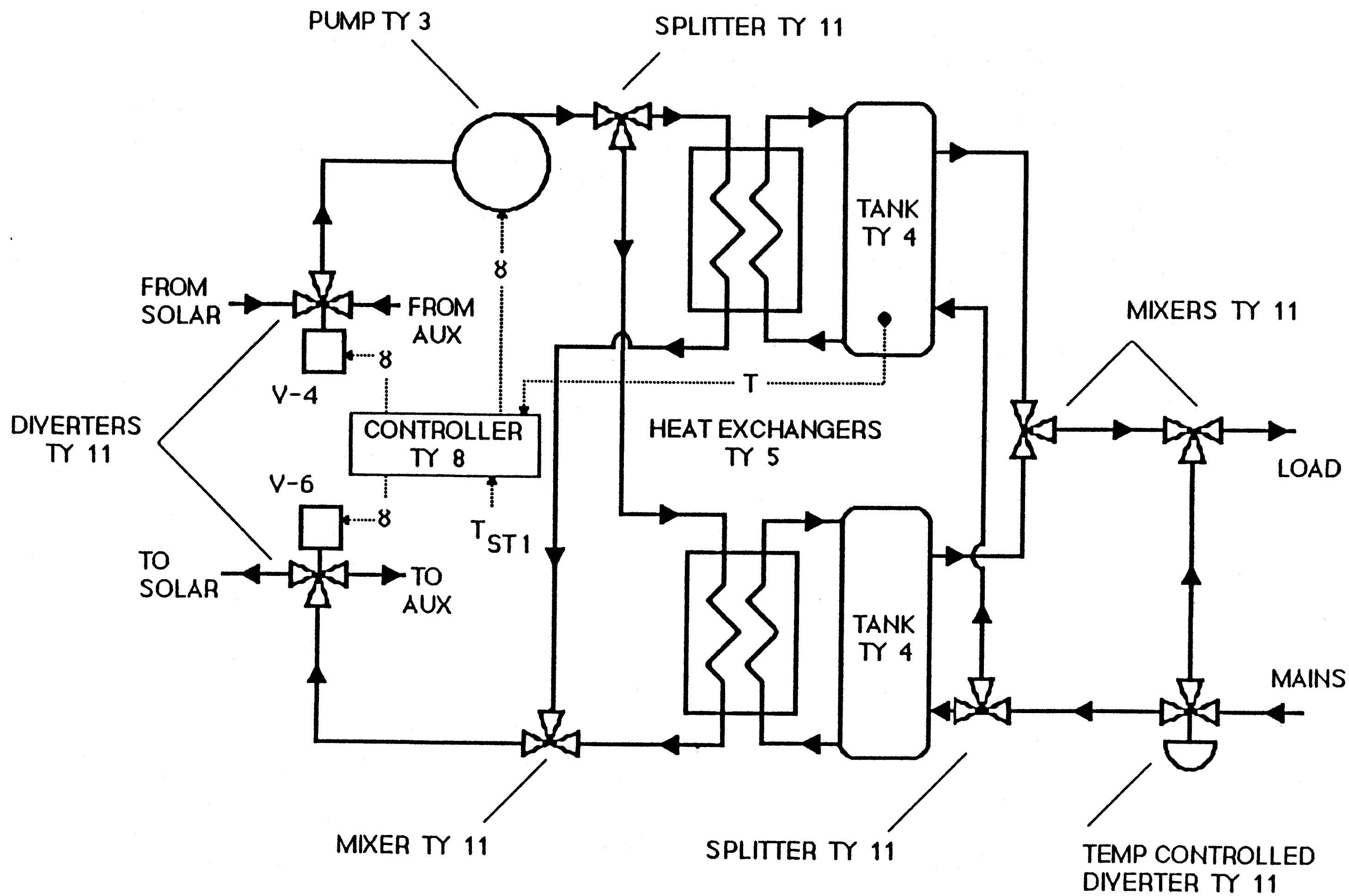

FIGURE 3.5 Chinle DHW loop TRNSYS model. Lines between components represent information flow paths and not actual system piping.

flow through the tank side of the heat exchanger. If the mass flow on the storage side is chosen so that its capacitance rate ($\dot{m}\,C_p$) is always higher than on the supply side of the heat exchanger, the effectiveness will be defined as:

$$\varepsilon = \frac{T_{h,i} - T_{h,o}}{T_{h,i} - T_t} \tag{3.2.1}$$

where:

$T_{h,i}$ = temperature of hot fluid (from solar storage or aux.) entering heat exchanger

$T_{h,o}$ = temperature of hot fluid at the outlet of the heat exchanger

T_t = average tank temperature

This is the same effectiveness used by Klett, *et al,* (1984) to evaluate submerged coil heat exchangers. The DHW storage tanks are modeled as fully mixed (TY 4 with 1 node). The temperature controlled diverter (TY 11) is used to mix the storage fluid to provide a constant temperature supply to the load. Since the actual load is not known, the load is specified as constant throughout the day (24 hrs.). Simulations made with various load profiles show an insignificant effect on yearly performance due to the small size of the DHW load relative to the SPH load. Since the actual Chinle DHW system equipment specifications are unknown, assumed values are chosen as shown in table 3.2.

Figure 3.6 shows the SPH and auxiliary boiler loops and the components used in the TRNSYS model. The Type 11 flow diverters along with the controller determine if the load is supplied by solar energy from the solar storage or auxiliary energy from theboilers. The type 12 space heating component determines the load by using an overall UA value for the building and the temperature difference between the inside of the

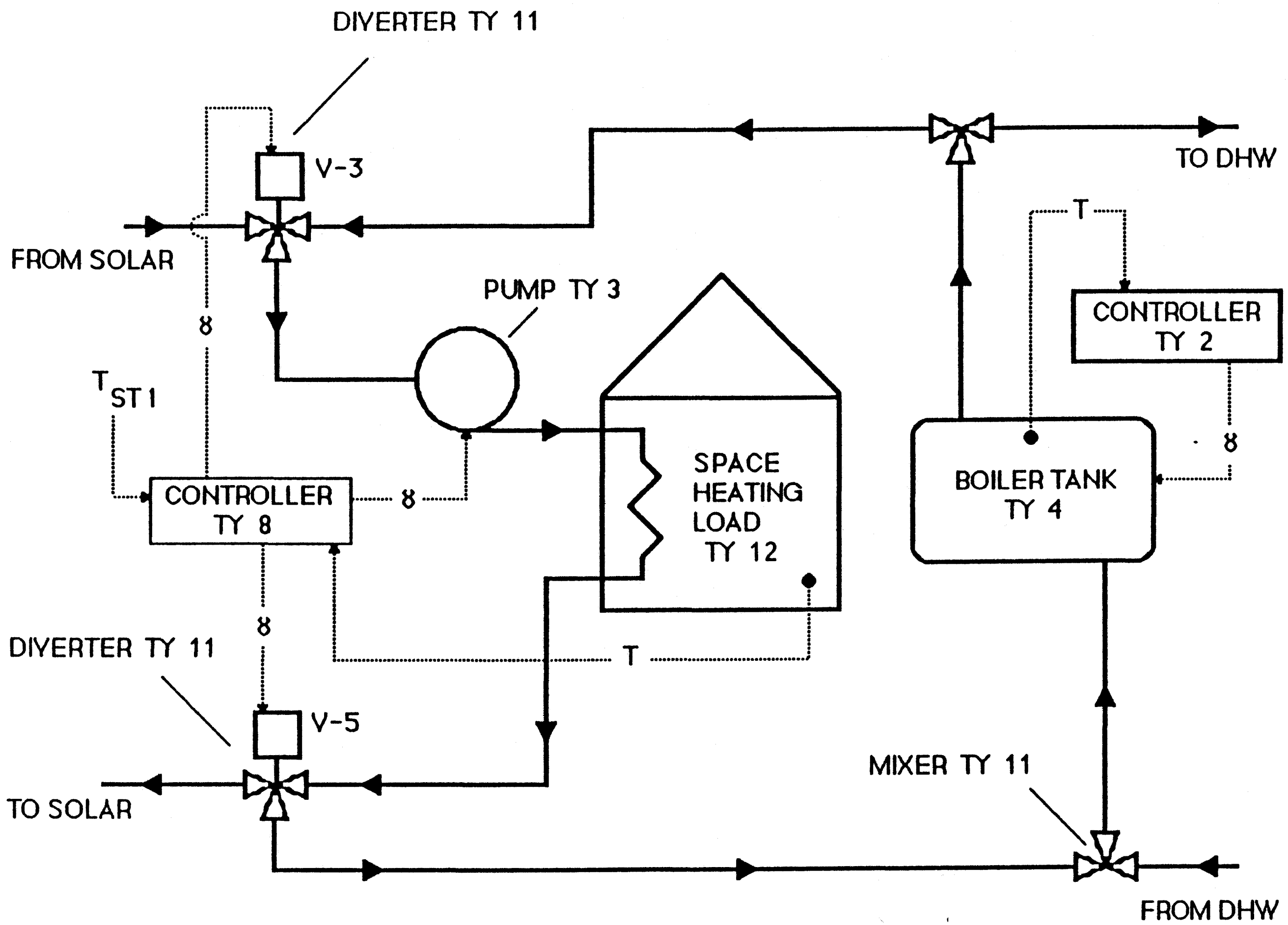

FIGURE 3.6 Chinle SPH and auxiliary loop TRNSYS model. Lines between components represent information flow paths and not actual system piping.

building and the ambient. Energy is input to the building through a water to air heat exchanger. The three auxiliary boilers are modeled as one fully mixed tank (TY 4 with 1 node), with an internal heater, as shown in figure 3.6. An external controller (TY 2) is used to control the heater. Equipment specifications for the Chinle system SPH and auxiliary loops were not available, so assumed values are used. The UA and capacitance of the building were determined by a trial and error method so that the simulated space heating load is approximately equal to the expected load as indicated by Schmidt (1985). The system parameters used are shown in table 3.2.

In order to run simulations, solar radiation and ambient temperature weather data must be provided. Typical Mean Year (TMY) data on an hourly basis for Albuquerque, New Mexico was used for the Chinle simulations. Albuquerque is located at a latitude of 35.05 degrees and has a total of 2385 degree days, compared to Chinle at a latitude of 36.2 degrees and 2948 degree days. The radiation processor (TY 16 mode 3) using Erbs (1980) correlation is used to process total hourly radiation on a horizontal surface from the TMY data, into total radiation on the tilted surface needed for the collector component model.

By choosing TRNSYS components and specifying parameters, many assumptions are being implied. The following list contains some of the assumptions used in he TRNSYS model of the Chinle system.

1. Constant collector performance parameters: $F'U_L$, $F'(\tau\alpha)$; the effect of wind and night time collector to sky radiation are neglected.
2. Linear collector efficiency based on ASHRAE collector tests.
3. Fully mixed collector inlet and outlet pipes, with an equivalent pipe length added to account for pipe metal capacitance.
4. Constant environment temperature (50 °F) throughout the year for

COLLECTOR:

Fluid: water
Gross collector area = 10112 ft^2
GTEST (flowrate / area; during performance tests) = 12.672 lbm / hr - ft^2
$F_R U_L$ = .750 Btu / hr - °F
$F_R (\tau\alpha)_n$ = .769
Incidence angle modifier (b_o) = .1
CAP_E = .410 Btu / ft^2 - °F
Total collector array fluid mass = 3171 lbm
Number of nodes: 10

COLLECTOR INLET AND OUTLET PIPES:

Length = 706 ft
Inside circumference = 1.054 ft
Inside cross-sectional area = .0884 ft^2
Inside diameter = .3355 ft (4" nominal pipe size)
U = .113 Btu / ft^2 - °F
Volume = 79.78 ft^3 (includes 17.355 ft^3 to account for pipe metal capacitance)
Environment temperature = 50 °F

COLLECTOR/STORAGE HEAT EXCHANGER: **

Constant effectiveness: ε = .6

COLLECTOR SIDE HX OUTLET PIPE AND COLLECTOR PUMP INLET PIPE: **

Length = 10 ft
Inside diameter = .3355 ft (4" nominal pipe size)
U = .113 Btu / ft^2 - °F
Environment temperature = 60 °F

DRAIN - BACK TANK:

Volume = 200.5 ft^3
Inside circumference = 15.71 ft
Inside cross-sectional area = 19.63 ft^2
U = .04 Btu / ft^2 - °F

COLLECTOR PUMPS:

Flowrate (each pump) = 80085 lbm / hr (160 gpm)

STORAGE LOOP PUMP:

Flowrate = 140650 lbm / hr (281 gpm)

COLLECTOR LOOP STORAGE TANKS (2):

EACH TANK:

Volume = 534.76 ft^3 (4000 gallons)
U = .04 Btu / ft^2 - °F
Environment temperature = 60 °F

Continued on next page.

TABLE 3.2 Chinle system model parameters and specifications.

Continued

SPH CONTROLLER: **
Room set temperature = 70 °F
Auxiliary heating if room temperature < 65 °F
Control temperature deadbands = 3 °F

SPH LOOP PUMP: **
Flowrate = 50000 lbm / hr

SPH LOAD: **
UA = 81225 Btu / hr - °F
CAP = 450000 Btu / °F
εC_{min} = 45000 Btu / hr - °F

DHW STORAGE TANKS (2): **
EACH TANK:
Volume = 66.8 ft^3 (468 gallons)
Height = 9.45 ft
U = .04 Btu / hr - ft^2 - °F
Heat exchanger effectiveness = .6

DHW CONTROL: **
Water supplied to load temperature = 120 °F
Auxiliary heating if tank temperature < 117 °F

DHW LOOP PUMP: **
Flowrate = 15000 lbm / hr

DHW LOAD: **
Load draw = 1753 lbm / hr (continuous)
City mains temperature = 46 °F

TRNSYS SIMULATION PARAMETERS:
Timestep = .03125 hr
Tolerances = -.001
Maximum iterations in one timestep = 100

** note: These values are assumed as no specifications were available for the Chinle system.

TABLE 3.2 Chinle system model parameters and specifications.

the collector pipes.

5. Collector loop drain-back in one TRNSYS timestep.
6. Ignore pipes in collector storage, DHW, SPH, and auxiliary loops.
7. Constant effectiveness heat exchangers, with no capacitance.
8. Fully mixed storage tanks.
9. Constant loss coefficients and environment temperature (60 °F) for all equipment located indoors.
10. Constant DHW load.
11. Single lumped capacitance and constant UA for the building load.
12. No solar or internal gains in the building load.
13. Pumping energy was not included in calculating energy loads and solar fractions.

III.3 DRAIN-BACK SYSTEMS AND SIMULATION RESULTS

The solar energy system at the Indian Health Facility in Chinle, Arizona was designed to incorporate either drain-back or dual fluid freeze protection. This section looks at the control strategies and thermal energy requirements of drain-back freeze protection, and presents simulation results using the TRNSYS model described in section III.2.

In a drain-back system the collector plate or fluid temperature is monitored and drain-back initiated if freezing conditions are approached. The fluid is drained from the collectors and collector loop piping into a storage tank. This not only prevents freezing, but reduces the heat losses from the collector loop by storing the warm fluid in a well insulated storage tank. The collector loop is refilled when the collector can provide useful energy. An alternate control strategy for drain-back consists of draining the collectors anytime that the collector pumps stop. This means that anytime useful energy cannot be collected, the fluid will be drained.

Table 3.3 summarizes the TRNSYS model results for the present Chinle system. This system drains the collector loop when the collector plate reaches 45 °F.

	$\underline{\text{Btu x}10^{-9}}$
A. Solar radiation incident on collector surface	7.159
B. Collected energy	2.788
Collector efficiency (A / B) .... 38.9 percent	
C. Solar energy delivered to load	2.628
D. Collector loop losses (pipes and drn-bck tank only).	0.136
Fraction of collected energy........... 4.8 percent	
E. DHW load..	1.132
F. SPH load..	10.560
G. Total load (E+F)......................................	11.690
H. Auxiliary energy	9.084
I. Total system losses.....................................	0.180
Fraction of total load.................. 1.5 percent	
J. Solar fraction (1 - H / G) .... 22.30 percent	

TABLE 3.3 Annual thermal energy usage predicted with the Chinle model using drain-back freeze protection.

The control parameter for drain-back is the drain temperature. By increasing this temperature, the collector loop fluid is removed at a higher temperature, which will reduce the heat losses. Figure 3.7 shows the effect, on the pipe and drain-back tank losses, of raising the drain temperature of the Chinle system. Losses are decreased 12% by draining at 75 °F versus 45 °F. However, the increased losses of the lower drain temperature systems are partially made up by better performance during start-up. The system that drains at a lower temperature will store cooler fluid and thus increase collector efficiency during morning start-up. Raising the drain temperature also increases the annual number of drain-backs as shown in figure 3.8. Increasing the

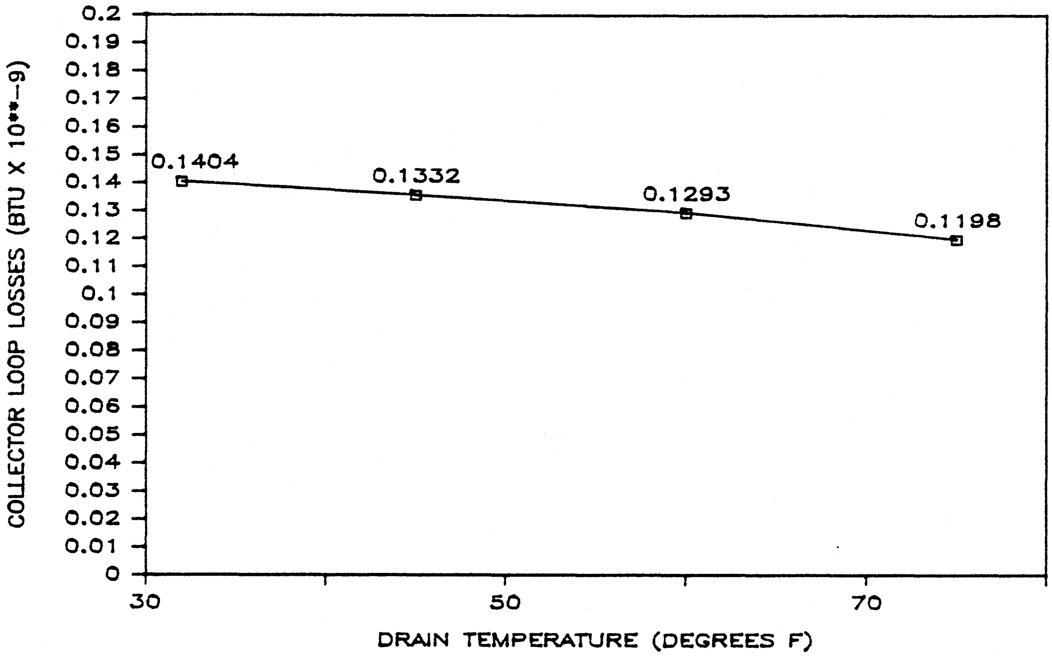

FIGURE 3.7 Annual collector loop heat losses versus drain temperature, as predicted with the Chinle model.

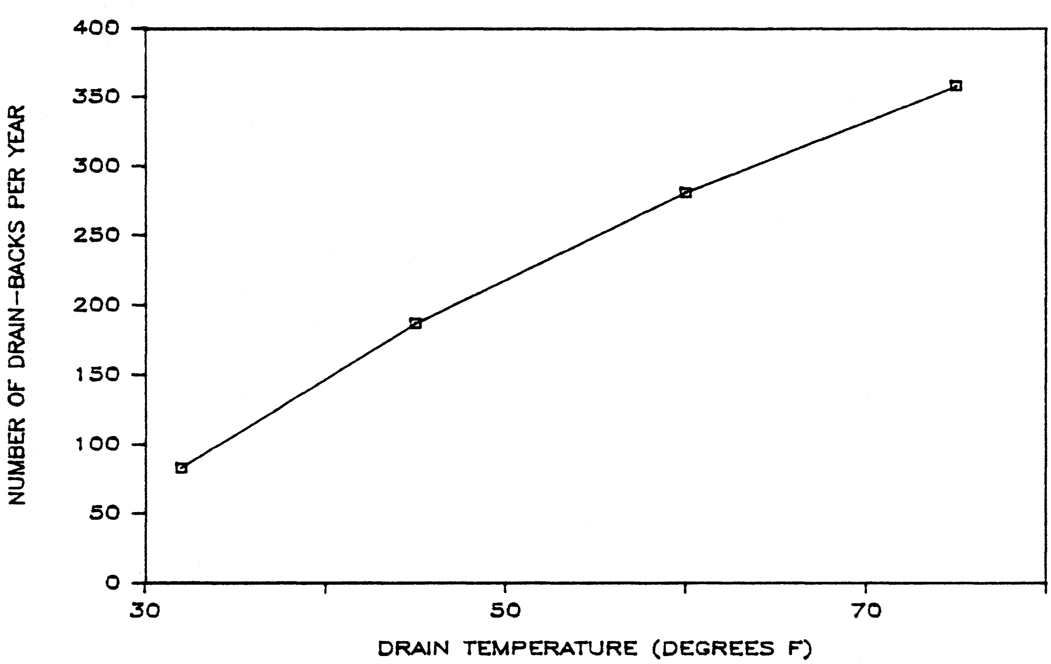

FIGURE 3.8 Annual number of drain-backs versus drain temperature, as predicted with the Chinle model.

number of drain-backs has negative affects such as increased pumping energy required to refill the collector loop and corrosion problems inside the empty collectors and pipes. (Heinemann, 1981)

Figure 3.9 shows that the effect of raising the drain temperature on system performance is insignificant. The solar fraction is approximately the same for all cases, at 22.3 percent. Figure 3.9 illustrates the relative magnitude of the energies involved. The energy saved by increasing the drain temperature is insignificant compared to the total energy collected. 10% of the collector loop pipe and drain-back tank losses represents only 0.2 % of the collected energy in the Chinle system.

In the Chinle system, drain-back is accomplished by opening a vent valve at the highest point of the collector array and letting gravity drain the fluid into the drain-back tank. This is known as "siphon return" drain-back. Another form of drain-back, called "open return", uses an oversized pipe from the collector outlet so that an air passage always exists between the collector and drain-back tank. Anytime the collector pump stops, fluid drains by gravity from the collectors and is replaced by air from the drain-back tank. The "open return" strategy could be incorporated in the Chinle system by programming the controller to drain the collectors anytime that the collector pump stops. The same TRNSYS model used for analyzing the effect of drain temperature was used to predict the performance of the "open return" strategy, except for the controller, which was modified to drain the collector loop anytime that the collector pumps stop. TRNSYS results for the Chinle system using both control strategies are shown in table 3.4. The "open return" strategy shows an increase in annual performance and has 21% less annual collector loop losses than the siphon return system.

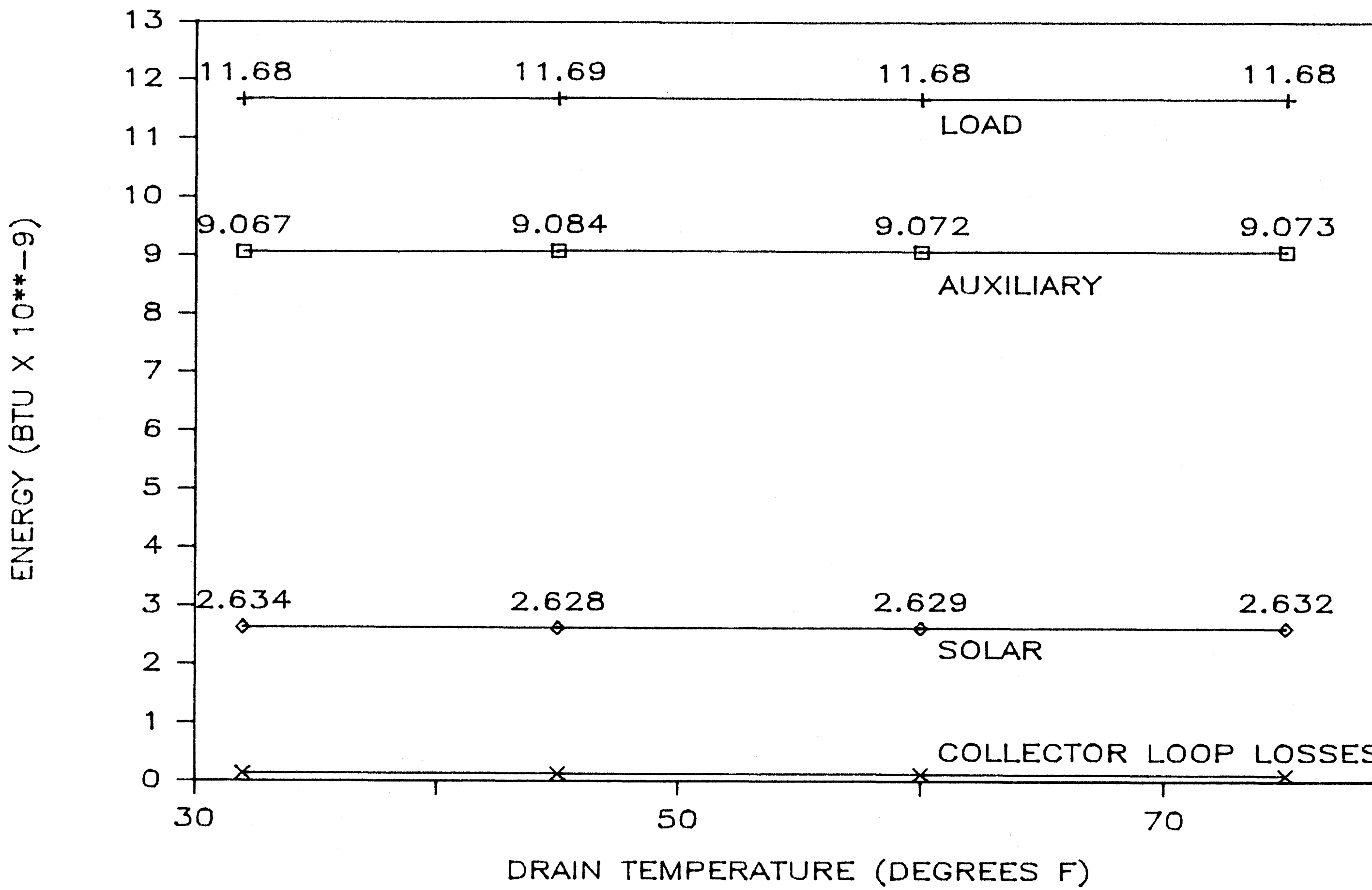

FIGURE 3.9 Annual energy usage versus the drain temperature, as predicted with the Chinle model.

CONTROL STRATEGY	Q_{col} Btu x10^{-9}	Q_{solar} Btu x10^{-9}	Q_{env} Btu x10^{-9}	Q_{aux} Btu x10^{-9}	Q_{load} Btu x10^{-9}	SF Percent
Drain at 45 °	2.788	2.628	.136	9.084	11.69	22.30
"Open return"	2.814	2.679	.110	9.025	11.68	22.75

TABLE 3.4 Annual thermal usage predicted with the Chinle model using two different drain-back control strategies.

Modeling drain-back systems required the development of drainable collectors and pipe components for TRNSYS as discussed in chapter II. It also required several standard TRNSYS components to account for the mass transfer when draining and filling the collector loop as discussed in section III.2. In this section it was shown that drain-back control strategy has a marginal effect on annual performance. In order to evaluate modeling requirements, a simulation of the Chinle system was made using the standard zero capacitance collector (type 1), with no freeze protection. The solar fraction for this model was 22.79%. This compares favorably with the predicted performance of the drain-back system using the "open return" control strategy (solar fraction = 22.75%). Before concluding that drain-back freeze protection has such a small effect on annual performance that it doesn't have to be modeled, further simulations should be made for other systems and other climates.

CHAPTER IV: RECIRCULATION FREEZE PROTECTION

In this section the thermal requirements of recirculation freeze protection applied to the Chinle system will be presented. Virtually no information was found on the design of recirculation systems, therefore several options were studied. Recirculation combines advantages of both drain-back and dual fluid systems. Like drain-back, it uses only water in the collector loop, thus eliminating the expense and thermal penalties of a water-glycol fluid. Like the dual fluid system, the collector loop is always filled, eliminating the extensive valving required for drain-back. The draw-back of recirculation freeze protection is that thermal energy is required to prevent freezing. The energy requirements of recirculation make this mode of freeze protection unattractive for severe climates.

IV.1 THE RECIRCULATION CYCLE

In a recirculation system, the collector temperature is monitored to determine the approach of freezing conditions. When the collector reaches a minimum set temperature, the collector loop pump or a secondary pump is turned on to recirculate warm fluid through the collector loop. Once the collector loop is warmed to a set temperature, the pump is turned off. The energy required to warm the collector loop can be supplied by solar or auxiliary sources. Warm fluid can be drawn directly from the collector storage tank or indirectly from the tank through a collector to storage heat exchanger. Auxiliary heaters can be placed in-line to the collector loop, in-line to the storage loop, or inside the collector storage tanks to provide the energy needed for the recirculating fluid. Systems using solar energy from the collector storage tanks must have back-ups in case there is not enough energy in the tanks to keep the collectors from freezing. This back-up can be auxiliary heaters or a secondary mode of freeze protection such as drain-back or drain-down.

In the most common form of recirculation, the energy required to keep the solar collectors warm is provided by the solar storage tank, as shown in figure 4.1. Energy collected during the day is used to prevent freezing at night or other times when freezing conditions are approached. The control parameters are the "recirculation temperature" and "recirculation deadband". The recirculation temperature is the minimum set temperature at which recirculation is begun. The sensor used to check for the recirculation temperature is normally located in the collector, but could be at any one or several system locations where freezing is of concern. The deadband is the increase in temperature over the recirculation temperature required to end the recirculation. The location of the sensor used for the deadband temperature is not necessarily the same as for the recirculation temperature.

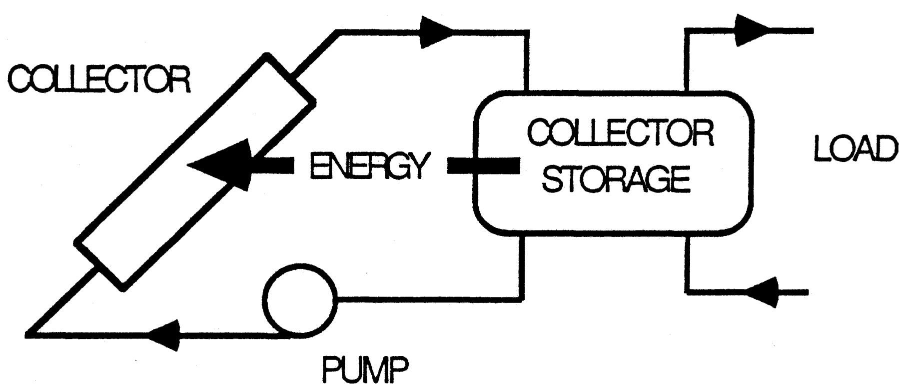

FIGURE 4.1 Typical recirculation system.

Consider the Chinle system, with long outdoor piping runs between the collector array and heat exchanger. A temperature sensor located on the collector absorber plate is used for the recirculation temperature. During a recirculation, warm water pushes the cold fluid out of the collectors. If the same collector absorber plate sensor is used for the deadband temperature, recirculation would end as soon as warm fluid reached the outlet of the collector. But this would only displace the cold fluid into the collector return piping, where it could eventually freeze. Therefore a second sensor should be located on the collector side heat exchanger inlet, which is the last point in the collector loop to receive warm fluid during recirculation. Both the collector absorber plate and the heat exchanger inlet should be checked for the deadband temperature before ending the recirculation. In systems with long piping, such that the collector outlet piping volume is greater than the collector array volume, a timer is required in addition to the temperature sensors to insure a long enough recirculation. Otherwise, a cold slug of fluid, as shown in figure 4.2, could be left in the middle of the return pipe. The timer insures that cold fluid from the collectors reach the deadband sensor before allowing recirculation shutdown because of fluid temperature.

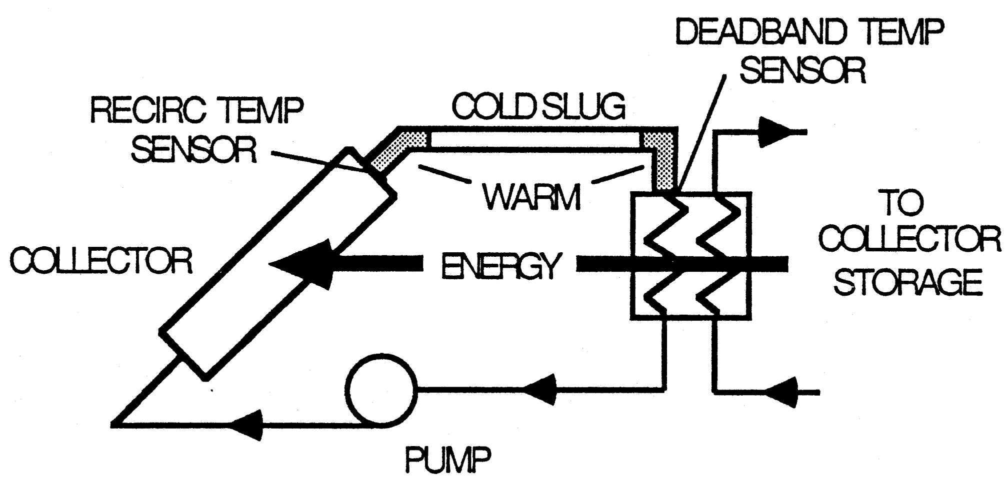

FIGURE 4.2 Chinle collector loop during recirculation.

During recirculation, the temperature of the fluid used to warm the collector loop is determined by the collector storage tank temperature. In a system with a collector to storage heat exchanger, the collector fluid will be heated at the heat exchanger to a temperature somewhat below the storage tank temperature (herein called the apparent tank temperature). In a system without the heat exchanger, fluid will be drawn directly from the collector storage tank. In either case, the warm fluid moves around the collector loop, first heating the collector inlet pipe, than the collectors, and finally the collector outlet pipe. It's important to note, that as the last point in the collector loop reaches the recirculation shut off temperature (recirc. temp. + recirc. deadband temp.), most of the collector loop will be at a much higher temperature, very close to the storage tank temperature or apparent tank temperature. In the Chinle simulations, the collectors are sometimes heated to over 100 °F during a recirculation, even though the shut-off temperature is 55 °F.

IV.2 CONVERTING CHINLE TO A RECIRCULATION SYSTEM

The present Chinle system, described in chapter III, could be modified to utilize recirculation freeze protection. This would require reprogramming the controller and possibly adding or changing some equipment.

The basic recirculation mode could be implemented by changing the control strategy so that both the collector loop and storage loop pumps run if freezing conditions are approached. In addition, a back-up is needed in case the collector storage tanks cannot meet the recirculation load. Several back-up configurations are available. Auxiliary heaters and appropriate controls, could be installed in the collector storage tanks, in-line to the collector loop, or in-line to the storage loop. These heaters could be self-contained units or consist of heat exchangers piped to the present auxiliary boilers. One method of back-up that would not require any mechanical changes to the Chinle system, would be to use the present drain-back mode as a back-up to the recirculation mode.

For the simulations, the back-up consisted of auxiliary heaters placed in both storage tanks. The heaters turned on when the tank temperatures reached 45 °F, and off at 50 °F.

IV.3 MODELING CHINLE AS A RECIRCULATION SYSTEM

In this section several TRNSYS models are analysed in order to determine the modeling requirements for recirculation. Simulations were made in order to determine the effect of timestep size, controller functions, and pipe models.

The collector loop model of the Chinle system is shown in figure 4.3, with mass volumes and circulation times for the fluid to move around the collector loop. During recirculation, the cold collector fluid must be pushed through to the heat exchanger, in other words, warm fluid at point C in figure 4.3 must be pushed through to point E. A timer for the recirculation pump is required to insure that the front of the cold fluid at point D, reaches point E. The timer for the Chinle model requires a minimum recirculation time of 2.92 minutes, after which the temperatures at points D and E are monitored until both reach the recirculation shut off temperature.

In order to simulate the controller dynamics, a plug-flow pipe model (Type 31) is used for the collector pipes, which keeps track of the fluid fronts. Chapter II.2 contains

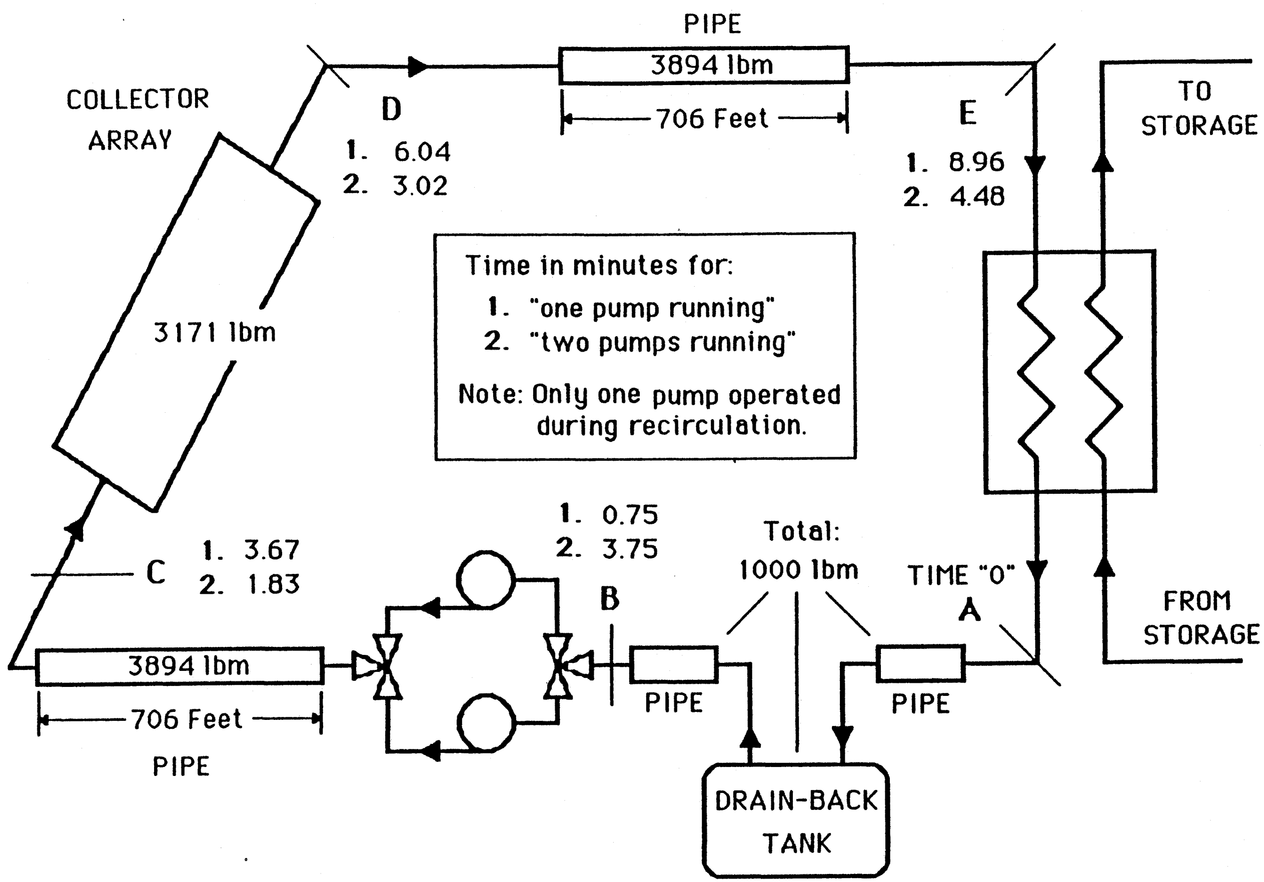

FIGURE 4.3 Mass volumes and circulation times for the Chinle model collector loop fluids, starting at the heat exchanger outlet.

a description of the plug-flow pipe model. A timestep was chosen so that the pipe would contain approximately 6 fluid plugs, in other words, it will take 6 timesteps for fluid to pass completely through the pipe. The timestep is calculated as:

$$\Delta t = \frac{2.92 \text{ minutes}}{6} \left(\frac{1 \text{ hour}}{60 \text{ minutes}}\right) = .0081 \text{ hours (29.2 seconds)} \qquad (4.3.1)$$

Simulations were made using the TRNSYS deck described in section 3.2 for the drain-back mode, with the following changes:

1. Plug flow pipe model.
2. Timestep size of .008 hours.
3. Auxiliary heaters in the collector storage tanks.
4. Controller parameters changed for the recirculation mode.

The control functions shown in table 3.1 for drain-back are used for recirculation except for the changes shown in table 4.1.

DESCRIPTION	PUMP P_{c1}	PUMP P_{c2}	PUMP P_{st}
*** 10a. T_c < Recirculation Temperature	on	off	on
b. (T_c and T_{chx}) > (Recirc temp. + Deadband) and P_{c1} on time > minimum recirc time	off	off	off
c. T_{st1} > 220 °F		"drain-back"	
d. T_{st1} < 50 °F		"Auxiliary tank heater on"	

*** Represents changes made to entry #10 of table 3.1.

TABLE 4.1 Changes made to the Chinle model control functions in order to use recirculation freeze protection.

In chapter III, figure 3.4, two control signals (γs) are shown input to the storage loop pump. One signal, from the storage loop controller (TY 2), is for operation when solar energy is being collected, and the second control signal is from the main controller (TY

"45" - fig. 3.3), which turns on the pump during recirculation.

Short term simulations, with the Chinle model, were made in order to observe the system dynamics. The controller had the following set points:

Recirculation temperature = 45 °F
Recirculation deadband = 10 °F
Minimum recirculation time = 3.0 minutes

The collector temperature during recirculation is important because it determines the heat losses and thus the energy required to keep the collectors warm. Figure 4.4 shows the collector temperature during a recirculation period. Three temperatures are shown. The temperature of the first node of the collector (10 node collector), the average collector temperature, and the collector outlet temperature. The sharp rise in temperatures occurs while the warming fluid is being circulated through the collectors. The longer temperature decay is the collector cooling between recirculations. The dip in curve A, at the top of a warm-up period, is caused by the cold slug of fluid that was pushed out of the collector during the last recirculation, traveling completely around the collector loop and entering the collector in the next recirculation.

Chapter II.1 explained that it was desired to use a fully mixed pipe model in order to include the effects of pipe wall thermal capacitance. The fully mixed pipe models were used in simulations of the Chinle drain-back system, therefore it is desired to use them in simulating the recirculation system for making comparisons. Fully mixed pipe models do not track fluid fronts, but will account for long term energy transfers. A second simulation was made using the fully mixed pipe model (TY "36") for the collector pipes, instead of the plug-flow model. Figure 4.5 shows the collector temperatures during recirculation cycles. Comparing figures 4.4 and 4.5, the Chinle model with fully mixed pipes show a higher frequency of recirculations and larger temperature spreads across

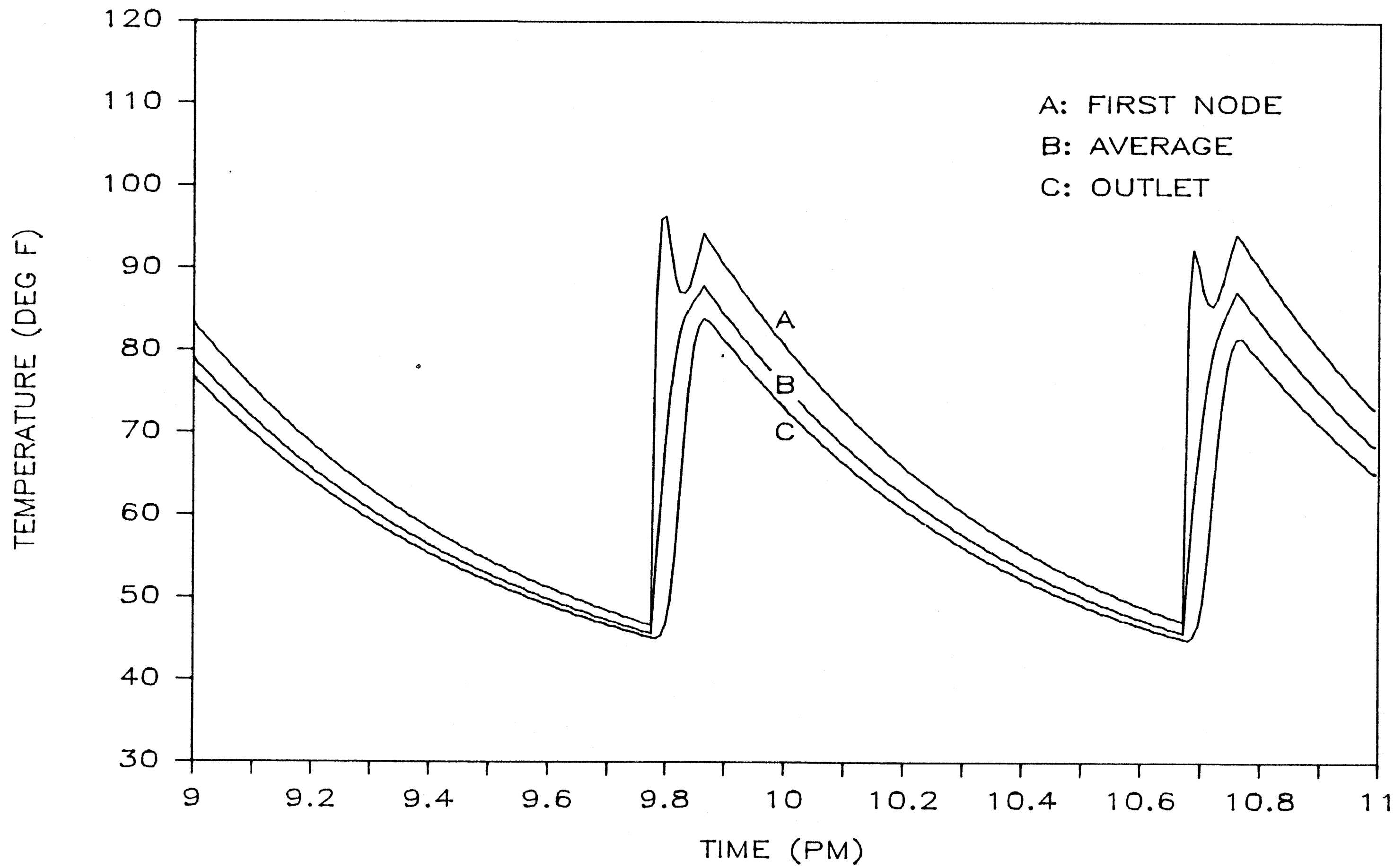

FIGURE 4.4 Collector temperatures during recirculations for the Chinle model with plug-flow pipes and a minimum recirculation time of 3 minutes. (10 node collector, .008 hr. timestep)

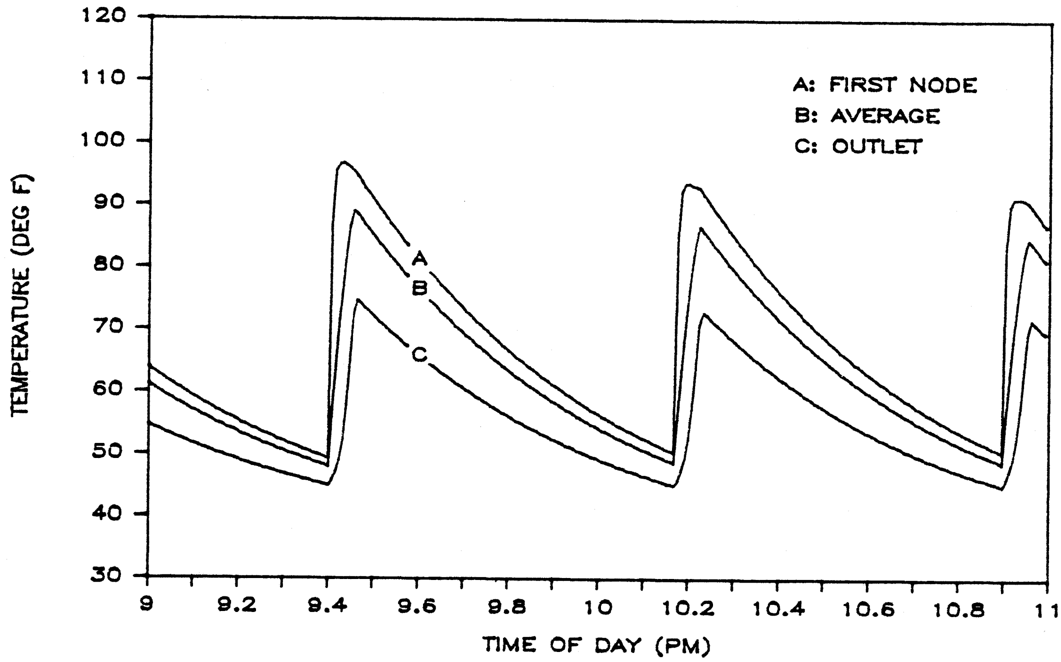

FIGURE 4.5 Collector temperatures during recirculations for the Chinle model with fully mixed pipes and a minimum recirculation time of 3 minutes. (10 nodel collector, .008 hour timestep)

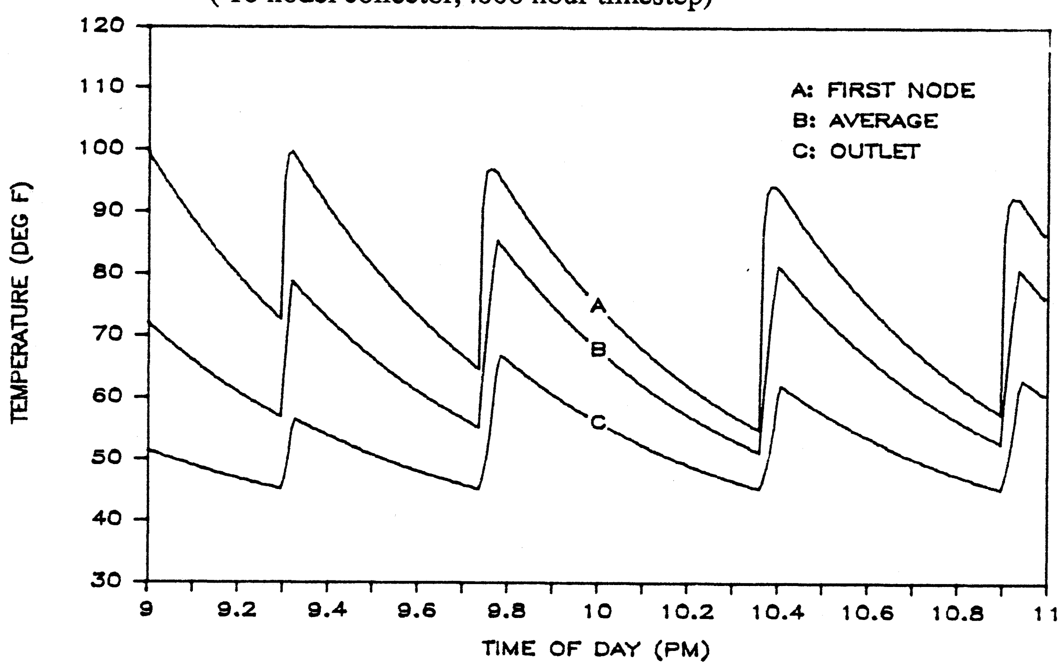

FIGURE 4.6 Collector temperatures during recirculations for the Chinle model with fully mixed pipes and no minimum recirculation time. (10 node collector , .008 hour timestep)

the collector. The fully mixed pipe model's outlet temperature reacts to changes at the inlet, faster than the plug-flow model. This means the recirculation deadband temperature will be reached sooner, shortening the recirculation time. Shorter recirculations leave less time for the collector to completely warm-up, thus the larger temperature spread across the collector.

Finally, simulations were made with the fully mixed pipe model and no minimum recirculation time. The recirculation stop criterion was only that the temperatures of the fluid entering the heat exchanger and exiting the collector be above the recirculation shut off temperature. Figure 4.6 shows the collector temperatures. An increase in both recirculation frequency and temperature spread across the collector is seen compared to figures 4.4 and 4.5.

Three simulation methods have been described for the Chinle recirculation system, which all produce quite different results in collector and controller dynamics. What's important is how they predict energy performance. Table 4.2 summarizes the results of simulations for the month of January.

MODEL	Q_{col} Btu x10^{-8}	Q_{rec} Btu x10^{-8}	Q_{solar} Btu x10^{-8}	Q_{aux} Btu x10^{-8}	Q_{load} Btu x10^{-8}	SF Percent
Plug-flow pipe min. recirc time = 3 min.	2.373	1.047	1.282	19.06	20.32	6.56
Fully mixed pipe min. recirc time = 3 min.	2.375	1.063	1.272	19.06	20.32	6.21
Fully mixed pipe no min. recirc time	2.377	1.057	1.281	19.05	20.32	6.23

TABLE 4.2 Thermal energy usage during the month of January predicted with three Chinle recirculation models.

The results in table 4.2 show that all of the models provide similar predictions of the energy performance of a recirculation system.

The simulations of table 4.2 all used .008 hour timesteps and required an excessive amount of computer time, which becomes unacceptable for yearly simulations. Yearly simulation results using three different timesteps are summarized in table 4.3. The model used the fully mixed pipes with no minimum recirculation time. The results show that the model predictions are somewhat irregular as the timestep is changed.

TIMESTEP hours	CPU hours	Q_{col} Btu x10^{-9}	Q_{rec} Btu x10^{-9}	Q_{solar} Btu x10^{-9}	Q_{aux} Btu x10^{-9}	Q_{load} Btu x10^{-9}	SF Percent
.008	22.	2.871	0.431	2.296	9.397	11.67	19.49
.03125	8.0	2.901	0.407	2.348	9.355	11.68	19.91
.250	2.3	2.904	0.483	2.276	9.382	11.64	19.37

CPU = approximate simulation computer time on Digital MicroVAX

TABLE 4.3 Annual thermal energy usage predicted with the Chinle recirculation model using three different timesteps. (Recirculation temp. = 45 °F)

For simulations with the larger timestep (.250 hr), the controller causes an increased amount of recirculation energy. Since control decisions must be constant over a TRNSYS timestep, a recirculation in a simulation using a timestep of .250 hours would have to last 15 minutes, while the actual recirculation lasts 2 to 4 minutes. Longer recirculation time means that the collector will be kept at the higher temperature for a longer duration, therefore losses will be higher. As the timestep is decreased below .03125 hours, the collector model begins to affect the recirculation energy. Chapter II explained that the multi-node collector model begins to show an ideal temperature front moving across the collector as the timestep is decreased. For the non-ideal model of the temperature front (ie. larger timestep), the collector outlet temperature reacts sooner to a change in inlet temperature, and thus reaches the deadband temperature sooner. Therefore, a smaller timestep will result in longer recirculations and higher collector temperatures, thus predicting higher losses.

The best timestep cannot be determined without actual performance data to show which timestep provides the most realistic results. One common timestep was chosen for all simulations, eliminating this as a variable. The timestep was chosen at .03125 hours (1.875 min.), because it is on the same order of size as the Chinle collector time constant of 1.28 minutes.

IV.4 SIMULATION RESULTS

In section IV.1 the control parameters "recirculation temperature" and "recirculation deadband" were explained as the turn on and turn off criterion for a recirculation. The effect of changing the set-points are considered in this section. The TRNSYS model is the same model used for simulating the drain-back Chinle system (Chap. III), with the controller changed for recirculation and auxiliary heaters added to the collector storage tanks as back-up for recirculation.

Yearly simulations were made with recirculation temperatures ranging from 32 °F to 50 °F. The deadband was kept constant at 10 °F. Figure 4.7 shows the load, auxiliary energy required, and solar energy delivered versus the set-point, and figure 4.8 shows the solar fractions. Recirculation temperature set-points of 32 °F and 50 °F represent two extremes. A setting of 32 °F would obviously result in freezing. Recirculating at 50 °F requires an excessive amount of energy to keep the collector loop at a temperature far

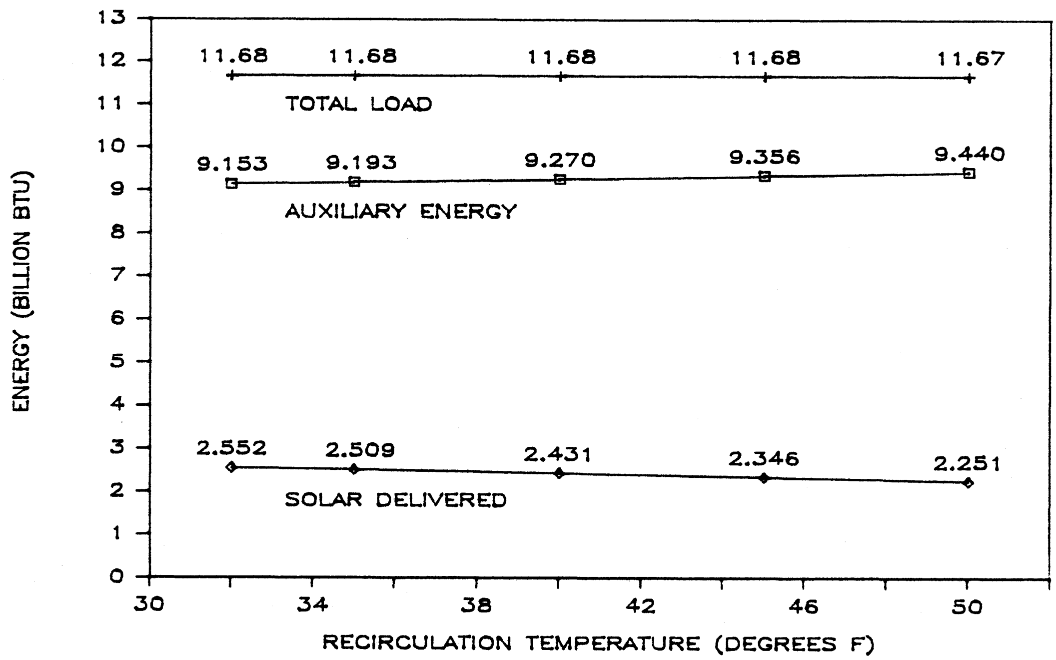

FIGURE 4.7 Chinle model predictions of annual energy usage versus the recirculation temperature set-point.

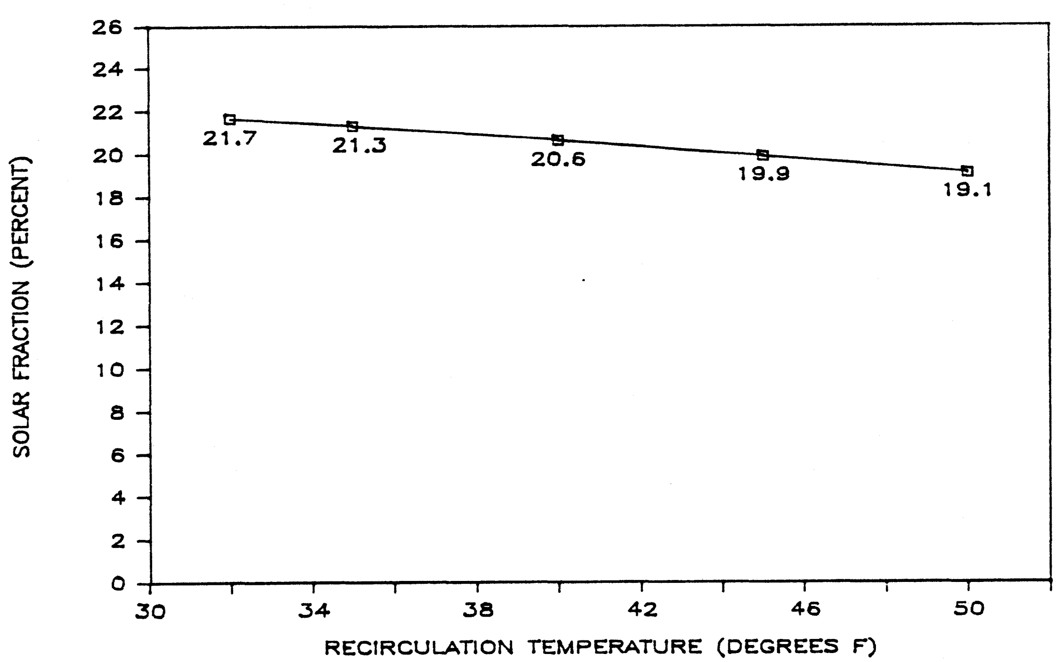

FIGURE 4.8 Chinle model predictions of annual solar fraction versus the recirculation temperature set-point. ($SF = 1 - Q_{aux} / Q_{load}$)

above freezing. Recirculation temperatures of between 35 °F and 45 °F are more reasonable. Table 4.4 shows the predicted recirculation energy requirements for systems recirculating at 35 and 45 °F. The annual savings in auxiliary energy from going from a set temperature of 45 °F to 35 °F is 163 million Btu or 1.8%.

Recirc Temp. °F	Q_{col} Btu x10^{-9}	Q_{rec} Btu x10^{-9}	Q_{solar} Btu x10^{-9}	Q_{rec} / Q_{col} Percent
35	2.851	0.186	2.509	6.5
45	2.901	0.407	2.346	14.0

TABLE 4.4 Annual recirculation energy requirements predicted with the Chinle model.

Simulations were made with the recirculation temperature at 45 °F and the deadband temperature ranging from 5 °F to 20 °F. As discussed in section IV.1, the deadband temperature requirement is applied to the temperature at the inlet to the heat exchanger. There was virtually no difference in performance. The deadband does affect the number of recirculations and the total time that fluid is recirculated as shown in figure 4.9. As the deadband is increased, the recirculating time increases as the system must be heated to a higher temperature. However, with the collector warmed to a higher temperature, the cooling time between recirculations also increases. This longer cooling time results in fewer recirculation cycles during freezing conditions.

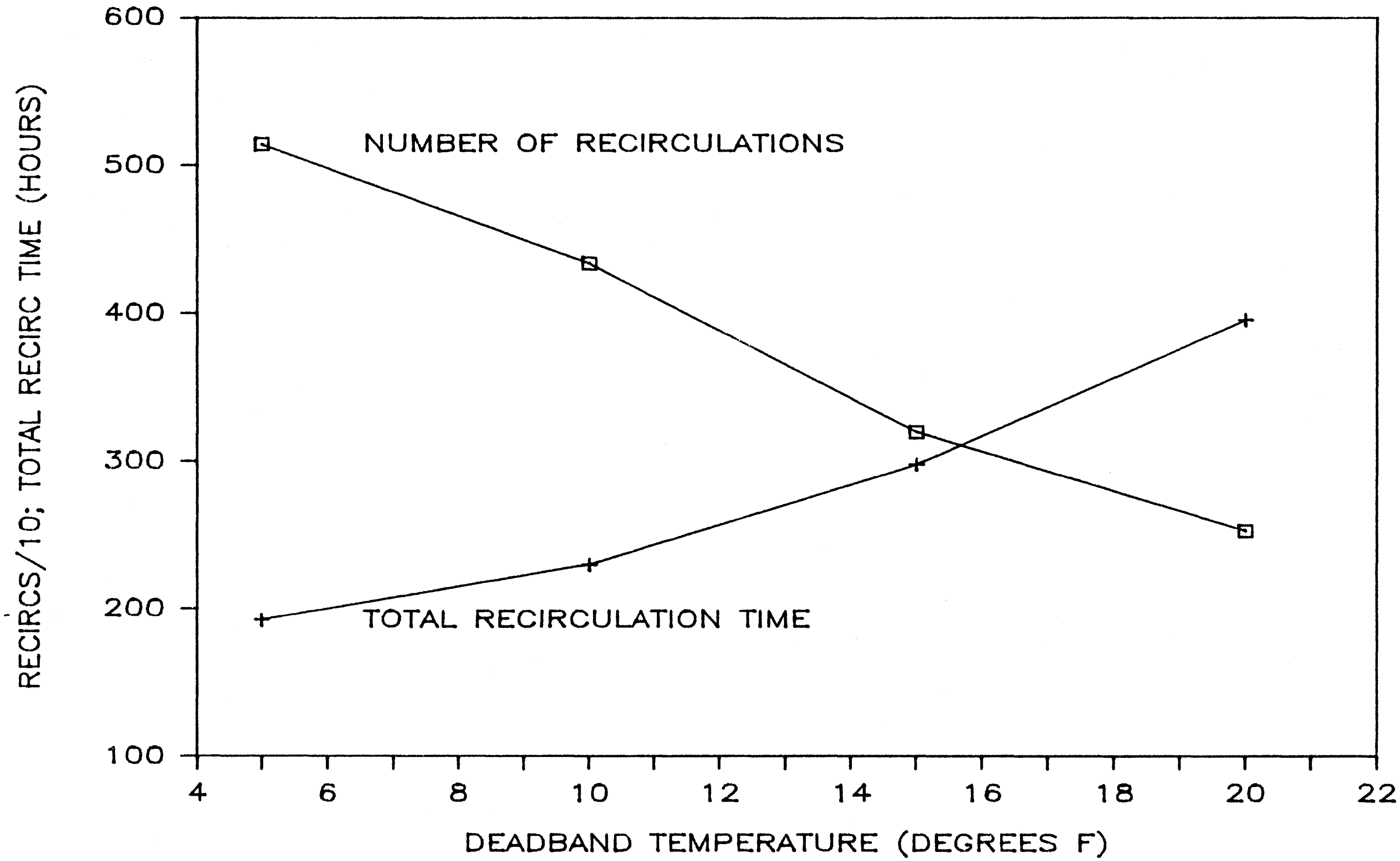

FIGURE 4.9 Annual recirculation dynamics versus the deadband temperature set-point, as predicted with the Chinle model.

IV.5 ALTERNATE RECIRCULATION SYSTEMS

In figure 4.4, the collector temperature was shown to reach up to 100 °F during a recirculation. Section IV.3 explained how this was due to the requirement that warm fluid pass completely around the collector loop to insure that all the cold fluid is heated. The extra time for the warm fluid to go from the exit of the collectors to the entrance of the heat exchanger allows the collectors to warm up almost to the warming fluid temperature. Since higher collector temperatures mean higher heat losses, methods for reducing the recirculation fluid temperature may prove economical.

Lower energy requirements for recirculation will result if the recirculating fluid temperature is kept to a minimum. One method available for the Chinle system would be to bypass fluid around the heat exchanger as shown in figure 4.10. A controller could monitor the temperature of the fluid returning from the collector field and control bypass valves around the heat exchanger in order to keep the returning fluid temperature just above freezing. A new TRNSYS component would be necessary to model the bypass controller. Instead, a controllable mixing valve (TY 11), shown in figure 4.11, was used to maintain a constant set temperature of the fluid going to the collector field. Various set temperatures were tried and the temperatures around the collector loop continuously checked to see if freezing occurred. For set temperatures of 40 °F and 45 °F, fluid temperatures never fell below 35 °F in the collector loop. Simulation results with various set temperatures are shown in table 4.5. One simulation was made with a set temperature of 32 °F. The fluid in this system would surely freeze, but the set point was used to establish the limiting case. The results for Q_{rec} in table 4.5 show the drastic effect of the recirculation fluid temperature.

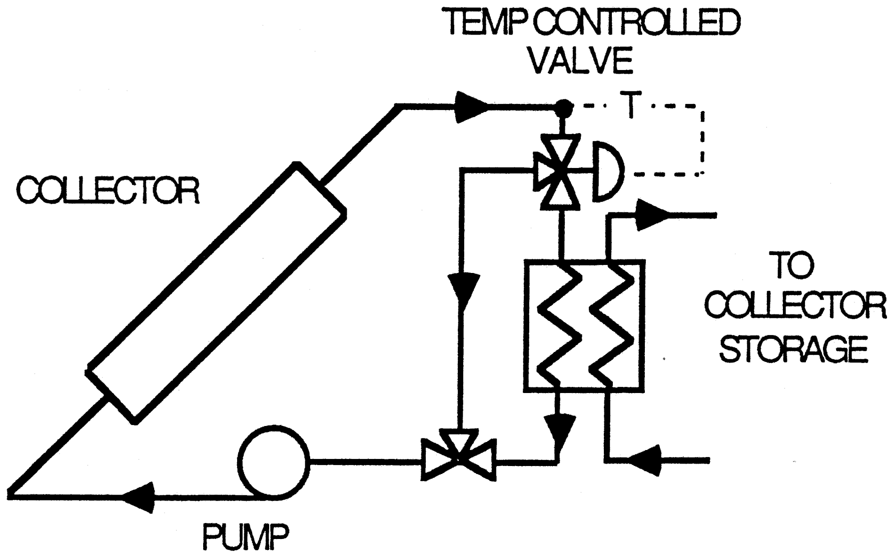

FIGURE 4.10 Possible Chinle system configuration in order to minimize the recirculation fluid temperature.

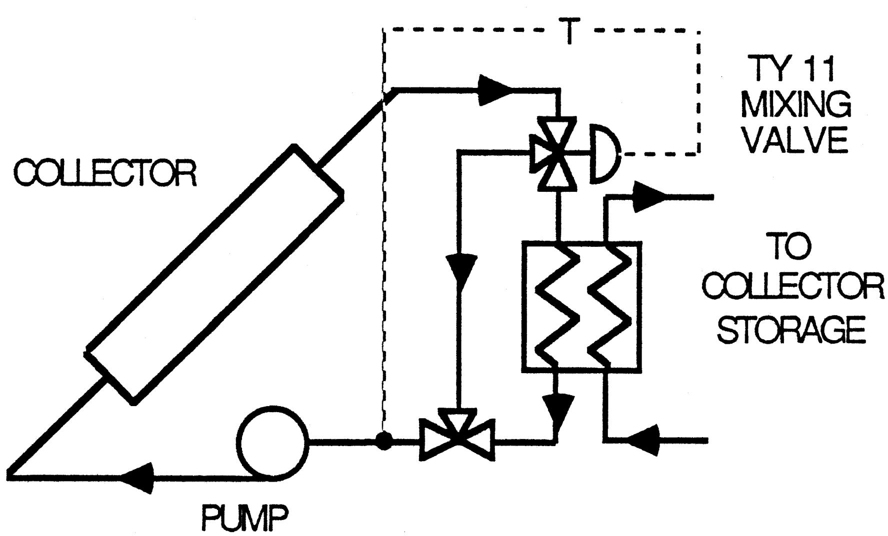

FIGURE 4.11 Chinle model configuration for reducing the recirculation fluid temperature.

Mixing Valve Set Temp	Q_{col} Btu x10^{-9}	Q_{rec} Btu x10^{-9}	Q_{solar} Btu x10^{-9}	Q_{aux} Btu x10^{-9}	Q_{load} Btu x10^{-9}	SF Percent
32 °F	2.828	0.073	2.578	9.106	11.68	22.06
40 °F	2.843	0.158	2.537	9.167	11.68	21.53
45 °F	2.855	0.226	2.487	9.215	11.68	21.10

TABLE 4.5 Annual thermal energy usage predicted with the Chinle model using a mixing valve to reduce the recirculation temperature.

Several methods could be applied to recirculation systems in order to minimize the recirculating fluid temperature. For the Chinle system with the collector to storage heat exchanger, variable speed pumps could be used in either the collector or storage loop to control the heat transfer across the heat exchanger. In most cases the thermal effects should be be similar to those found in the system simulated here. A cost study is required to determine the feasibility of each method. One draw-back to recirculation methods to limit the fluid temperature, is the added complexity. The advantages of recirculation is its simplicity, low equipment cost, and dependability. Any added mixing valves or controllers will negate some of the advantages of the standard system.

CHAPTER V: DUAL FLUID FREEZE PROTECTION

The dual fluid system, using an anti-freeze solution in the collector loop and a collector to storage loop heat exchanger, is a common means of freeze protection. The advantages of this freeze protection method is its simplicity and performance, as it doesn't require the extra valving of drain-back or the energy penalties of recirculation. The drawback of dual fluid freeze protection is the requirement of a heat exchanger which raises operating temperatures and increases system losses. Freeze protection is provided by the fact that the freezing point of the collector fluid is well below the expected ambient temperatures. Four disadvantages of an anti-freeze solution (50% by weight ethylene glycol to water) are summarized below:

1. High price of ethylene glycol versus pure water.
2. The toxicity of ethylene glycol requires the use of two metal interfaces between the toxic fluid and potable water supply. This can be accomplished by the use of either two heat exchangers or a double walled heat exchanger.
3. The viscosity of a water-glycol mixture is an average of 3 times higher than pure water over a typical range of flat plate collector temperatures of 75 °F to 200 °F.
4. The heat capacity of the water-glycol mixture is lower than pure water by an an average of 18% over the temperature range of 75 °F to 200 °F.

In this chapter, a TRNSYS model will be used to predict the thermal performance of the Chinle system using dual fluid freeze protection. A 50-50 water-glycol fluid, with a freezing point around -20 °F, will be used in the collector loop. The present Chinle drain-back system could be easily modified for dual fluid freeze protection by replacing the water in the collector loop with a water-glycol fluid and reprogramming the controller to inhibit drain-back.

V.1 EFFECTS OF WATER-GLYCOL IN SYSTEM PERFORMANCE

Replacing the collector loop water with a 50-50 water-glycol has two major effects which decrease collector and system performance. Increasing the collector fluid viscosity lowers the heat transfer coefficient between the collector fluid and collector tube walls, and lowering the specific heat of the fluid increases the mean operating temperature of the collector for any given inlet fluid temperature.

Not only do the properties of a water-glycol solution differ from pure water, but the viscosity and specific heat of a water-glycol solution are very temperature dependent. The properties of both fluids are summarized in table 5.1 over a temperature range typical to liquid flat plate collector solar systems. The specific heat of water is relatively constant over the temperature range, therefore an average value is normally used in calculations and simulations, whereas, the specific heat of water-glycol changes by 10% over the temperature range in table 5.1.

The collector performance parameters were calculated considereing the water-glycol properties to be independent of temperature. Three different sets of properties were used to establish the operating range for the collector. The collector performance parameters are calculated in appendix A and summarized in table 5.2.

FLUID	Density ρ lbm / ft^3	Viscosity μ lbm / ft-hr	Specific Heat C_p Btu / lbm-°F	Conductivity k Btu / hr-ft-°F	Prandtl # Pr
*Water-glycol at:					
75 °F	66.17	8.474	0.7943	.24	28.0
140 °F	64.93	3.632	0.8421	.23	13.0
200 °F	63.36	1.816	0.8779	.23	6.9
Water at:					
75 °F	62.27	2.218	0.998	.350	6.34
140 °F	61.38	1.129	1.000	.376	3.00
200 °F	60.11	0.734	1.006	.390	1.89

* 50-50 (by weight) water - ethylene glycol solution
water properties from Chapman (1984)
water-glycol properties from Duffie and Beckman (1980)

TABLE 5.1 Water and water-glycol properties at various temperatures.

FLUID	F'	F_R	U_L Btu /hr-ft^2-°F	$F_R U_L$ Btu /hr-ft^2-°F	$F_R(\tau\alpha)_n$
Glycol at:					
75 °F	.948	.912	.809	.738	.752
140 °F	.947	.913	.809	.739	.753
200 °F	.947	.916	.808	.740	.755
Water at:					
140 °F	.962	.933	.804	.750	.769

TABLE 5.2 Calculated collector parameters under test conditions with the same mass flowrate for both the pure water and water-glycol fluids. Calculations are shown in appendix A.

The increased viscosity of the water-glycol fluid decreases the heat transfer coefficient between the fluid and absorber tubes by about 45% from that of pure water, but that only decreases the collector efficiency factor (F') by about 1.6%. The effect of the decreased collector efficiency factor and decreased specific heat of the water-glycol reduces the heat removal factor (F_R) by about 2%.

Using the water-glycol solution over water also has an effect on the collector pumps. If the present Chinle system pumps are used with water-glycol, a significant decrease in flowrate will result from the large increase in fluid viscosity. Reducing the flowrate will increase the operating temperature of the collectors, thereby decreasing the collector efficiency. In order to predict the decrease in flowrate, data would be needed on the pressure drop versus flowrate for the system and flowrate versus pressure drop for the pumps. Since this information was not available, a variety of flowrates were used in the simulations. Goumaz (1981) recommends that the pump size be increased, to raise the flowrate by up to 22%, to offset the effect of the reduced specific heats.

V.2 SIMULATION RESULTS

The Chinle system was modeled as a dual fluid system using the TRNSYS model described in chapter III, for Chinle as a drain-back system, with the following exceptions.

1. Collector performance factors changed for the effect of the water-glycol fluid.
2. Collector loop fluid densities and specific heats changed to those for the water-glycol fluid.
3. The controller was changed to inhibit drain-back.

Annual simulations were made with the water-glycol properties evaluated at various temperatures, but held constant during any one simulation The collector loop flowrates were varied from + 20% to - 20% of the Chinle flowrate using water as the collector fluid. The decreased flowrates represent the case of replacing the collector loop water of the present Chinle system, with a water-glycol solution, but using the same Chinle pumps. The increased flowrates are for the water-glycol fluid with larger collector loop pumps. The simulation results are summarized in table 5.3.

The largest estimated effect from using a water-glycol fluid in the collector loop is represented in table 5.3 by the water-glycol system with properties evaluated at 75 °F and the flowrate reduced by 20% from that used for pure water as the collector fluid. This case shows a 2% decrease in collected solar energy and a 2% relative reduction in solar fraction from the pure water system. As the flowrate is increased, the water-glycol

FLUID	Flowrate % of "Base"	Q_{col} Btu x10^{-9}	Q_{solar} Btu x10^{-9}	Q_{aux} Btu x10^{-9}	Q_{load} Btu x10^{-9}	SF Percent
Water-glycol:						
props at 75 °F:						
	-20.	2.731	2.564	9.120	11.66	21.80
	-10.	2.741	2.583	9.105	11.66	21.98
	0.	2.763	2.596	9.100	11.67	22.06
	+10.	2.773	2.604	9.092	11.67	22.13
	+20.	2.769	2.602	9.092	11.67	22.11
props at 140 °F:						
	0.	2.768	2.606	9.099	11.68	22.08
props at 200 °F:						
	0.	2.774	2.607	9.091	11.68	22.15
*Water:						
props at 140 °F						
	0.	2.785	2.626	9.096	11.70	22.26

* This simulation used water as the collector fluid and drain-back freeze protection.

Flowrate = collector flowrate ("Base" = 160170 lbm / hr total collector array flow)

TABLE 5.3 Annual thermal energy usage predicted with the Chinle model using dual fluid freeze protection.

performance approaches the pure water system. The simulation with the water-glycol properties evaluated at 200 °F performs close to the pure water system. Water-glycol properties evaluated at 200 °F and 75 °F represent the two end points of typical operating conditions for liquid flat plate collector systems. The difference in performance with properties evaluated at either of these end points is small, which justifies using an average temperature to evaluate the water-glycol properties and considering them independent of temperature.

V.3 HEAT EXCHANGER PENALTY

Koenigshofer (1977) estimated a 10% decrease in collected energy and Goumaz (1981) found a relative decrease in solar fraction of 17% in one case, in going from drain-back to dual fluid freeze protection, because of the penalty incurred by the addition of a collector to storage heat exchanger. The decrease in performance of the Chinle system is much smaller because the present system already incorporates a collector to storage heat exchanger, even though it operates in a drain-back freeze protection mode. Therefore the performance of the system using water-glycol versus pure water in the collector loop is only reduced due to the difference in properties between water and water-glycol. A simulation was made of the Chinle system without the heat exchanger and the results are compared to drain-back and dual fluid freeze protection in table 5.4.

The results in table 5.4 show that the heat exchanger penalty decreases the collected energy by 3% to 4%, which is much lower than referenced above. The heat exchanger penalty is very system dependent and will be influenced by the total collector area, flowrates, and heat exchanger effectiveness.

System	Q_{col} Btu x10^{-9}	Q_{solar} Btu x10^{-9}	Q_{aux} Btu x10^{-9}	Q_{load} Btu x10^{-9}	SF Percent
Drain-back:					
without heat exchanger[1]	2.873	2.720	9.012	11.71	23.05
with heat exchanger[1]	2.785	2.626	9.096	11.70	22.26
Dual fluid:[2]	2.768	2.606	9.099	11.68	22.08

1. This simulation used water as the collector fluid and drain-back freeze protection.
2. This simulation used a 50-50 water-ethylene glycol solution with the properties evaluated at 140 °F.

TABLE 5.4 Annual simulation results for the Chinle system, showing the effect of the collector to storage heat exchanger.

CHAPTER VI: SUMMARY

The three most common types of freeze protection for solar energy systems using liquid flat plate collectors, are drain-back, recirculation, and dual fluid. Each freeze protection scheme was modeled using the computer simulation program TRNSYS. The models were based on the large solar energy system installed at the Indian Health Facility in Chinle, Arizona and the simulations were used to predict the annual thermal energy performance of the system incorporating each of the freeze protection methods.

VI.1 COMPARISONS

The predicted performance of the Chinle system incorporating several different freeze protection schemes is summarized in table 6.1. The legend below applies to the entries in table 6.1.

Q_{col} = total solar energy collected

Q_{solar} = solar energy delivered to the DHW and SPH loops (energy delivered from the collector storage tanks)

Q_{aux} = total auxiliary energy required by system

Q_{load} = total energy delivered to the load (space heating plus hot water)

SYSTEM	Q_{col}		Q_{solar}		Q_{aux}		Q_{load}		SF	
	Btu x 10^{-9}	Δ	Btu x 10^{-9}	Δ	Btu x 10^{-9}	Δ	Btu x 10^{-9}	Δ	PERCENT	Δ
Drain-back:										
No heat exchanger [1]	2.873	-	2.720	-	9.012	-	11.71	-	23.1	-
"Open return"	2.814	2.1	2.679	1.5	9.025	0.1	11.68	0.3	22.8	1.3
Drain temperature [1]	2.788	3.0	2.628	3.4	9.084	0.8	11.69	0.2	22.3	3.5
Dual fluid: [2]	2.768	3.7	2.606	4.3	9.099	1.0	11.68	0.3	22.1	4.4
Recirculation:										
Mixed recirc. [3]	2.843	1.0	2.537	7.0	9.167	1.7	11.68	0.3	21.5	7.2
Recirc. temperature [4]	2.851	0.8	2.509	8.1	9.193	2.0	11.68	0.3	21.3	8.1

1. These systems have a drain-back set point temperature of 45 °F.
2. This system uses a 50-50 (by weight) water-ethylene glycol solution in the collector loop.
3. This system has a mixed fluid temperature of 40 °F.
4. This system has a recirculation set point temperature of 35 °F.

Δ = relative difference with the drain-back system with no heat exchanger (percent)

TABLE 6.1 Annual thermal energy usage predicted with the Chinle models utilizing various freeze protection methods.

VI.2 CONCLUSIONS

The following is a list of conclusions, drawn from this study, regarding the modeling requirements for simulating solar energy systems utitlizing freeze protection schemes and the thermal performance of freeze protection methods as applied to the Chinle system.

1. Fully mixed pipe models can be used instead of plug-flow pipe modes for simulating most solar energy systems with little or no difference in the prediction of annual thermal performance. Only in energy systems where very long pipe lengths may introduce a time lag, that affects control decisions, might a plug-flow pipe model be required.
2. The effect of modeling collector thermal capacitance on the predicted thermal performance of a system is can be significant. The Chinle system model including collector capacitance predicts 1.5% less collected energy than the model neglecting capacitance.
3. The annual thermal performance of drain-back systems using a drain-back temperature set-point, is insensitive to the magnitude of the set-point. (over a reasonable range of set-points, such as 35 °F to 75 °F)
4. The best thermal performance for systems incorporating drain-back freeze protection is with the "open return" control strategy, which drains-back anytime the system pumps shut down. In the Chinle system the solar fraction increases by a relative amount of 2% when changing from draining-back at 45 °F to an "open return" strategy.
5. Accuarate modeling of the dynamics of a solar energy system incorporating recirculation freeze protection is not required to obtain reasonable predictions of annual thermal performance. Models that can

approximate the recirculation time provide satisfactory results.

6. The annual thermal performance of a recirculation system is strongly dependent on the set-point temperature used to initiate recirculation and only slightly affected by the set-point temperature for ending a recirculation, as much of the system will be heated to temperatures close to the solar storage tank temperature, independent of the shut-off temperature.

7. The annual performance of a recirculation system is improved by using a mixing valve to minimize the temperature of the recirculating fluid. In the Chinle system the amount of energy required for recirculation is reduced as much as 50% by using a mixing valve. However, this only amounts to an increase in solar fraction by a relative amount of 1%.

8. Although the specific heat and viscosity of a 50-50 (by weight) water-ethylene glycol solution are temperature dependent, satisfactory simulation results of dual fluid systems are obtained from evaluating the properties of the water-glycol at the average operating temperature, for typical systems using liquid flat plate solar collectors.

9. Using dual fluid freeze protection on the Chinle system only slightly reduces the annual energy performance because the collector to storage heat exchanger already exists in the system and it penalizes the performance of all of the freeze protection methods.

10. The collector to storage heat exchanger in the Chinle system reduces the collected solar energy by 3 to 4 percent.

VI.3 RECOMMENDATIONS

The following are recommendations for future work.

1. Simulations should be made for solar energy systems of different sizes and types with and without pipe models accounting for pipe wall thermal capacitance, in order to determine if the effects are significant. Preliminary studies showed that the pipe wall thermal effects were not always insignificant.
2. The existing plug-flow model in TRNSYS version 12.1 should be modified to account for pipe wall thermal capacitance. The user should have the option to include or not include capacitance when modeling pipes with TRNSYS.
3. The multi-node drainable collector model developed in order to model the various freeze protection schemes should be verified against experimental data and further developed if necessary.
4. Simulations should be performed with models based on several systems utilizing drain-back and recirculation freeze protection and the results used to develop simple methods to correct the predicted performance from models ignoring the freeze protection. This correction could be useful for F-chart (F-chart 1985) type programs.
5. The results from this and/or similar studies on the thermal performance of solar energy systems with various freeze protection methods should be combined with studies on pumping requirements, equipment costs, energy costs, and reliability to form a comprehensive study of freeze protection.

APPENDIX A

This appendix shows the calculations for determining the effect, on collector performance, of replacing water with a water-glycol solution. Table A.1 shows the collector data used for the calculations. First the equations used are presented, then a set of example calculations shown. All the equations used in this section are from Duffie and Beckman (1980).

Collector manufacturer and model:
Novan Energy, Inc.
Optima 498SC

Gross Area: 31.6 ft^2

Absorber Plate:
Material: All copper alloy
plate emittance: .75
Copper conductivity: 227 Btu / hr-ft-°F
Plate thickness: .0035"
Tubes: 22 copper tubes
Tube size: 3 / 8 ": I.D = .43" O.D. = .50" Length = 92-3 / 8"
Tube spacing: 2" on center
Manifolds: copper
Manifold size: Diameter 1"; Length = 49"

Covers:
Number of covers: one

Main frame:
Sidewall insulation: 1" Polyisocyanurate foam with aluminum foil facing (R8)
Bottom insulation: 1" unbonded fiberglass insulation and 1" fiberglass reinforced Polyisocyanurate foam with aluminum foil facing (R12)
Width: 46.5"
Length: 98"

Performance (based on gross collector area):
Test fluid: water
Test flowrate: .8 gpm
$F_R(\tau\alpha)_n = .769$
$F_R U_L = .750$ Btu / hr-ft^2-°F

Data from product specifications (1982,1983) and photographs.

TABLE A.1 Collector specifications used in calculations.

The following equations were used to calculate collector performance factors.

$$F = \frac{\tanh [\, m (W - D) / 2 \,]}{m (W - D) / 2} \tag{A.1}$$

$$m^2 = \frac{U_L}{k_p \, \delta} \tag{A.2}$$

where:

F = standard fin efficiency for a straight fin
W = center to center distance between tubes
δ = absorber plate thickness
U_L = collector overall loss coeficient
D = outside tube diameter
k_p = conductivity of absorber plate

$$F' = \frac{\dfrac{1}{U_L}}{W \left[\dfrac{1}{U_L (D + (W - D) F)} + \dfrac{1}{C_b} + \dfrac{1}{\Pi D_i h_{f,i}} \right]} \tag{A.3}$$

$$C_b = \frac{k_b \, b}{\gamma} \tag{A.4}$$

where:

F' = collector efficiency factor
D_i = absorber plate tube inside diameter
$h_{f,i}$ = heat transfer coefficient between fluid and tubes
C_b = bond conductance (see figure A.1)
γ = average bond thickness
b = bond width
k_b = bond thermal conductivity

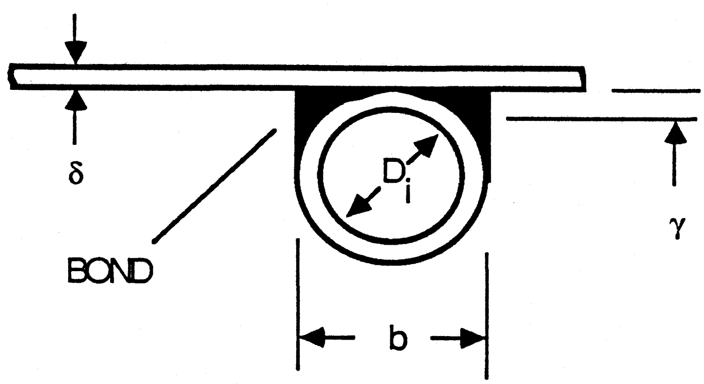

FIGURE A.1 Plate to tube bond dimensions.

$$V = \frac{GPM}{tubes\ \Pi\ (D_i / 2)^2} \tag{A.5}$$

$$Re = \frac{\rho\ V\ D_i}{\mu} \tag{A.6}$$

$$h_{f,i} = \frac{Nu\ k_f}{D_i} \tag{A.7}$$

where:

V = velocity of fluid in absorber tubes
GPM = flowrate of fluid through collector in gallons per minute
tubes = total number of absorber tubes
Re = Reynolds number of fluid in absorber tubes
ρ = collector fluid density
μ = collector fluid viscosity
Nu = Nusselt number between fluid and absorber tubes
k_f = conductivity of collector fluid

$$F_R = \frac{\dot{m}\ C_P}{A_c\ U_L} \left[1 - \exp \left(\frac{-F'\ U_L\ A_c}{\dot{m}\ C_P} \right) \right] \tag{A.8}$$

where:

F_R = collector heat removal factor
$\dot{m}$ = collector flowrate
A_c = gross collector area
C_P = collector fluid specific heat

$$T_{f,m} = T_{f,i} + \frac{Q_u / A_c}{U_L F_R} \left(1 - \frac{F_R}{F'}\right) \tag{A.9}$$

$$T_{p,m} = T_{f,i} + \frac{Q_u / A_c}{U_L F_R} \left(1 - F_R \right) \tag{A.10}$$

$$Q_u = A_c F_R \left[S - U_L (T_{f,i} - T_a) \right] \tag{A.11}$$

where:

$T_{p,m}$ = mean collector plate temperature
$T_{f,i}$ = collector inlet fluid temperature
Q_u = useful energy gain
S = absorbed solar radiation

$$U_t = \left\{ \frac{N}{\frac{C}{T_{p,m}} \left[\frac{(T_{p,m} - T_a)}{(N + f)} \right]^{e}} + \frac{1}{h_w} \right\}^{-1} + \frac{\sigma (T_{p,m} + T_a) (T^2_{p,m} + T^2_a)}{(\varepsilon_p + 0.00591\, N\, h_w)^{-1} + \frac{2N + f - 1 + 0.133\, \varepsilon_p}{\varepsilon_g} - N} \tag{A. 12}$$

$$U_b = \frac{k}{L} \tag{A.13}$$

$$U_e = \frac{(UA)_{edge}}{A_c} \tag{A.14}$$

$$U_L = U_t + U_b + U_e \tag{A.15}$$

where:

U_L = overall collector loss coefficient
U_e = collector edge loss coefficient
$(UA)_{edge}$ = edge loss coefficient-area product
U_b = collector back loss coefficient
k= back insulation thermal conductivity
L = back insulation thickness
U_t = collector top loss coefficient (W / m^2-deg C)
N = number of glass covers
$f = (1 + 0.089\, h_w - 0.1166\, h_w\, \varepsilon_p)(1 + 0.07866\, N)$
$C = 520\,(1 - 0.000051\, \beta^2)$ for $0° < \beta < 70°$. For $70° < \beta < 90°$, use $\beta = 70°$
$e = 0.43\,(1 - 100 / T_{p,m})$
β = collector tilt angle (degrees)
ε_g = emittance of glass (0.88)
ε_p = emittance of absorber plate
σ = Stefan-Boltzmann constant and is equal to 5.6697×10^{-8} W / m^2-K^4
T_a = ambient temperature (K)
$T_{p,m}$ = mean absorber plate temperature (K)
h_w = wind heat transfer coefficient (W / m^2-deg C)

For both fluids, the following conditions were assumed as the test conditions for determining the collector performance parameters.

Collector flowrate: m = 393.9 lbm / hr (.8 gpm for water at 140 °F)
Ambient temperature: T_a = 60 °F
Inlet fluid temperature: $T_{f,i}$ = 135 °F
Absorbed solar radiation: S = 193.7 Btu / hr-ft^2

The test conditions were chosen so that the collector operating with water as the fluid would have a mean fluid temperature of 140 °F, which is the temperature used to evaluate the water properties.

Equations A.1 through A.8 were first used in a trial and error method to determine the U_L for the collector during test conditions with water as the fluid. An initial guess was made for U_L, equations A.1 through A.8 used to calculate F_R, then the $F_R U_L$ product compared to the collector performance specifications. The final trial is shown in this section. Water properties were evaluated at 140 °F.

Assume $U_L = .8041$ Btu / hr-ft^2-°F

$$m = \left(\frac{.8041 \text{ Btu / hr-ft}^2\text{-°F}}{(227 \text{ Btu / hr-ft-°F})(.0035 \text{ in.})(1 \text{ ft / 12 in})} \right)^{1/2}$$

$m = 3.485 \;\; 1$ / ft

$$F = \frac{\tanh[(3.485 \;\; 1/\text{ft})(\;(2 \text{ in} - .50 \text{ in})/2)(1 \text{ ft} / 12 \text{ in})]}{(3.485 \;\; 1/\text{ft})((2 \text{ in} - .50 \text{ in})/2)(1 \text{ ft} / 12 \text{ in})}$$

$F = .984\,5$

$$V = \frac{(.8 \text{ gal / min})(1 \text{ ft}^3 / 7.4805 \text{ gal})}{(22 \text{ tubes})(\Pi\;((.43 \text{ in.})/2)^2)(1 \text{ ft}^2 / 144 \text{ in}^2)}$$

$V = 4.82$ ft / min

$$Re = \frac{(61.38 \text{ lbm / ft}^3)(4.82 \text{ ft / min})(.43 \text{ in})(60 \text{ min / hr})(1 \text{ ft} / 12 \text{ in})}{1.129 \text{ lbm / ft-hr}}$$

$Re = 563.4$ (laminar flow)

$(D_i / L)\, Re\, Pr = ((.43 \text{ in}) / (92.375 \text{ in}))(563.4)(3.0)$

$(D_i / L)\, Re\, Pr = 7.87$

From Duffie and Beckman (1980; p.134; "Fig. 3.14.1 Average Nusselt numbers in short tubes for various Prandtl numbers")

$Nu = 4.2$

$$h_{fi} = \frac{(4.2)(.3760 \text{ Btu / hr-ft-°F})}{(.43 \text{ in})(1 \text{ ft} / 12 \text{ in})}$$

$h_{fi} = 44.07$ Btu / hr-fr^2-°F

Assume: k_b is the same as copper, b is approx. the tube diameter, γ is approx. 1 / 4 the tube dia.

$$C_b = \frac{(227\ \text{Btu / hr-ft-°F})(.43\ \text{in})}{(1/4)(.43\ \text{in})}$$

$$C_b = 908\ \text{Btu / hr-ft-°F}$$

$$F' = \frac{(1 / .8041\ \text{Btu / hr-ft}^2\text{-°F})}{\left[(2\ \text{in})\left[\dfrac{1}{(.8041\ \text{Btu /hr-ft}^2\text{-°F})[.43\ \text{in} + (2\ \text{in} - .43\ \text{in})(.9845)]}\right] + \dfrac{1}{(908\ \text{Btu / hr-ft}^2\text{-°F})(12\ \text{in} / 1\ \text{ft})} + \dfrac{1}{\Pi(.43\ \text{in})(44.07\ \text{Btu / hr-ft}^2\text{-°F})}\right]}$$

$$F' = \frac{.6218}{.6295 + .0000918 + .0168} = .962$$

$$m = (.8\ \text{gal / min})(1\text{ft}^3 / 7.4805\ \text{gal})(60\ \text{min / hr})(61.38\ \text{lbm / ft}^3)$$

$$m = 393.9\ \text{lbm /hr}$$

$$F_R = \frac{(393.9\ \text{lbm / hr})(1.00\ \text{Btu / lbm-°F})}{(31.6\ \text{ft}^2)(.8041\ \text{Btu / hr-ft}^2\text{-°F})} \times \left[1 - \exp\left(\frac{-(31.6\ \text{ft}^2)(.8041\ \text{Btu / hr-gt}^2\text{-°F})(.962)}{(393.9\ \text{lbm / hr})(1.00\ \text{Btu / lbm-°F})}\right)\right]$$

$$F_R = .933$$

Check against the collector performance parameters given in the collector specifications. From table A.1, $F_R U_L = .750$.

Then:

$$U_L = \frac{F_R U_L}{F_R} = \frac{.750\ \text{Btu / hr-ft}^2\text{-°F}}{.933} = .8039\ \text{Btu / hr-ft}^2\text{-°F}$$

Which is close enough to the initial guess of .8041 Btu / hr-ft^2-°F

Equation A.9 and A.11 can be used to check for the proper mean fluid temperature.

$$Q_u / A_c = .933\ (\ 193.7 \text{ Btu / hr-ft}^2 - (.8041 \text{ Btu / hr-ft}^2\text{- °F})\ (135\ \text{°F} - 60\text{° F})$$

$$Q_u / A_c = 124.46 \text{ Btu / hr-ft}^2$$

$$T_{f,m} = 135\ \text{°F} + \frac{124.46 \text{ Btu / hr -ft}^2}{.750 \text{ Btu/ hr-ft}^2\text{-°F}} \left(1 - \frac{.933}{.962}\right)$$

$$T_{f,m} = 140.0\ \text{°F}$$

Equation A.10 can be used to find the mean plate temperature, which is used in equations A.12 through A.15 to find the overall collector loss coefficient. Since U_L is already known, equation A.12 can be used to determine the wind heat transfer coefficient that gives the same U_L as calculated with equations A.1 through A.8. The wind heat transfer coefficient will be used in equation A.12 to calculate the U_L for the collector using water-glycol as the fluid.

Equation A.13:

$$U_b = \frac{1}{R_{tot}} = \frac{1}{8 \text{ hr-ft}^2\text{-°F / Btu} + 12 \text{ hr-ft}^2\text{-°F / Btu}}$$

$$U_b = .050 \text{ Btu / hr-ft}^2\text{-°F}$$

Equation A.14:

$$U_e = \frac{\dfrac{A_{edge}}{\text{R-factor}}}{A_c} = \frac{\dfrac{(4.25 \text{ in})\ (2\ (\ 98 \text{ in} + 46.5 \text{ in}\ )\ (1 \text{ ft}^2 / 144 \text{ in}^2)}{8 \text{ hr-ft}^2\text{-°F /Btu}}}{31.6 \text{ ft}^2}$$

$$U_e = .0337 \text{ Btu / hr-ft}^2\text{-°F}$$

Rearranging equation A.15:

$$U_t = U_L - U_e - U_b = .8041 - .050 - .0337 = 0.7204 \text{ Btu / hr-ft}^2\text{-°F}$$

Equation A.12 can be used to find h_w. The calculations are not shown. Note that equation A.12 is used with SI units and then converted to English units.

$$h_w = 3.005 \text{ W / m}^2\text{-deg C} = .529 \text{ Btu / hr-ft}^2\text{-°F}$$

A trial and error method is now used to find the performance parameters for the collector using the water-glycol fluid. First a value for U_L is estimated. Then equations A.1 through A.8 are used to determine the collector parameters. Equations A.10 through A.15 are then used to calculate U_L, which is compared to the initial guess. The new U_L can be used as a new guess, and the iterative process will converge quickly. The water-glycol properties are evaluated at three temperatures. These properties are assumed constant for all the calculations, even though the fluid in the test condition is at a different temperature. This was done to establish a range of operating conditions. The results of the calculations are summarized in table A.2.

FLUID	V	Re	Pr	Nu	h	F	F'	F_R	U_L	F_RU_L	$F_R(\tau\alpha)_n$
Glycol at:											
75 °F	4.47	75	28.0	4.2	28.13	.984	.948	.912	.809	.738	.752
140 °F	4.56	175	13.0	4.3	27.60	.984	.947	.913	.809	.739	.753
200 °F	4.67	350	6.9	4.4	28.24	.984	.948	.916	.808	.740	.755
Water at:											
140°F	4.82	563	3.0	4.2	44.07	.984	.962	.933	.804	.750	.769

TABLE A.2 Results of collector calculations for determining the collector test performance parameters.

APPENDIX B

This appendix contains the FORTRAN program for the collector component used in TRNSYS for the Chinle models. This collector model includes thermal capacitance and allows for the fluid to be drained and filled.

```
C
C  THIS COMPONENT IS A MODIFIED TYPE1 COLLECTOR WHICH INCLUDES
C  THE CAPACITANCE OF THE COLLECTOR.  THE COLLECTOR IS HANDLED AS
C  A MULTI-NODE MODEL.  FIRST ORDER DIFFERENTIAL EQUATIONS ARE
C  SOLVED SEQUENTIALLY FOR EACH NODE.
C
C  THIS VERSION ASSUMES 0 CONDUCTANCE BETWEEN NODES WHEN THERE
C  IS NO FLOW. IT ALSO ALLOWS DRAINING AND FILLING.
C
C  THE COMPONENT WAS ONLY MODIFIED FOR MODE 1.
C
      SUBROUTINE TYPE44(TIME,XIN,OUT,T,DTDT,PAR,INFO)
      IMPLICIT REAL M
      INTEGER CMODE,EMODE,OMODE,GAMMA
      COMMON/SIM/TIME0,TFINAL,DELT
      COMMON/STORE/NSTORE,IAV,S(5000)
      COMMON/LUNITS/LUR,LUW,IFORM
      DIMENSION PAR(16),XIN(16),OUT(20),INFO(10)
      DIMENSION TM(200)
      DATA IUNIT/0/,RDCONV/0.017453/,PI/3.1415927/,SQRT2/1.41421356/

C
      TAUALF(THETA)=1.-B0*(1./AMAX1(0.5,COS(THETA*RDCONV))-1.)
     .             - (1.-B0)*(AMAX1(60.,THETA)-60.)/30.
C
      IF(INFO(7).GT.-1) GO TO 5
C  FIRST CALL OF SIMULATION
C
      INFO(6)=20
      CMODE=INT(PAR(1)+0.1)
C
      NP=16
      NI=11
      NODES=PAR(12)
      INFO(10)=2*NODES+2
C
      OMODE=INT(PAR(14)+0.1)
C
1     CALL TYPECK(1,INFO,NI,NP,0)
      ISTORE=INFO(10)
C
C  STORE INITIAL VALUES FOR FIRST CALL OF THE SIMULATION
C
      DO 4 I=1,NODES
        S(ISTORE+NODES+I)=PAR(13)
4     CONTINUE
      S(ISTORE+2*NODES+1)=PAR(16)
5     IF(INFO(1) .EQ. IUNIT) GO TO 55
      IUNIT=INFO(1)
```

```
C
C  SET PARAMETERS
      CMODE=INT(PAR(1)+0.1)
      NS=INT(PAR(2)+0.1)
      XNS=FLOAT(NS)
      A=PAR(3)
      CPC=PAR(4)
C
C  MODE 1
10    EMODE=INT(PAR(5)+0.1)
      GTEST=PAR(6)
      FRTAN=PAR(7)
      FRUL=PAR(8)
      EFFEC=PAR(9)
      CPF=PAR(10)
      IF(EFFEC.LE.0.) CPF=CPC
C  MODIFY TEST RESULTS TO BE BASED ON (TI-TA)/GT
      GO TO (16,17,18) ,EMODE
16    RATIO=1.
      GO TO 19
17    RATIO=1./(1.+FRUL/GTEST/CPC/2.)
      GO TO 19
18    RATIO=1./(1.+FRUL/GTEST/CPC)
19    FRTAN=RATIO*FRTAN
      FRUL=RATIO*FRUL
C
      FPUL=-GTEST*CPC*ALOG(1.-FRUL/GTEST/CPC)
      RTEST=GTEST*CPC*(1.-EXP(-FPUL/GTEST/CPC))
      FPFR=1./(GTEST*CPC/FPUL*(1.-EXP(-FPUL/GTEST/CPC)))
      CAPE=PAR(11)
      NODES=PAR(12)
      AN=A/NODES
C  OPTICAL PARAMETERS
      OMODE=INT(PAR(14)+.1)
52    BO=PAR(15)
      MASVOL=PAR(16)
      CAPW=MASVOL*CPC/A
      CAPNW=CAPE-CAPW
C  CHECK TO SEE THAT SUBTRACTING THE CAPACITANCE OF THE WATER
C  DOES NOT RESULT IN A CAP (WITH NO WATER) LESS THAN ZERO.
      IF (CAPNW .GT. 0.) GO TO 55
        WRITE(LUW,1000)
        STOP
C
C
55    ISTORE=INFO(10)
      IF(INFO(7) .GT. 0) GO TO 61
C
C  STORE FINAL TEMPERATURES AND MASS FROM LAST TIMESTEP AS
```

```
C  INITIAL VALUES FOR THIS TIMESTEP.
C
        DO 56 I=1,(NODES+1)
          S(ISTORE+I-1)=S(ISTORE+NODES+I)
56      CONTINUE
C
C  INPUTS
C
61      TIN=XIN(1)
        MIN=XIN(2)
        FLWF=XIN(3)
        TA=XIN(4)
        GT=XIN(5)
62      XKAT=1.
        GH=XIN(6)
        GD=XIN(7)
        RHO=XIN(8)
        THETA=XIN(9)
        SLP=XIN(10)
        GAMMA=IFIX(XIN(11)+.1)
C  GAMMA=1 FOR DRAINBACK
C
65      IF(INFO(7).GT.0) GO TO 100
C**DETERMINE INCIDENCE ANGLE MODIFIER, ONCE EACH TIMESTEP
        IF(GT .GT. 0. .AND. THETA .LT. 90.) GO TO 70
C
C  NO RADIATION
        XKAT=0.
        GO TO 100
C
C
C  FLAT PLATES
C
C
C    USE RELATIONS OF BRANDEMUEHL FOR EFFECTIVE INCIDENCE ANGLES
C    FOR DIFFUSE
70      EFFSKY=59.68-0.1388*SLP+0.001497*SLP*SLP
        EFFGND=90.-0.5788*SLP+0.002693*SLP*SLP
        COSSLP=COS(SLP*RDCONV)
        FSKY=(1.+COSSLP)/2.
        FGND=(1.-COSSLP)/2.
        GDSKY=FSKY*GD
        GDGND=RHO*FGND*GH
C
C    USE CONSTANT FROM ASHRAE TESTS
71      XKATB=TAUALF(THETA)
        XKATDS=TAUALF(EFFSKY)
        XKATDG=TAUALF(EFFGND)
75      XKAT=(XKATB*(GT-GDSKY-GDGND)+XKATDS*GDSKY+XKATDG*GDGND)/GT
```

```
C
C
C**THERMAL PERFORMANCE
C
100   IF(INFO(7).LE.0) OUT(10)=XKAT
      XKAT=OUT(10)
      IFLAG=0
      MASBEG=S(ISTORE+NODES)
CCCCCCCCCCCCCCCCCCCCCCCCCCCCCCCCCCCCCCCCCCCCCCCCCCCCCCCCCCCCCCCCCCC
C
C
C
C  THE FOLLOWING OUTLINE SUMMARIZES THE DECISION PROCESS
C
C     A. IF DRAINBACK (GAMMA=1)
C
C         1. IF COLLECTOR IS INITIALLY EMPTY (MASBEG=0.)
C
C             a. CAPACITANCE OF EMPTY COLLECTOR
C
C             b. CALL DIFFEQ - NO FLOW COLLECTOR
C
C         2. IF COLLECTOR IS INITIALLY NOT EMPTY (MASBEG .GT. 0.)
C
C             a. CAPACITANCE OF EMPTY COLLECTOR PLUS ANY FLUID CAP
C
C             b. CALL DIFFEQ - NO FLOW COLLECTOR
C
C             c. MIX FLUID TEMPERATURE AND DRAIN
C
C     B. IF NO DRAINBACK (GAMMA=0)
C
C         1. IF NO FLOW INTO COLLECTOR (MIN=0)
C
C             a. CAPACITANCE OF EMPTY COLLECTOR PLUS ANY FLUID
C
C             b. CALL DIFFEQ - NO FLOW COLLECTOR
C
C         2. IF FLOW INTO COLLECTOR (MIN .GT. 0)_
C
C             a. IF COLLECTOR IS NOT FULL
C
C               - MIX TEMPERATURES OF FLUID TO FILL COLLECTOR OR
C
C                 FLUID THAT ENTERS COLLECTOR WITH THE EMPTY
C
C                 COLLECTOR AND ASSUME A UNIFORM TEMPERATURE
C
C               - CALL DIFFEQ, TREAT AS A NO FLOW COLLECTOR FOR
```

```
C
C                   THE TIME THAT IT TOOK TO FILL THE COLLECTOR
C
C                 - CALL DIFFEQ, FOR THE TIME THAT FLUID LEAVES THE
C
C                   COLLECTOR
C
C              b. IF COLLECTOR IS FULL
C
C                 - CALL DIFFEQ WITH A CONSTANT FLOW RATE
C
C                   THROUGHOUT THE TIMESTEP
C
C
C
CCCCCCCCCCCCCCCCCCCCCCCCCCCCCCCCCCCCCCCCCCCCCCCCCCCCCCCCCCCCCCCCCCCCCCC
C
      IF (GAMMA .EQ. 0) GO TO 111
         IF (MASBEG .EQ. 0.) GO TO 112
            CAP=CAPNW+MASBEG*CPC/A
            GO TO 113
111      IF (MIN .GT. 0.) GO TO 116
            IF (MASBEG .EQ. 0.) GO TO 112
               CAP=CAPNW+MASBEG*CPC/A
               GO TO 113
112   CAP=CAPNW
113   QU=0.
      TTOTAL=0.
      SOLAR=XKAT*GT
      AA=-FPUL/CAP
      BB=(FRTAN*FPFR*SOLAR+FPUL*TA)/CAP
      DO 114 I=1,NODES
        TM1=S(ISTORE+I-1)
        CALL DIFFEQ(TIME,AA,BB,TM1,TM(I),TMBAR)
        S(ISTORE+NODES+I)=TM(I)
        TTOTAL=TTOTAL+TMBAR
114   CONTINUE
      TOAVE=TMBAR
      MOUT=0.
      IF (GAMMA .EQ. 1 .AND. MASBEG .GT. 0.) GO TO 115
         MDRAIN=0.
         MASEND=MASBEG
         ENTHAL=0.
         GO TO 300
115   TOAVE=TTOTAL/NODES
      MDRAIN=MASBEG/DELT
      MASEND=0.
      ENTHAL=MDRAIN*CPC*TOAVE
      GO TO 300
```

```
116   MOUT=MIN
      MDRAIN=0.
      MASEND=AMIN1(MASVOL,(MIN*DELT+MASBEG))
      IF (ABS(MASBEG-MASVOL) .LT. .001) GO TO 119
         TTOTAL=0.
         DO 117 I=1,NODES
           TTOTAL=TTOTAL+S(ISTORE+I-1)
117      CONTINUE
         TTOTAV=TTOTAL/NODES
         CAP=MASEND*CPC/A+CAPNW
         TMIX=((MASEND-MASBEG)*CPC*TIN/A+MASBEG*CPC*TTOTAV/A
     .        +CAPNW*TTOTAV)/CAP
         TIMFIL=(MASEND-MASBEG)/MIN
         SOLAR=XKAT*GT
         AA=-FPUL/CAP
         BB=(FRTAN*FPFR*SOLAR+FPUL*TA)/CAP
         DO 118 I=1,NODES
            TM1=TMIX
            CALL DIFF2(TIME,TIMFIL,AA,BB,TM1,TM(I),TMBAR)
            S(ISTORE+NODES+I)=TM(I)
118      CONTINUE
         TOAVE=TMBAR
         MOUT=AMAX1((MIN*DELT+MASBEG-MASVOL)/DELT,0.)
         MDRAIN=0.
         QU=0.
         ENTHAL=-MIN*CPC*TIN
         IF (MOUT .EQ. 0.) GO TO 300
C
C  IFLAG INDICATES THAT THE COLLECTOR FILLED DURING THIS TIMESTEP
         IFLAG=1
119   FLWC=MOUT
C    PUMP ON
120   R1=XNS*FLWC*CPC/A*(1.-EXP(-FPUL*A/XNS/FLWC/CPC))/RTEST
      XK=R1*A*FRUL/FLWC/CPC/XNS
      R2=(1.-(1.-XK)**NS)/XNS/XK
C  NOTE: RATIO IS NOT USED IN THIS PROGRAM, BUT LEFT OVER FROM
C        THE TYPE1 COLLECTOR MODEL.
      RATIO=R1*R2
      SOLAR=XKAT*GT
      AA=-((FPUL+FLWC*CPC/AN)/CAP)
      TTOTAL=0.
      DO 150 I=1,NODES
         TM1=S(ISTORE+I-1)
         IF (IFLAG .EQ. 1) TM1=TM(I)
            IF(I .EQ. 1) THEN
              TIND=TIN
            ELSE
              TIND=TMBAR
            END IF
```

```
          BB=(FRTAN*FPFR*SOLAR+FPUL*TA+FLWC*CPC/AN*TIND)/CAP
          IF (IFLAG .EQ. 1) GO TO 130
          CALL DIFFEQ(TIME,AA,BB,TM1,TM(I),TMBAR)
          GO TO 140
130       CALL DIFF2(TIME,(DELT-TIMFIL),AA,BB,TM1,TM(I),TMBAR)
140       TTOTAL=TTOTAL+TM(I)
          S(ISTORE+NODES+I)=TM(I)
150    CONTINUE
       TMEAN=TTOTAL/NODES
       TOAVE=TMBAR
       QU=FLWC*CPC*(TOAVE-TIN)
       ENTHAL=CPC*(MOUT*TOAVE-MIN*TIN)
C
C  OUTPUTS
300    S(ISTORE+2*NODES+1)=MASEND
       OUT(1)=TOAVE
       OUT(2)=MOUT
       OUT(3)=ENTHAL
       OUT(4)=MDRAIN
       OUT(5)=QU
       IF (NODES .GT. 10) GO TO 400
         DO 350 I=1,NODES
           OUT(10+I)=TM(I)
350      CONTINUE
400    RETURN
1000   FORMAT(1X,'****ERROR IN COLLECTOR COMPONENT,
      . (CAP FLUID + CAP NO FLUID) IS .GT. CAPE****')
       END
C
C THIS SUBROUTINE WAS COPIED FROM TRNSYS AND MODIFIED TO SOLVE
C THE DIFFERENTIAL EQUATIONS FOR TIME PERIODS OTHER THAN A
C FULL TIMESTEP
C
       SUBROUTINE DIFF2(TIME,DELT2,AA,BB,TI,TF,TBAR)
       COMMON /SIM/ TIMEO,TFINAL,DELT
C
       IF(TIME .GT. TIMEO) GO TO 10
C  MAINTAIN INITIAL CONDITIONS AT ZERO TIME
       TF = TI
       TBAR = TI
       RETURN
10     IF(ABS(AA) .GT. 0.) GO TO 20
C  SOLUTION TO DIFFERENTIAL EQUATION IS LINEAR
       TF = BB*DELT2 + TI
       TBAR = (TF + TI)/2.
       RETURN
C  SOLUTION TO DIFFERENTIAL IS EXPODENTIAL
20     TF = (TI + BB/AA)*EXP(AA*DELT2) - BB/AA
       TBAR = (TI + BB/AA)/AA/DELT2*(EXP(AA*DELT2) - 1.) - BB/AA
```

```
RETURN
END
```

APPENDIX C

This appendix contains the FORTRAN program for the pipe component used in TRNSYS for the Chinle models. This model includes pipe wall thermal capacitance and allows for the fluid to be drained and filled.

```
C
C  THIS COMPONENT IS AN ALTERED TYPE39 VARIABLE VOLUME TANK.
C  IT WAS CREATED FOR USE IN A DRAIN-BACK SYSTEM.
C  IT DRAINS IN ONE TIMESTEP WHEN GIVEN A DRAIN SIGNAL AND
C  MODELS THE PIPE WALL CAPACITANCE USING AN EQUIVALENT PIPE
C  LENGTH.
C
      SUBROUTINE TYPE36(TIME,XIN,OUT,T,DTDT,PAR,INFO)
C THIS SUBROUTINE MODELS A VARIABLE VOLUME TANK WHICH
C HAS UPPER AND LOWER VOLUME LIMITS
      DIMENSION PAR(13),XIN(4),OUT(20),INFO(10)
      REAL MIN,MOUT,LHTAV,MFIN,MAV,MFST,MZERO,MRET
      COMMON/SIM/TIMEO,TFINAL,DELT
      DATA IUNIT/0/
      DATA TUNE/10000.0/
C
      IF(INFO(7).GT.-1) GO TO 5
      INFO(6)=9
      NI = 4
      NP = 13
      ND = 0
      CALL TYPECK(1,INFO,NI,NP,ND)
C STORE T INITIAL AND M INITIAL FOR FIRST CALL OF SIMULATION
      OUT(19)=PAR(11)
      OUT(20)=PAR(12)
C SET PARAMETERS
5     IF(INFO(1).EQ.IUNIT) GO TO 10
      IUNIT=INFO(1)
      MODE=INT(PAR(1)+0.1)
      VOL = PAR(2)
      VMIN=AMAX1(PAR(3),.001*VOL)
      VMAX=AMIN1(PAR(4),.999*VOL)
C SET T-ZERO AND M-ZERO FOR DELT-E CALCULATION
      TZERO = PAR(11)
      MZERO = PAR(12)*PAR(10)
      CIRC=PAR(5)
      AEND=PAR(6)
      HEIGHT=VOL/AEND
      UW = PAR(7)
      UD = PAR(8)
      CP = PAR(9)
      DEN = PAR(10)
      LACT=PAR(13)
10    IF(INFO(7) .NE. 0 ) GO TO 12
C SET T INITIAL AND M INITIAL
      OUT(19)=OUT(10)
      OUT(20)=OUT(11)
12    CONTINUE
      TFST = OUT(19)
```

```
      VFST = OUT(20)
      MFST=VFST*DEN
C READ INPUTS
      TIN = XIN(1)
      MIN = XIN(2)
      DRAIN = XIN(3)
      TAMB = XIN(4)
      MRET=0.
      MOUT=0.
      LEVEL=0
      IF(TIME.GT.TIME0) GO TO 15
C  USE INITIAL CONDITIONS AT START OF SIMULATION
      TAV=TFST
      VOLAV=VFST
      TFIN=TFST
      VOLFIN=VFST
      MFIN=VOLFIN*DEN
      GO TO 150
C  CHECK FOR DRAIN BACK SIGNAL
15    IF(DRAIN .LT. .9) GO TO 16
      MOUT=(MFST-VMIN*DEN)/DELT
C CHECK FOR MAXIMUM OR MINIMUM LIQUID VOLUME
16    VFTEST=VFST+DELT*(MIN-MOUT)/DEN
      IF((VFTEST-VMAX) .LT. -1.E-6) GO TO 19
      MRET=MIN-MOUT-AMAX1((VMAX*DEN-MFST)/DELT,0.)
      IF (MRET .LT. 1.E-6) MRET=0.
      LEVEL = 1
      GO TO (17,18) ,MODE
17    MOUT=MOUT+MRET
      GO TO 20
18    MIN=MIN-MRET
      GO TO 20
   19 IF((VFTEST-VMIN) .GT. 1.E-6) GO TO 20
      MOUT=AMAX1((MFST-VMIN*DEN)/DELT,0.)+MIN
      LEVEL = -1
   20 CONTINUE
C CALCULATE FINAL AND AVERAGE FOR TANK FLUID MASS AND VOLUME
      MFIN = MFST +DELT*(MIN-MOUT)
      MAV = (MFST+MFIN)/2.0
      VOLFIN = MFIN/DEN
      VOLAV = MAV/DEN
      LHTAV = VOLAV/AEND
C CALCULATE TANK UA USING ACTUAL PIPE INSIDE AREA
C (DOESN'T INCLUDE EQUIVALENT LENGTH)
      UA = UW * CIRC * LACT
C CHECK FOR MIN = MOUT
      CHECK = ABS(MIN-MOUT)
      XXTEST = (MIN + UA/CP)/TUNE
      IF(CHECK .LT. XXTEST) GO TO 75
```

```
C CHECK FOR NO FLOW
      IF(MIN .LT. 0.001 .AND. MOUT .LT. 0.001) GO TO 75
C EQUATIONS FOR FLOW CONDITION
   50 CONTINUE
      B = MIN + UA/CP
      C = MIN - MOUT
      D = MIN * TIN + (UA/CP) * TAMB
      CC = TFST-D/B
      DD = (1+(C*DELT)/MFST)**(-B/C)
      TFIN = CC*DD+D/B
      AA = (TFST-D/B)/(C-B)
      BB = (1+(C*DELT)/MFST)**(1-B/C)
      TAV = AA*(MFST/DELT)*(BB-1.0) + D/B
      GO TO 150
   75 CONTINUE
C EQUATIONS FOR MIN = MOUT CONDITION
      B = MIN + UA/CP
      D = MIN *TIN + (UA/CP) * TAMB
      G = -B/MFST
      H = 1.0/(DELT*(-B))
      A1 = D - B*TFST
      E = A1 * EXP(DELT*G)
      TFIN = (E-D)/(-B)
      TAV =H*((E-A1)/G)+D/B
  150 CONTINUE
      DE = CP*(MFIN*TFIN-MZERO*TZERO)
      HIN=CP*MIN*TIN
      HOUT=CP*MOUT*TAV
      QLOSS = UA*(TAV - TAMB)
C SET OUTPUTS
      OUT(1) = TAV
      OUT(2) = MOUT-MRET
      OUT(3)=TAV
      IF(MODE.EQ.2) OUT(3)=TIN
      OUT(4) = MRET
      OUT(5) = VOLAV
      OUT(6) = HIN-HOUT
      OUT(7) = QLOSS
      OUT(8) = DE
      OUT(9)  = LEVEL
      OUT(10) = TFIN
      OUT(11) = VOLFIN
      OUT(12) = MAV
      OUT(13) = LHTAV/HEIGHT
      RETURN
      END
```

APPENDIX D

This appendix contains the FORTRAN program for the type "49" mixing valve component used in TRNSYS for the Chinle models. This model determines the mass flowrates from each storage tank in order to supply the DHW and SPH loops with fluid at the proper temperature.

```
C
C  THIS PROGRAM WAS WRITTEN TO SIMULATE THE MIXING VALVE IN THE
C  CHINLE SOLAR ENERGY SYSTEM.  USING TWO INLET TEMPERATURES AND
C  A DEMAND FLOW RATE IT DETERMINES THE FLOW RATE OF EACH
C  TEMPERATURE SOURCE IN ORDER TO OUTPUT THE SET TEMPERATURE
C  (IF POSSIBLE).
C
      SUBROUTINE TYPE49(TIME,XIN,OUT,T,DTDT,PAR,INFO)
      REAL LOAD
      DIMENSION XIN(3),OUT(4),PAR(2),INFO(20)
      INFO(6)=4
      TSET=PAR(1)
      NSTK=PAR(2)
      TST1=XIN(1)
      TST2=XIN(2)
      LOAD=XIN(3)
      IF(INFO(7) .GT. NSTK) GO TO 100
C
C  CHECK FOR NO FLOW
C
      IF(LOAD .GE. 0.01) GO TO 10
       FLWST1=0.
       FLWST2=0.
       TMIX=TST2
       GO TO 100
C
C  CHECK INPUT STATES
C
10    IF((TST2-TSET) .GE. 0.) GO TO 30
      IF((TST2-TST1) .GE. -.1) GO TO 30
      IF((TSET-TST1) .GT. -.1) GO TO 20
C
C  MIX SOURCE STREAMS
C
        FRAC=(TSET-TST2)/(TST1-TST2)
        FLWST1=FRAC*LOAD
C  THE NEXT TWO LINES WERE NEEDED TO PREVENT EXCESSIVE ITERATING.
        IF (INFO(7) .EQ. 0) OUT(3)=FLWST1
        IF (ABS((FLWST1-OUT(3))/(OUT(3)+.001)) .LT. .01)
     .  FLWST1=OUT(3)
        FLWST2=LOAD-FLWST1
        TMIX=(FLWST1*TST1+FLWST2*TST2)/(FLWST1+FLWST2)
      GO TO 100
C
C  USE ONLY FISRT SOURCE
C
20    FLWST1=LOAD
      FLWST2=0.
      TMIX=TST1
```

```
      GO TO 100
C
C  USE ONLY SECOND SOURCE
C
30    FLWST1=0.
      FLWST2=LOAD
      TMIX=TST2
C
C  OUTPUT
C
100   OUT(1)=TMIX
      OUT(2)=LOAD
      OUT(3)=FLWST1
      OUT(4)=FLWST2
      END
```

APPENDIX E

This appendix contains the FORTRAN program for the collector loop controller used in TRNSYS for the Chinle models.

```
C
C  THIS TRNSYS COMPONENT WAS WRITTEN TO SIMULATE THE CONTROLLER USED

C  IN THE CHINLE,AZ. SOLAR ENERGY SYSTEM.
C
C
      SUBROUTINE TYPE45(TIME,XIN,OUT,T,DTDT,PAR,INFO)
      DIMENSION OUT(11),XIN(3),INFO(10),PAR(15)
      INTEGER NSTK,COUNTA,COUNTB,COUNTC,OKAON,OKAOFF,OKBON,OKBOFF
      INTEGER TOTALH,TOTALL,HIFLAG,LIST,TMODE
      REAL LASTA,LASTB,LEAD,LAG
      COMMON/SIM/TIME0,TFINAL,DELT
      COMMON /LUNITS/ LUR,LUW,IFORM
      INFO(6)=5
C
C SET PARAMETERS  AND INITIAL VALUES FIRST CALL OF SIMULATION
C
      IF(INFO(7) .GT. -1) GO TO 10
      TONA=PAR(1)
      TOFFA=PAR(2)
      TONB=PAR(3)
      TOFFB=PAR(4)
C  TIMEA AND TIMEB ARE MINIMUM TIME LIMITS FOR PUMPS TO BE
C  ON OR OFF.
      TIMEA=PAR(5)
      TIMEB=PAR(6)
      NSTK=PAR(7)
      THIGH=PAR(8)
      TLOW=PAR(9)
      DEADB=PAR(10)
      LIST=IFIX(PAR(11)+.1)
      IMODE=IFIX(PAR(12)+.1)
C  IMODE = 0 FOR DRAINBACK; 1 FOR RECIRC
      RECDB=PAR(13)
      TSTORLO=PAR(14)
      TMODE=IFIX(PAR(15)+.1)
C  TMODE = 0 FOR COLLECTOR TEMP; 1 FOR BOTH COLLECTOR AND HEAT
C  EXCHANGER
      TOTALH=0
      TOTALL=0
      OKAON=0
      OKAOFF=0
      OKBON=0
      OKBOFF=0
      STATEA=0.
      STATEB=0.
      STATED=0.
      STATER=0.
      TIMEHI=0.
```

```
      TIMELO=0.
      AOFF=(TIME-TIMEA-1.)
      AON=(TIME-TIMEA-1.)
      BOFF=(TIME-TIMEB-1.)
      BON=(TIME-TIMEB-1.)
      LEAD=0.
      LAG=0.
      DRNBK=0.
      RECIRC=0.
      COUNTA=0
      COUNTB=0
      COUNTC=0
      GO TO 75
10    IF(INFO(7) .GT. 0) GO TO 75
      COUNTA=0
      COUNTB=0
      COUNTC=0
      ITERFL=1000
C
C  KEEP TRACK OF DRAINBACK AND/OR RECIRCULATION TIME
C
      IF (OUT(3) .LT. .01 .AND. OUT(4) .LT. .01) GO TO 15
      IF (HIFLAG .EQ. 0) GO TO 12
         TIMEHI=TIMEHI+DELT
         GO TO 15
12    TIMELO=TIMELO+DELT
C
C  CHECK TO SEE IF THE OUTPUTS CHANGED DURING THE LAST TIMESTEP AND
C  IF SO SET THE TIMERS AND/OR COUNTERS AS REQUIRED.
C
C  CHECK PUMP A
15    IF(ABS(STATEA-OUT(1)) .LT. .001) GO TO 30
      STATEA=OUT(1)
      IF(OUT(1) .GT. .9) GO TO 20
      AOFF=TIME-DELT
      GO TO 30
20    AON=TIME-DELT
30    OKAON=0
      OKAOFF=0
C  CHECK TO SEE IF PUMP A CAN TURN ON OR OFF.
      IF((TIME-AON) .GE. TIMEA) OKAOFF=1
      IF((TIME-AOFF) .GE. TIMEA) OKAON=1
C  CHECK PUMB B
      IF(ABS(STATEB-OUT(2)) .LT. .001) GO TO 50
      STATEB=OUT(2)
      IF(OUT(2) .GT. .9) GO TO 40
      BOFF=TIME-DELT
40    BON=TIME-DELT
50    OKBON=0
```

```
      OKBOFF=0
C  CHECK TO SEE IF PUMP B CAN TURN ON OR OFF.
      IF((TIME-BOFF) .GE. TIMEB) OKBON=1
      IF((TIME-BON) .GE. TIMEB) OKBOFF=1
C  CHECK FOR DRAINBACK OR RECIRCULATION
      IF(ABS(OUT(3)-STATED) .LT. .001) GO TO 60
        STATED=OUT(3)
        IF(OUT(3) .LT. .1) GO TO 70
      GO TO 65
60    IF(ABS(OUT(4)-STATER) .LT. .001) GO TO 70
        STATER=OUT(4)
        IF(OUT(4) .LT. .1) GO TO 70
65    IF(HIFLAG .EQ. 0) GO TO 66
         TOTALH=TOTALH+1
         GO TO 70
66    TOTALL=TOTALL+1
70    IF(ABS(TFINAL-TIME) .GT. .001) GO TO 75
      WRITE(LUW,*)
      STKPER=100*STUCK/((TFINAL-TIMEO)/DELT)
      IF(STKPER .GE. 5.) WRITE(LUW,590) STKPER
      WRITE(LUW,600) TOTALH,TOTALL
      WRITE(LUW,610) TIMEHI
      WRITE(LUW,620) TIMELO
C
C  IF CONTROL FUNCTIONS HAVE CHANGED NSTK TIMES. STICK CONTROLLER
C
75    IF(COUNTA .LT. NSTK) GO TO 80
        LEAD=1.
        IF (STATEA .LT. .001) LAG=1.0
        DRNBK=0.
        RECIRC=0.
        GO TO 90
80    IF(COUNTB .GE. NSTK) GO TO 90
      IF(COUNTC .LT. NSTK) GO TO 100
        IF(IMODE .EQ. 0) THEN
          LEAD=0.
          LAG=0.
          DRNBK=1.
          RECIRC=0.
        ELSE
          LEAD=0.
          LAG=0.
          DRNBK=0.
          RECIRC=1.
        END IF
90    IF (INFO(7) .GT. ITERFL) GO TO 190
      ITERFL=INFO(7)
      STUCK=STUCK+1.
      GO TO 190
```

```
C
C  READ INPUTS
C
100    TCOLL=XIN(1)
       TSTOR=XIN(2)
       TCOLHX=XIN(3)
       IF(TSTOR .LT. TSTORLO) WRITE(LUW,630) TSTOR,TIME
C
C  DECISION ROUTINE
C
C  CHECK FOR DRAIN BACK CONDITIONS
       IF (DRNBK .GT. .9 .OR. RECIRC .GT. .9) GO TO 110
       IF (TSTOR .GT. THIGH) GO TO 160
       IF (TCOLL .LT. TLOW) GO TO 170
       GO TO 120
110    IF ((THIGH-TSTOR) .LT. DEADB) GO TO 180
       IF (HIFLAG .GT. 0) GO TO 120
       IF (IMODE .EQ. 0) THEN
         IF((TCOLL-TLOW) .LT. DEADB) GO TO 180
       ELSE
           IF(TMODE .EQ. 1) THEN
             IF((TCOLHX-TLOW) .LT. RECDB .OR. (TCOLL-TLOW) .LT. RECDB
)
     .          GO TO 180
           ELSE
             IF((TCOLL-TLOW) .LT. RECDB) GO TO 180
           END IF
       END IF
       IF (LIST .EQ. 1) WRITE(LUW,580) TIME
120    DRNBK=0.
       RECIRC=0.
C  CHECK LEAD PUMP
       IF(LEAD .EQ. 1.) GO TO 130
       IF(OKAON .EQ. 0 .OR. (TCOLL-TSTOR) .LT. TONA) GO TO 190
       LEAD=1.
       LAG=1.
       GO TO 190
130    IF(OKAOFF .EQ. 0 .OR. (TCOLL-TSTOR) .GT. TOFFA) GO TO 140
       LEAD=0.
       LAG=0.
       GO TO 190
C  CHECK LAG PUMP
140    IF(LAG .EQ. 1.) GO TO 150
       IF(OKBON .EQ. 0 .OR. (TCOLHX-TSTOR) .LT. TONB) GO TO 190
       LAG=1.
       GO TO 190
150    IF(OKBOFF .EQ. 0 .OR. (TCOLHX-TSTOR) .GT. TOFFB) GO TO 190
       LAG=0.
       GO TO 190
```

```
C
C  INITIATE DRAINBACK
C
160    IF(LIST .EQ. 1) WRITE(LUW,560) TIME
       HIFLAG=1
       GOTO 180
170    IF(LIST .EQ. 1) WRITE(LUW,570) TIME
       HIFLAG=0
180    LEAD=0.
       LAG=0.
       DRNBK=1.
       RECIRC=0.
       IF (IMODE .EQ. 0 .OR. HIFLAG .EQ. 1) GO TO 190
       DRNBK=0.
       RECIRC=1.
190    OUT(1)=LEAD
       OUT(2)=LAG
       OUT(3)=DRNBK
       OUT(4)=RECIRC
C  SET CONTROL SIGNALS FOR THE COLLECTOR LOOP PUMPS FLOW DIVERTER
C  AND THE STORAGE LOOP PUMP.
C
       FLOW=0.
       IF(LAG .GT. .9) FLOW=.5
       OUT(5)=FLOW
       IF(OUT(1) .NE. OUT(6)) COUNTA=COUNTA+1
       IF(OUT(2) .NE. OUT(7)) COUNTB=COUNTB+1
       IF(OUT(3) .NE. OUT(8) .OR. OUT(4) .NE. OUT(9)) COUNTC=COUNTC+1

       OUT(6)=OUT(1)
       OUT(7)=OUT(2)
       OUT(8)=OUT(3)
       OUT(9)=OUT(4)
       OUT(10)=TOTALL
       OUT(11)=TOTALH
300    RETURN
560    FORMAT(1X,'WARNING: HIGH TEMP. DRAIN AT TIME=',1X,F8.3)
570    FORMAT(1X,'WARNING: LOW TEMP. DRAIN OR RECIRC AT TIME=',1X,F8.
3)
580    FORMAT(1X,'DRAINBACK OR RECIRC CONDITION END AT TIME=',1X,F8.3
)
590    FORMAT(1X,'**WARNING** COLLECTOR CONTROLLER STUCK',1X,F5.1,1X,
     .       'PERCENT OF THE TIMESTEPS.')
600    FORMAT(1X,' **** NOTE **** ',I6,'  HIGH TEMP. DRAINS;  ',I6,
     .       '  LOW TEMP. DRAINS OR RECIRCS.(REVISED 4-21-86)')
610    FORMAT(1X,'TOTAL TIME AT HIGH TEMPERATURE CONDITION=',F8.3,1X,
     .        'HOURS.')
620    FORMAT(1X,'TOTAL TIME AT LOW TEMPERATURE CONDITION= ',F8.3,1X,
     .        'HOURS.')
```

```
630   FORMAT(1X,'STORAGE TEMP.= ',F6.2,1X,'AT TIME ',F7.2)
      END
```

APPENDIX F

This appendix contains the TRNSYS deck used to model the Chinle system. The deck is presently set up for modeling Chinle as a drain-back system. Ony the parameters of the collector loop controller need to be changed in order to model Chinle with recirculation freeze protection.

```
NOLIST
*
*  THIS DECK WAS CREATED TO SIMULATE THE DHW AND SPACE HEATING
*  SOLAR ENERGY SYSTEM ON THE INDIAN HEALTH FACILITY AT CHINLE,AZ.
*  IT INCLUDES PIPE WALL CAPACITANCE, COLLECTOR CAPACITANCE, AND
*  DRAIN-BACK.
*
*  WRITTEN 1986, J.P. KUMMER
*
*
SIMULATION 1. 8760. .03125
WIDTH 132
TOLERANCES -.001 -.001
LIMITS 100 50 90
*
CONSTANTS 5
TDHW=46. MDHW=1753.
UA=81225. CAP=450000. ECMIN=45000.
*
UNIT 1 TYPE 9      DATA READER
PARAMETERS 10
2 1. -1 .08808 0. 2 .18 32. 10 1
(14X,F4.0,1X,F4.0)
*
UNIT 2 TYPE 16     RADIATION PROCESSOR(ALBUQUERQUE)(ERBS CORR.)
PARAMETERS 7
3 1 1 35.03 429.05 0. -1
INPUTS 6
1,1 1,19 1,20 0,0 0,0 0,0
0. 0. 1. .2 55. 0.
*
UNIT 3 TYPE 44         SOLAR COLLECTOR (MULTI-NODE; DRAINBACK)
PARAMETERS 16
1 1 10112. 1 1 12.672 .769 .750 0. 1. .410
10 45. 1 .1 3171.
INPUTS 11
14,3 14,4 0,0 1,2 2,6 2,4 2,5 0,0 2,9 2,10 10,3
45. 0. 0 50. 0 0 0 .2 0 0. 0.
*
UNIT 4 TYPE 36     COLL. OUTLET PIPE (INCLUDES PIPE WALL CAP.)
PARAMETERS 13
1 79.78 17.355 79.78 1.054 .0884 .113 0. 1. 62.4 50. 79.78 706.
INPUTS 4
3,1 3,2 10,3 0,0
45. 0. 0. 50.
*
UNIT 5 TYPE 5      HEAT EXCHANGER
PARAMETERS 4
4 .6 1. 1.
```

```
INPUTS 4
4,3 4,4 17,1 17,2
45. 0. 100. 0.
*
UNIT 6 TYPE 31     COLL. SIDE X-CHANGER OUTLET PIPE (PLUG FLOW)
PARAMETERS 6
.3355 10. .113 62.4 1. 55.
INPUTS 3
5,1 5,2 0,0
55. 0. 60.
*
UNIT 72 TYPE 11    COLL. PIPES DRAIN TEE PIECE
PARAMETER 1
1
INPUTS 4
4,1 4,2 14,1 14,2
45. 0. 45. 0.
*
UNIT 70 TYPE 11    COLLECTOR AND PIPES DRAIN TEE PIECE
PARAMETER 1
1
INPUTS 4
3,1 3,4 72,1 72,2
45. 0. 45. 0.
*
UNIT 73 TYPE 11    COLL. LOOP RUN/DRAIN TEE PIECE
PARAMETER 1
1
INPUTS 4
70,1 70,2 6,1 6,2
45. 0. 50. 0.
*
UNIT 7 TYPE 39     DRAIN BACK TANK
PARAMETERS 12
1 200.5 10. 200.5 15.71 19.63 .04 .04 1. 62.4 100. 15.
INPUTS 4
73,1 73,2 13,2 0,0
55. 0. 0. 60.
*
UNIT 8 TYPE 31     COLL. PUMP INLET PIPE (PLUG FLOW)
PARAMETERS 6
.3355 10. .113 62.4 1. 55.
INPUTS 3
7,1 7,2 0,0
55. 0. 60.
*
UNIT 9 TYPE 11     FLOW DIVERTER
PARAMETERS 1
2
```

```
INPUTS 3
8,1 8,2 10,5
55. 0. .5
*
UNIT 10 TYPE 45    COLLECTOR LOOP CONTROLLER
PARAMETERS 15
10. 2. 5. 2.5 .233 .233 4 220. 45. 10. 0. 0. 10. 40. 1   (DB,HX)
INPUTS 3
3,1 20,1 4,3
55. 100. 55.
*
UNIT 68 TYPE 15    ALG. OPERATOR (.OR. FUNCTION)
PARAMETERS 1
12
INPUTS 2
10,1 10,4
0. 0.
*
UNIT 11 TYPE 3     COLLECTOR LEAD PUMP
PARAMETERS 2
80085. 1.
INPUTS 3
9,1 9,2 68,1
60. 0. 0.
*
UNIT 12 TYPE 3     COLLECTOR LAG PUMP
PARAMETERS 2
80085. 1.
INPUTS 3
9,3 9,4 10,2
60. 0. 0.
*
UNIT 13 TYPE 11    TEE PIECE
PARAMETERS 1
1
INPUTS 4
11,1 11,2 12,1 12,2
55. 0. 55. 0.
*
UNIT 14 TYPE 36    COLL. INLET PIPE (INCLUDES PIPE WALL CAP.)
PARAMETERS 13
1 79.78 17.355 79.78 1.054 .0884 .113 0. 1. 62.4 50. 79.78 706.
INPUTS 4
13,1 13,2 10,3 0,0
45. 0. 0. 50.
*
UNIT 16 TYPE 2     STORAGE LOOP PUMP CONTROLLER
PARAMETERS 3
5 200. 3.
```

```
INPUTS 3
4,3 20,1 10,1
55. 100. 0.
*
UNIT 69 TYPE 15    ALG. OPERATOR (.OR. FUNCTION)
PARAMETERS 1
12
INPUTS 2
16,1 10,4
0. 0.
*
UNIT 17 TYPE 3     STORAGE LOOP PUMP
PARAMETERS 2
140650. 1.
INPUTS 3
21,1 21,2 69,1
100. 0. 0.
*
UNIT 22 TYPE 49    LOAD MIXER
PARAMETERS 2
135. 50
INPUTS 3
20,1 21,1 41,2
100. 100. 0.
*
UNIT 20 TYPE 4     STORAGE TANK 1
PARAMETERS 6
1 534.76 1. 62.4 .04 -5.
INPUTS 5
5,3 5,4 21,3 22,3 0,0
130. 0. 130. 0. 60.
DERIVATIVES 1
100.
*
UNIT 21 TYPE 4     STORAGE TANK 2
PARAMETERS 6
1 534.76 1. 62.4 .04 -5.
INPUTS 5
20,1 20,2 41,1 22,2 0,0
130. 0. 130. 0. 60.
DERIVATIVES 1
100.
*
*****************************************************************
*                           LOAD SECTION                        *
*****************************************************************
*
UNIT 24 TYPE 11     DHW FLOW MIXER
PARAMETERS 1
```

```
3
INPUTS 5
52,1 39,2 22,1 39,4 26,1
130. 0. 130. 0. 0.
*
UNIT 26 TYPE 8     DHW PUMP AND VALVE CONTROLLER
PARAMETERS 7
4 0 128. 500. 250. 117. 10.
INPUTS 2
34,1 20,1
125. 130.
*
UNIT 27 TYPE 15    DHW ALGEBRAIC OPERATOR
PARAMETERS 1
12
INPUTS 2
26,1 26,2
0 0
*
UNIT 28 TYPE 3     DHW PUMP
PARAMETERS 2
15000. 1.
INPUTS 3
24,1 24,2 27,1
130. 0. 0.
*
UNIT 31 TYPE 11    DHW FLOW DIVERTER
PARAMETERS 1
2
INPUTS 3
28,1 28,2 0,0
130. 0. .5
*
UNIT 32 TYPE 5     DHW HEAT X-CHANGER 1
PARAMETERS 4
4 .6 1. 1.
INPUTS 4
31,1 31,2 34,1 0,0
130. 0. 125. 15000.
*
UNIT 33 TYPE 5     DHW HEAT X-CHANGER 2
PARAMETERS 4
4 .6 1. 1.
INPUTS 4
31,3 31,4 35,1 0,0
130. 0. 125. 15000.
*
UNIT 74 TYPE 11    DHW LOAD SPLITTER
PARAMETERS 1
```

```
2
INPUTS 3
37,1 37,2 0,0
TDHW MDHW .5
*
UNIT 34 TYPE 4      DHW STORAGE 1
PARAMETERS 6
1 66.8 1. 62.4 .04 -9.45
INPUTS 5
32,3 32,4 74,1 74,2 0,0
130. 0. 55. 0. 60.
DERIVATIVES 1
125.
*
UNIT 35 TYPE 4      DHW STORAGE 2
PARAMETERS 6
1 66.8 1. 62.4 .04 -9.45
INPUTS 5
33,3 33,4 74,3 74,4 0,0
130. 0. 55. 0. 60.
DERIVATIVES 1
125.
*
UNIT 36 TYPE 11     DHW TEE PIECE
PARAMETERS 1
1
INPUTS 4
32,1 32,2 33,1 33,2
130. 0. 130. 0.
*
UNIT 75 TYPE 11     DHW LOAD MIXER
PARAMETERS 1
1
INPUTS 4
34,3 34,4 35,3 35,4
125. 0. 125. 0.
*
UNIT 37 TYPE 11     DHW TEMP. CONTROLLED LOAD DIVERTER
PARAMETERS 2
5 50
INPUTS 4
0,0 0,0 75,1 0,0
TDHW MDHW 125. 120.
*
UNIT 38 TYPE 11     DHW TEE PIECE (LOAD OUT)
PARAMETERS 1
1
INPUTS 4
75,1 75,2 37,3 37,4
```

```
125. 0. 125. 0.
*
UNIT 39 TYPE 11    DHW FLOW DIVERTER
PARAMTERS 1
2
INPUTS 3
36,1 36,2 26,1
130. 0. 0
*
UNIT 40 TYPE 11    SPACE HEATING FLOW MIXER
PARAMETERS 1
3
INPUTS 5
52,1 48,2 22,1 48,4 42,1
130. 0. 130. 0. 0
*
UNIT 42 TYPE 8     SPACE HEATING CONTROLLER
PARAMETERS 7
4 0 125. 500. 70. 65. 3.
INPUTS 2
47,4 20,1
75. 130.
*
UNIT 43 TYPE 15    SPH ALGEBRAIC OPERATOR (.OR. FUNCTION)
PARAMTERS 1
12
INPUTS 2
42,1 42,2
0 0
*
UNIT 45 TYPE 3     SPACE HEATING PUMP
PARAMETERS 2
50000. 1.
INPUTS 3
40,1 40,2 43,1
130. 0. 0
*
UNIT 47 TYPE 12      SPACE HEATING LOAD
PARAMETERS 6
4 UA  CAP. 75. 1. ECMIN
INPUTS 6
45,1 45,2 1,2 0,0 0,0 0,0
75. 0. 75. 0. 0. 0.
*
UNIT 48 TYPE 11    SPH FLOW DIVERTER
PARAMETERS 1
2
INPUTS 3
47,1 47,2 42,1
```

```
130. 0. 0
*
UNIT 49 TYPE 11    SPH TEE PIECE
PARAMETERS 1
1
INPUTS 4
39,1 39,2 48,1 48,2
130. 0. 80. 0.
*
UNIT 44 TYPE 2    AUX. HEATER CONTROL
PARAMETERS 3
4 35 3
INPUTS 3
0,0 52,1 44,1
200. 200. 0.
*
UNIT 52 TYPE 4     AUX. BOILER(TANK)
PARAMETERS 13
1 600. 1. 62.4 .04 -10. 4000000. 1 1 250. 10. 0. 75.
INPUTS 6
49,1 49,2 0,0 0,0 0,0 44,1
200. 0. 0. 0. 60. 0.
DERIVATIVES 1
200.
*
UNIT 41 TYPE 11    LOAD TEE PIECE
PARAMETERS 1
1
INPUTS 4
39,3 39,4 48,3 48,4
130. 0. 130. 0.
*
*****************************************************************
*                     SIMULATION SUMMARY DEVICES                *
*****************************************************************
*
UNIT 29 TYPE 15    SUMMER    (DECOLPIPES,QENVCOLPIPES)
PARAMETERS 20
0 0 3 0 3 0 3 0 3 -4 0 0 3 0 3 0 3 0 3 -4
INPUTS 10
14,8 4,8 6,5 8,5 7,8 14,7 4,7 6,3 8,3 7,7
0. 0. 0. 0. 0. 0. 0. 0. 0. 0.
*
UNIT 30 TYPE 15    SUMMER    (COLSTOR:QIN,QOUT,DE,QENV; QTDHWHX)
PARAMETERS 20
0 0 3 -4 0 0 3 -4 0 0 3 -4 0 0 3 -4 0 0 3 -4
INPUTS 10
20,9 21,9 20,6 21,6 20,7 21,7 20,5 21,5 32,5 33,5
0. 0. 0. 0. 0. 0. 0. 0. 0. 0.
```

```
*
UNIT 46 TYPE 15    SUMMER    (DHWSTOR:QIN,QOUT,DE,QENV)
PARAMETERS 16
0 0 3 -4 0 0 3 -4 0 0 3 -4 0 0 3 -4
INPUTS 8
34,9 35,9 34,6 35,6 34,7 35,7 34,5 35,5
0. 0. 0. 0. 0. 0. 0. 0.
*
UNIT 59 TYPE 15    SUMMER     (DETOTAL,QENVTOT)
PARAMETERS 16
0 0 3 0 3 0 3 -4 0 0 3 0 3 0 3 -4
INPUTS 8
29,1 30,3 46,3 52,7 29,2 30,4 46,4 52,5
0. 0. 0. 0. 0. 0. 0. 0.
*
UNIT 25 TYPE 28    COLLECTOER LOOP
PARAMTERS 24
-1 0. 8762 0 2 2 0 0 0 -4 0 -4 -4 0 -4 0 -4 0 -4 0 -4 -4 0 -4
INPUTS 9
30,3  29,1 3,5 3,3 29,2 5,5 30,1 30,2 30,4
LABELS 9
QCOLL DELTAH DECOPI QECOPI QCOLHX QINST QOTST DEST QEST
*
UNIT 15 TYPE 28    LOAD LOOP
PARAMETERS 24
-1 0. 8762. 0 2 2 0 0 0 -4 0 -4 0 -4 -4 0 -4 0 -4 -4 0 -4 0 -4
INPUTS 9
52,7 46,3 30,5 46,1 46,2 46,4 52,8 52,5 47,5
LABELS 9
QDHWX QINDHW QOTDHW DEDHW QEDHW QAUX DEAUX QEAUX QSPHT
*
UNIT 60 TYPE 28    TOTALS
PARAMETERS 41
-1 0. 8762 0 2 1 0 0 -4 0 -2 2 -4 0 0 3 -3 -14 -7 2 -1 100.
1 -4 0 0 3 -4 0 -4 -4 -1 1. -15 -3 -16 -17 3 2 4 -4
INPUTS 8    (DETOT,IT,TAMB,DELTAHCOL,QAUX,DHWOUT,QINSPH,QENVTOT)
59,1 2,6 1,2 3,3 52,8 46,2 47,5 59,2
LABELS 9
IT TAMB QIN PERCQC QOUT QENV DE QAUX SOLFRC
*
UNIT 66 TYPE 28    PUMPING ENERGY
PARAMETERS 26
-1. 0. 8762. 0 2 2 -11 -12 -13 -3 -14 -3 3 -3 -15 -3
-16 -3 -17 -3 3 3 3 -4 -4 -4
INPUTS 7
10,10 10,11 11,3 12,3 17,3 28,3 45,3
LABELS 9
CLEAD CLAG COLTOT STOR DHW SPH TOTAL TOTALH TOTALL
*
```

```
UNIT 61 TYPE 28    ENERGY BALANCE
PARAMETERS 18
-1 0. 8762. 0 2 1 0 0 0 3 -4 -4 0 -4 0 0 3 -4
INPUTS 6    (DETOT,DELTAHCOL,QAUX,QENVTOT,DHWOUT,QINSHP)
59,1 3,3 52,8 59,2 46,2 47,5
LABELS 4
QIN DE QENV QOUT
CHECK 20. 1 -2 -3 -4
*
END
```

REFERENCES

American Society of Heating, Refrigerating, and Air-Conditioning Engineers, ASHRAE Standard 93-77, Methods of Testing to Determine the Thermal Performance of Solar Collectors, (1977).

Chapman, A.J., Heat Transfer, Macmillan Publishing Company, (1984).

Chiou, J.P., "The Effect of Nonuniform Fluid Flow Distribution on the Thermal Performance of Solar Collector," Solar Energy 29/6, pp. 487 - 502, (1982).

De Ron, A.J., "Dynamic Modeling and Verification of a Flat-Plate Solar Collector," Solar Energy 24, pp. 117 - 128, (1979).

Duffie, J.A. and Beckman, W.A., Solar Engineering of Thermal Processes, John Wiley and Sons, Inc., New York, (1980).

Erbs, D.G., "Methods for Estimating the Diffuse Fraction of Hourly, Daily, and Monthly Average Global Solar Radiation," M.S. Thesis University of Wisconsin-Madison, (1980).

FChart 4.2 User's Manual, University of Wisconsin-Madison, Solar Energy Laboratory, Engineering Experiment Station Report 50, (1985).

Goumaz, J.,"Comparison of Drain-back and Dual Liquid Solar Heating and Domestic Hot WAter Systems," M.S. Thesis, Colorado State University, (1981).

Hall, I.J., *et al* ,"Generation of a Typical Meteorological Year," Proceedings of 1978 Annual Meeting, American Section of ISES, 2., p 669 (1978).

Heineman, K.W., Thermal Applications of Solar Energy, GArland STPM Press, New York, N.Y., (1981)

Hicks, M.J., personal communications, Lac Du Flambeau, Wisconsin, (1986).

Kays, W.M. and London, A.L., Compact Heat Exchangers, McGraw-Hill, New York, N.Y., (1964).

Klein, S.A., Duffie, J.A., and Beckman, W.A. "Transient Considerations of Flat-Plate Solar Collectors," ASME, Journal of Engineering Power 96A, pp. 109 - 113, (1974).

Klein, S.A., "The Effects of Thermal Capacitance Upon the Performance of Flat-Plate Solar Collectors," M.S. Thesis, University of Wisconsin-Madison, (1973).

Klein, S.A., *et al.*, TRNSYS 12.1 User's Manual, University of Wisconsin-Madison, Solar Energy Laboratory, Engineering Experiment Station Report 38-12, (1983).

Klett, D.E., Goswami, D.Y., and Saad, M.T., "Thermal Performance of Submerged Coil Heat Exchangers Used in Solar Energy Storage Tanks," Journal of Solar Energy Engineering 106, pp. 373 - 375, (1984).

Koenigshoffer, D.R., "Freeze Protection for Solar Collectors," Sunworld 3, pp. 10 - 11, (1977).

Myers, G.E., Mitchell, J.W., and Lindeman Jr., C.F., "The Transient Response of Heat Exchangers Having an Infinite Capacitance Rate Fluid," Transactions of the ASME Journal of Heat Transfer, paper 70 - HT - B, (1970).

Myers, G.E., Mitchell, J.W., and Norman, R.F.,"The Transient Response of Crossflow Heat Exchangers, Evaporators, and Condensers," Transactions of the ASME Journal of Heat Transfer, paper 66 - WA / HT - 34, (1966).

Product Specifications, P-01-7-0003, Novan Energy, Inc., Boulder, Co., (1982).

Schmidt, D., Engineer, ETEC Division of Rockwell International, telephone conversations, (1885,1986).

Solar Products Specifications Guide, June, p. 169, Solar Vision, Inc., (1983).